ABSTRACT

Dissertation Title:	The Role of Adipocyte Lipid Droplet Lipolysis in Thermogenesis and Metabolic Health
	Hyunsu Shin, Doctor of Philosophy, 2017
Dissertation directed by:	Liqing Yu, Associate Professor Department of Animal and Avian Sciences University of Maryland at College Park Professor Center for Molecular and Translational Medicine Institute for Biomedical Sciences Georgia State University

My thesis was focused on the role of Comparative Gene Identification-58 (CGI-58)-mediated adipocyte lipid droplet (LD) lipolysis in thermogenesis and metabolic health. LD lipolysis in energy-dissipating brown adipose tissue (BAT) was believed to play a central role in cold-induced non-shivering thermogenesis, but this concept has not been tested in whole animal in vivo. We created a mouse line that lacks BAT CGI-58, a coactivator of Adipose Triglyceride Lipase (ATGL) that initiates the first step of cytosolic LD lipolysis by cleaving a fatty acyl chain from a triglyceride (TG) molecule. We found that BAT-specific CGI-58 knockout (BAT-KO) mice defend against the cold normally when food is absent, despite a defect in BAT LD lipolysis. Interestingly, BAT-KO versus control mice display higher body temperature when food is present during cold exposure. This cold adaptation in

BAT-KO mice is associated with increases in BAT glucose uptake, insulin sensitivity, white adipose tissue (WAT) browning, energy expenditure, and sympathetic innervation. To identify the sources of fuels for thermogenesis of BAT-KO mice in the fasted state, we hypothesized that WAT lipolysis is a major source of thermogenic fuels during fasting. To test this hypothesis, we genetically inactivated CGI-58 expression in the whole fat tissues (both BAT and WAT) of mice (FAT-KO mice). We observed that FAT-KO mice are cold sensitive when food is absent, but tolerate cold normally when food is present, demonstrating that WAT lipolysis is essential for cold-induced thermogenesis during fasting and that dietary nutrients can substitute WAT lipolysis for fueling whole-body thermogenesis. Intriguingly, FAT-KO mice display a dramatic increase in cardiac glucose uptake under both basal and insulin-stimulated conditions, which is associated with significant increases in glucose tolerance, insulin sensitivity, and cardiac expression levels of natriuretic peptides. In conclusion, our studies demonstrate that 1) BAT LD lipolysis is not essential for cold-induced whole-body thermogenesis due to increased BAT uptake of circulating fuels and WAT browning; 2) WAT lipolysis is required for fueling thermogenesis during fasting; and 3) Adipose lipolysis is critically implicated in whole-body energy metabolism and cardiac function.

THE ROLE OF ADIPOCYTE LIPID DROPLET LIPOLYSIS IN THERMOGENESIS AND METABOLIC HEALTH

BY

Hyunsu Shin

Dissertation submitted to the Faculty of the Graduate School of the University of Maryland, College Park, in partial fulfillment of the requirements for the degree of

Doctor of Philosophy

2017

Advisory Committee:

Associate Professor Liqing Yu, Chair

Professor Richard A. Erdman

Director of Mouse Metabolism Core at NIH Oksana Gavrilova

Associate Professor of University of Maryland at Baltimore Carole Sztalryd

Professor Thomas W. Castonguay, Dean's Representative

© Copyright by

Hyunsu Shin

2017

ACKNOWLEDGEMENTS

The completion of this dissertation could not have been possible without the support and encouragement from people around me. I would like to thank my advisor Dr. Liqing Yu. He has been a patient mentor and taught me how to learn and think independently. He provided me with great opportunities to learn logic thinking in science. His curiosity and passion on science always inspired me when I encountered difficulties in my studies. I am very grateful for the invaluable experience I had under the guidance of Dr. Yu.

I appreciate Dr. Richard Erdman who has served as a member of my thesis committees during last eight years of my graduate studies. The completion of this study must have been impossible without Dr. Oksana Gavrilova's valuable advices and generous support in research resources. Insights from Dr. Carole Sztalryd have guided me to complete and define my story. I am also grateful to Dr. Thomas Castonguay. His advice and wisdom on life have stamped on my heart.

I also appreciate all the former and current lab members, including Anil Kadegowda, Youlin Wang, Yinyan Ma, Weiqing Tang, Jianming He, Shun Lei, Xing Wei, and Pan Yang who have helped my studies in many ways. My former advisor Dr. Ian Mather has inspired me through his unlimited passion for science. I also thank Haarin Chun who has long been my discussion partner and become a best friend of mine. I would like to thank facility managers and all people I met at UMD and GSU, especially Drs. Hang Shi and Bingzhong Xue and their lab members for many good suggestions and helps in my research projects.

I especially thank my parents and sister. They have encouraged me endlessly and always stood on my side. I am very thankful for my best firends Dongwon Lee, Heejung Byun and Chul Kim. They have been there whenever I needed them. Also, I would like to thank my lovely fiancée Irene Cho for her invaluable encouragement and love. Finally, I dedicate my dissertation to all people who have been around me. Without the endless support and encouragement from their hearts, I could not have endured the challenges I had during my study.

TABLE of CONTENTS

LIST of TABLES

LIST of FIGURES

FIGURES FOR OBJECTIVE 2

LIST of ABBREVIATIONS

2-deoxyglucoe 6-phosphate	2-DGP
2-Deoxyglucose	2-DG
Adipose triglyceride lipase	ATGL
anterior subcutaneous WAT	asWAT
Artrial NP	ANP
Bone morphogenetic protein	BMP
Brain NP	BNP
Brown adipose tissue	BAT
Brown adipose-specific CGI-58 knockout	BAT-KO
Brown-in-white	brite
Brown-like	beige
CCAAT-enhancer binding protein-beta	C/EBP-β
Cell death activator	Cidea
Cluster of differentiation 36	CD36
cyclic Guanosine monophosphate	cGMP
Diacylglycerol	DG
Electron transport chain	ETC
epididymal WAT	eWAT
Fatty acid transporter protein 1	FATP1
Fibronectin type III domain containing 5	FNDC5
Free cholesterol	FC
Free fatty acid	FFA
G0/G1 switch gene 2	G0S2
Gastrocnemius	Gas.
Glucose tolerance test	GTT
Glucose transporter	Glut
Glycosylphosphatidylinositol-anchored high density lipoprotein binding protein 1	GPIHBP1
Green fluorescent protein	GFP
Hematoxylin and Eosin	H&E
High fat diet	HFD
Hormone sensitive lipase	HSL
inguinal subcutaneous WAT	iWAT
Inner mitochondrial membrane	IMM
Insulin tolerance test	ITT
interscacular BAT	iBAT
Intraperitoneal	i.p.
Iodothyronine 5' deiondinase	Dio2

Lateral hypothalamic area	LHA
Lipid droplet	LD
Lipocalin prostaglandin D synthase	L-PGDS
Lipoprotein lipase	LPL
Long chain fatty acid	LCFA
Mammalian target of rapamycin	mTOR
mesenteric WAT	mWAT
Mitogen activated protein kinase	MAPK
Monoacylglycerol	MG
Myogenic factor 5	Myf5
Natriuretic peptide	NP
Nitric oxide	NO
Non-shivering Thermogenesis	NST
NP receptor A	NPRA
NP receptor C	NPRC
Orexin	Ox
Perilipin 1	Plin1
peri-renal WAT	pWAT
Peroxisome proliferator-activated receptor	PPAR
PPAR coactivator 1 α	PGC1-α
PR-domain containing protein 16	PRDM16
Protein kinase A	PKA
Protein kinase G	PKG
Quadriceps	Quad.
Respiratory exchange ratio	RER
Short chain fatty acid	SCFA
Sulfo-N-succinimidyloleate	SSO
TG-rich lipoprotein	TRL
Thyroxine	T4
Total cholesterol	TC
Transcription co-regulator for adiposity and energy metabolism SERTA domain containing 2	TRIP-Br2
Triacylglyceride	TG
Triiodothyronine	T3
Tyrosine hydroxylase	TH
Uncoupling protein 1	UCP1
Vascular endothelial growth factor	VEGF
Ventromedial nucleus of the hypothalamus	VMH
Very long chain fatty acid	VLCFA
Visceral WAT	vWAT

White adipose tissue	WAT
Whole adipose tissue CGI-58 knockout	FAT-KO

INTRODUCTION

Body temperature maintenance is critical for survival of animals and humans. During cold exposure, heat is produced mainly through shivering thermogenesis and non-shivering thermogenesis (NST). Shivering thermogenesis is the rapid heat production through skeletal muscle shivering, which is a mechanism against acute cold exposure. NST is an adaptive mechanism against chronic cold exposure, which occurs in brown adipocytes present in specific fat depots. Due to the role of NST in energy dissipation, there has been growing interest in studying NST regulation and its impact on obesity and associated metabolic disorders.

Fat tissues can be broadly divided into two major types: white adipose tissue (WAT) and brown adipose tissue (BAT), each has distinct morphology (**Figure 1**). WAT stores energy as a single large lipid droplet (LD) in each adipocyte and mobilizes it during increased energy demand or fasting. BAT

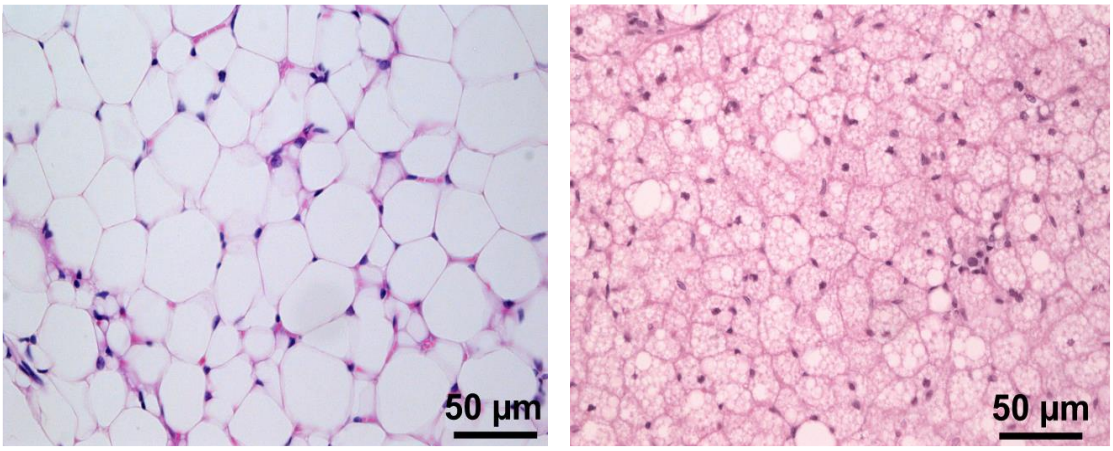

Figure 1. Hematoxylin and Eosin (H&E) staining of WAT and BAT. WAT contains a unilocular lipid droplet (LD) in a cell (left), whereas BAT contains multilocular LDs in a cell (right).

contains brown adipocytes, each of which is filled with multiple small LDs and dissipates energy as heat through NST during cold adaption [1-11]. Since the 1970s, BAT has been recognized as the main non-shivering thermogenic organ, which was initially thought to be relevant only to rodents, hibernating mammals, and newborn humans [1-3, 5]. However, positron emission tomography (PET) and ^{18}fluorodeoxyglucose uptake studies have recently revealed that adult humans have dispersed BAT [12-16], which has revitalized interest in basic and clinical research of BAT biology. A major function of BAT is to defend against the cold in a nonshivering manner by generating heat using fatty acids, glucose and other chemicals [2, 17-19]. Uncoupling protein-1 (UCP-1) plays an essential role in this process because it uncouples mitochondrial oxidation of substrates from ATP synthesis [2].

In addition to white and brown adipocytes, a third type of adipocyte has been discovered in humans and rodents [3, 20, 21]. These cells appear in WAT depots and have a different developmental origin from brown adipocytes [22, 23]. They attain brown adipocyte features under β-adrenergic or cold stimulation and are called the brown-like (beige) or brown-in-white (brite) adipocytes [24-30]. Although the thermogenic capacity of beige/brite cells is lower than that of classical brown adipocytes, beige/brite cells have been shown to be thermogenic [17, 28, 29]. Recruitment of these beige adipocytes to WAT is called WAT Browning. It was shown that the presence of BAT or beige adipocytes is negatively correlated with obesity in humans and rodents [31]. Therefore,

inducing beige or brown adipocytes in humans may have a therapeutic potential for treating obesity and associated metabolic diseases.

I. Origins of Brown/Beige Adipocytes

NST is solely dependent on brown adipocytes. However, under prolonged cold stimulation, beige adipocytes are recruited to meet increased demand for heat. While classical brown adipocytes are reportedly derived from engrailed-1-expressing cells in the central dermomyotome [32] and a *Myf5*-positive lineage [24], the origins of beige/brite adipocytes in the browned WAT are under hot debate [33-35]. Some studies showed that they can arise ***de novo*** **from precursor cells** [27, 28, 36-41], but others showed that they can originate from "**transdifferentiation**" of existing white adipocytes [25, 34, 42-50] that are likely derived from the progenitors residing in the adipose vasculature [51], or sometimes from *Myf5*+ lineage [24, 52], or both [53, 54]. These observations may imply that beige adipocytes likely have multiple cellular origins, depending on pathological conditions, and are composed of heterogeneous cell populations.

II. Regulation of Brown/Beige Adipocyte Thermogenesis

1. Transcriptional Regulators

Transcriptional factors involved in the thermogenic programming during brown/beige cell recruitment are described in **Figure 2** [55].

1) Peroxisome Proliferator-Activated Receptors (PPARs) and CCAT-Enhancer-Binding Protein-beta (C/EBP-β)

Among three members of the PPARs family, PPAR-γ is specific for adipogenesis by promoting differentiation of pre-adipocytes into mature adipocytes [56]. Besides PPAR-γ, C/EBPs also regulates the differentiation program in the adipose lineage [57]. These two factors not only control white adipose tissue homeostasis, but also the development of brown and beige adipocytes. For example, C/EBP-β expression in BAT is higher than that in WAT [58]. White

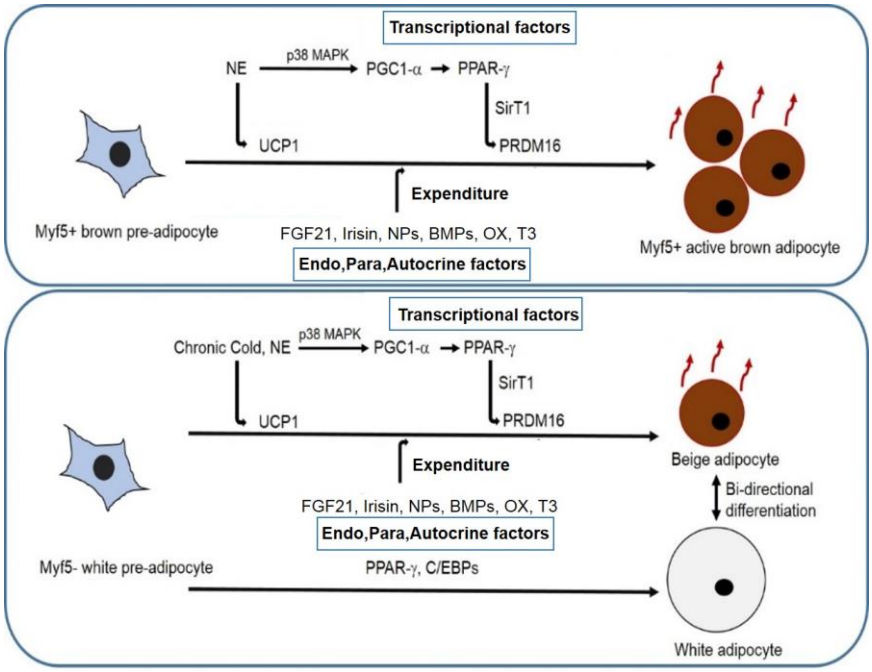

Figure 2. Transcriptional and Hormonal Regulation of the Thermogenic Program.
Activation of themogenic brown adipocytes (top) and beige adipocytes in white adipocytes (bottom). Endocrinologic factors, such as Neuronal factors, norepinephrine; cardiac factors, natriuretic peptides (NPs); liver and brown adipose tissue (BAT) factors, fibroblast growth factor (FGF)21; thyroid factors, thyroxine (T3); bone morphogenic proteins (BMPs) and muscle factors, irisin. Adapted from Harms and Seale, 2013 [55].

adipocyte C/EBP-β induces the brown fat transcriptional pattern. C/EBP-β null mice fail to generate heat and their UCP1 mRNA and protein levels in BAT are lower than those of control mice [58]. A recent study showed that high-fat diet

(HFD)-induced expression of PPAR-γ is associated with vagal neuronal innervation and subsequently stimulates beige cell programing in inguinal subcutaneous fat (iWAT) [59]. Mice with a PPAR-γ dominant-negative mutation show cold intolerance and reduced expression of UCP1 in BAT and WAT [60]. PPAR-γ, as an adipocyte development-associated gene, is essential for adipocytes to undergo thermogenic differentiation. Many studies have shown that precursor cells in WAT can express UCP1 mRNA and develop a beige fate in response to PPAR-γ agonist treatment [61]. It is well known that thiazolidinediones, as PPAR-γ agonists, trigger thermogenic program in BAT and WAT by activating genes involved in UCP1 activation and mitochondrial biogenesis [26, 61]. The thermogenic effect of PPAR-γ agonists is mediated by direct activation of thermogenic genes via the PPAR response element in their promoters and enhancers [62, 63], and some of these genes are involved in provision of thermogenic fuels by increasing BAT uptake of free fatty acids (FFAs) [64]. In contrast to many observations in which PPAR-γ induces the brown/beige phenotypes, TLE3 competes with PR (PRD1-BF1-RIZ1 homologous)-domain-containing protein 16 (PRDM16) for binding sites in PPAR-γ, which allows PPAR-γ to repress brown/beige cell recruitment while inducing white adipocyte recruitment. [65]. In addition to PPAR-γ, PPAR-α is implicated in thermogenic program by stimulating mitochondrial respiration and β oxidation of FFAs [66].

2) PRDM16

PRDM16 was initially identified at a chromosome breakpoint in myeloid leukemia [67]. A later study found that PRDM16 controls brown fat/skeletal muscle switch [24]. When PRDM16-expressing fibroblasts are implanted subcutaneously into nude mice, the fat pads derived from PRDM16-expressing cells relative to the controls show at least a five-fold increase in expression levels of brown fat selective genes, such as UCP1, Cidea, PPAR-γ coactivator 1-α **(**PGC1-α), and PPAR-α [24]. Furthermore, PRDM16 is sufficient to induce browning of subcutaneous fat [26]. When the PRDM16 DNA binding domain is mutated, the brown fat phenotype is no longer present, suggesting that it may function as a transcriptional co-regulator [24]. A subsequent investigation determined that PRDM16 acts through binding and co-activating PGC-1β, PGC-1α, and PPAR-γ [68]. PRDM16 can form a transcriptional complex with the active form of C/EBP-β [26]. As mentioned above, C/EBP-β is required for initiating the myoblast-to-BAT conversion [57, 58]. Co-transplantation studies with myoblasts expressing PRDM16 and C/EBP-β suggest that C/EBP-β mediates the myoblast-to-BAT conversion in a PRDM16-dependent manner [58]. In addition, PRDM16 has been shown to be a key factor for full functioning of PPAR-γ in response to the PPAR-γ agonist rosiglitazone [61]. Transgenic expression of PRDM16 in adipose tissues of mice increases expression levels of UCP1 and other browning-related genes in iWAT in response to rosiglitazone [26]. Several factors have been reported to regulate Whitening or Browning differentiation by modulating PRDM16 [24, 26]. The iWAT in adipose tissue-specific PRDM16 knockout (KO) mice induced by adiponectin-cre expression display visceral white adipose tissue

(vWAT)-like features [69], suggesting an epistatic relationship between a PRDM16 thermogenic program and a WT1 visceral program (WT1 is one of the visceral signature genes including WT1, TCF21, and BNC1) [69]. Interestingly, miR-133, a muscle specific microRNA, can directly antagonize PRDM16 [70-73]. It was shown that cold represses miR-133 expression in fat cells and subsequently induces PRDM16 expression, which increases expression of its downstream thermogenesis-associated genes [72].

3) PGC1-α

PGC1-α is considered as a master regulator of mitochondrial biogenesis. As a transcription factor closely associated with oxidative metabolism, it is involved in regulation of nuclear receptors, estrogen-related receptors, and FoxO transcription factors in multiple tissues [74-78]. Especially, PGC1-α expression in adipocytes is strongly correlated with UCP1 expression as well as other thermogenic components [76, 79]. Mechanistically, there is a robust activation of the sympathetic nervous system (SNS) stimulation under the cold condition. Upon SNS stimulation, β-adrenoceptor triggers cAMP and activates protein kinase A (PKA) that phosphorylates lipolytic-associated enzymes and p38 mitogene activated protein kinase (MAPK). MAPK is essential for cAMP-dependent transcription of PGC1-α in BAT. A previous study showed that p38 MAPK is required for a β-adrenergic agonist to induce PGC1-α mRNA expression [80, 81]. Furthermore, the nuclear co-repressor Rip140 recruited by liver X receptor-α to the DR-4 element in the UCP1 enhancer adjacent to

PPAR/Retinoid X receptor binding DR-1 domain represses PGC1-α, which leads suppression of UCP1 expression [82, 83].

4) Sirtuin 1 (SirT1)

SirT1 is a member of the sirtuin protein family and is characterized by a sirtuin core domain grouped into four classes. SirT1 is involved in glucose metabolism and insulin secretion by repressing protein tyrosine phosphatase activity [84]. SirT1-associated protection against metabolic damages occurs via stimulating PGC1-α and lowering proinflammatory inactivation by cytokines, such as tumor necrosis factor-α and interluekin-6 [85]. The specific mechanism for SirT1 to regulate the thermogenic program was recently identified. SirT1 serves as an NAD-dependent protein deacetylase linking transcriptional regulation to intracellular energetics and mitochondrial oxidation. SirT1 specifically regulates PPAR-γ activity by deacetylating PPAR-γ Lys268 and Lys293 sites. A deacetylated PPAR-γ mutant in 3T3-L1 cells promotes lipid accumulation, increases expression of the insulin sensitizing adipokine, adiponectin, and induces degradation of anti-adipogenic β-catenin, indicating that deacetylation of PPAR-γ is required for its full activity. SirT1-dependent deacetylation of Lys293 and Lys268 on PPAR-γ is required to recruit PRDM16 to PPAR-γ [71]. Additionally, dietary supplementation of a SirT1 activator, resveratrol, results in higher energy expenditure and lower fat accumulation in mice [86].

2. Endocrine, Paracrine, and Autocrine Factors

Some endocrine, paracrine, and autocrine factors produced by brown adipocytes and other cells can promote brown/beige adipocyte thermogenesis, such as fibroblast growth factor 21 (FGF21) from liver, thyroid hormone from thyroid gland, natriuretic peptides (NPs) from heart, and bone morphogenetic proteins (BMPs) from brown adipocytes (**Figure 2**).

1) FGF21

FGF21 is a polypeptide growth factor that is mainly expressed in liver and acts as a hormone on adipose tissue, skeletal muscle [87, 88] and other tissues. The effect of FGF21 on adipocytes is controversial. Although FGF21 activity is known to enhance energy expenditure and mitochondrial biogenesis, the role of FGF21 treatment in intracellular lipolysis is somewhat controversial [89-92]. Some studies have shown induction of adipose triglyceride lipase (ATGL) in adipocytes [93], whereas other studies showed reduced ATGL expression and circulating FFA level after administrating FGF21 [90]. More recently, the suppressive effect of FGF21 on growth hormone-induced lipolysis in adipocytes has been reported [94]. However, considering that energy expenditure and mitochondrial activity are heavily dependent on oxidation of FFAs, products of lipolysis, FGF21 seems to be positively correlated with lipolysis. Signaling to release hepatic FGF21 involves increased FFAs, which act as ligands for PPAR-α. Activated PPAR-α increases FGF21 expression during fasting [95]. FGF21 treatment increases phosphorylation of AMPK in 3T3-L1 cells, stimulating SirT1 through modulation of intracellular NAD+/NADH levels. When SirT1 is knocked-down by shRNA *in vitro*, FGF21 cannot further deacetylate PGC1-α, which results in inactivation of

the thermogenic program [96]. The effect of FGF21 on mitochondrial energy expenditure is likely mediated by serine/threonine kinase 11 that activates AMPK activity to induce SirT1, causing deacetylation of PGC1-α [96].

Hormonal regulation of FGF21 has been reported. FGF21 interacts with β-klotho, an FGF21 signaling cofactor that is ubiquitously expressed. The FGF21/β-klotho interaction in hypothalamus stimulates energy expenditure and browning of iWAT by enhancing the SNS activity [93]. Although the main source of FGF21 is the liver, other organs, such as muscle and adipose tissues, produce FGF21 under some circumstances. When the autophagy pathway is inhibited in mice by genetically deleting autophagy related 7, skeletal muscle releases FGF21 as a myokine for recruitment of beige cells to compensate for failure of autophagy-dependent energy degradation in skeletal muscle [97]. These mice have a lean phenotype and less adipose hypertrophy. FGF21 has a beneficial insulin-sensitizing effect by regulating insulin action [98]. However, high circulating FGF21 levels in humans are correlated with the occurrence of metabolic diseases, including type 2 diabetes and non-alcoholic fatty liver disease [99], suggesting FGF21 resistance or metabolic stress when administered at a supraphysiological dose. Further studies are needed to examine the mechanisms underlying FGF21 resistance or metabolic stress associated with high doses of FGF21 before its clinical use in metabolic diseases and thermoregulation.

2) Thyroid Hormone

Thyroid hormone reduces the proton motive force by facilitating the leak of protons through the inner mitochondrial membrane (IMM). Hafner et al. showed that hyperthyroidism is correlated with increased respiration, without ATP turnover, suggesting that thyroid hormone-induced energy expenditure may occur via mitochondrial uncoupling [100]. This implication is consistent with that Na+-K+-ATPase in liver membranes increases in a thyrotoxic state [101]. In BAT, cold adaptation increases type II iodothyronine 5' deiodinase (Dio2), which converts thyroxine (T4) to triiodothyronine (T3), the active form of thyroid hormone, to activate the thermogenic program T3 [102, 103]. UCP1 levels in response to SNS stimulation are modest without thyroid hormone, whereas the expression levels of UCP1 are 18-20-fold higher after SNS activation than the basal condition in the presence of thyroid hormone, specifically T3 [102]. In agreement, hypothyroidism reduces the number of β-adrenergic receptors [104] and the induction of $G_i\alpha$ or $G_b\gamma$ protein subunits in WAT [105, 106]. Although Dio2, UCP1, and PGC1-α mRNA levels are normal, thyroid hormone receptor (TR)-α KO mice fails to adapt to cold [107].

3) Natriuretic Peptides (NPs)

The cardiac NPs, atrial NP (ANP) and brain NP (BNP), are cardiometabolic hormones released from the heart and regulate hemodynamic homeostasis. Plasma ANP and BNP increase with severity of heart failure [108]. They promote natriuresis (sodium excretion in the urine) through vasodilation by inhibiting the renin-angiotensin-aldosterone system. The role of NPs in regulating thermogenesis via a catecholamine-independent mechanism was recently

identified [109]. There are two NP receptors. NP receptor A (NPRA) binds ANP/BNP and this binding increases cyclic guanosine monophosphate (cGMP). Increased cGMP activates the α- and β- subunits of protein kinase G (PKG) to phosphorylate p38 MAPK. The activated p38 MAPK subsequently phosphorylates the transcriptional regulator PGC1-α and further activates transcription factors for the UCP1 enhancer, PPRE, and CRE2 [109]. It was shown that ANP binding to NPRA induces UCP1 expression and respiration in human multipotent adipose-derived stem cells [109]. Similar to catecholamine effects, activation of NP signaling also induces phosphorylation of hormone sensitive lipase (HSL)- and perilipin 1 (Plin1) to promote cytosolic LD lipolysis in adipocytes [110, 111]. In addition, ANP and BNP upregulate mitochondrial genes associated with FFA oxidation and mitochondrial biogenesis in adipocytes via NPRA [112]. Compared with NARA, NP receptor C (NPRC) has an opposite effect on NPs. It mediates degradation of ANP/BNP and therefore clearance of NPs from the circulation.

4) Bone morphogenetic proteins (BMPs)

BMPs are growth factors implicated in the regulation of tissue architecture. Various BMP family members recruit precursor cells into the adipocyte lineage. BMP2 and 4 are involved in white adipogenesis [113, 114], whereas BMP7 is related to brown adipogenesis [115]. Some studies have reported that BMP4, 7, and 8B promote beige adipocyte recruitment [116, 117]. The BMP8B level increases in mature BAT in response to increased catecholamines, which activates p38 MAPK/CREB signaling and increases lipase activity. BMP8B KO

mice display reduced metabolic rates and impaired thermogenesis [117]. Mice lacking the type 1A BMP receptor in brown adipocyte progenitor cells exhibit a severe paucity of interscapular brown adipose tissue (iBAT), which in turn, increases sympathetic innervation into iWAT to induce beige cell recruitment [118].

In addition to autocrine functions of BMPs in BAT, BMP8B may have a central role for modulating BAT thermogenesis by activating the AMPK-orexin (OX) axis [119]. Hunger regulation is modulated by the lateral hypothalamic area (LHA). Satiety is regulated in the ventromedial nucleus of the hypothalamus (VMH). Suppression of AMPK in the VMH [120, 121] or stimulation of orexigenic tone in the LHA activates the brown/beige thermogenic program. BAT development and differentiation require OX neurons in the LHA [122, 123]. In a recent study, a significant elevation in body temperature was observed in mice after treatment with BMP8B within the VMH [119]. These studies suggest a central role of BMP8B in regulating thermogenesis via influencing the VMH-LHA interplay.

5) Vasculature factors

Nitric oxide (NO) is synthesized in endothelial cells and promotes BAT mitochondrial respiration and biogenesis [124]. Soluble guanylyl cyclases are activated by NO, increase cGMP, and subsequently stimulate PKG activity to promote brown/beige recruitment and UCP1 expression [125-127].

Overexpression of vascular endothelial growth factor (VEGF) A increases vascularization and upregulates UCP1 and downstream brown markers [128]. Similarly, deletion of VEGF receptor 2, one of two tyrosine kinase receptors for

VEGF, in mice results in impaired beige recruitment [129]. Both NO and VEGF seem to use a paracrine mechanism in endothelial cells for control of the brown adipocyte phenotype.

III. The Role of FFA in Thermogenesis

FFAs are essential for mitochondrial respiration, β-oxidation, and activation of UCP1 in mitochondria (**Figure 3**) [2]. First, FADH2, NADH, and acetyl-coA are generated via β-oxidation of FFAs in the mitochondria. These products are further utilized in the electron transport chain (ETC). The ETC or so-called, mitochondrial respiratory chain, consists of five complexes. Complexes I, III, and IV pump protons out of the inner membrane by oxidizing NADH and FADH2 to NAD+ and FAD+. The proton gradient generated by ETC is subsequently coupled to generate ATP by complex V, an ATP synthase. However, protons in

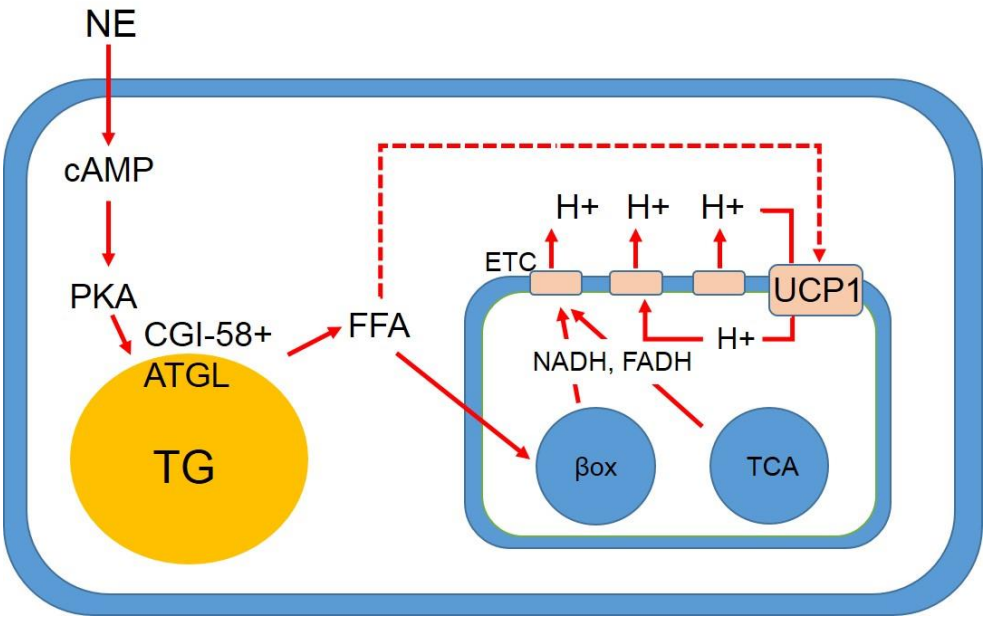

Figure 3. Proposed Model of Thermogenic Regulation in Brown/Beige Adipocytes. Norepinephrine stimulates a signaling cascade that activates intracellular lipolysis of lipid droplets (LDs). FFAs that are released either directly bind to UCP1 or undergoes β-oxidation. The Generated proton gradient is subsequently utilized via UCP1 to generate heat. ETC, Electron transport chain; TCA, Tricarboxylic acid cycle; βox, β-oxidation. Adapted from Cannon and Nedergaard, 2004 [2].

brown adipocytes are dissipated as heat via UCP1 that increases the permeability of the inner membrane causing protons returned to the mitochondrial matrix from the intermembrane space of mitochondria. In addition to mitochondrial β-oxidation for the uncoupling process, FFAs are required for activation of UCP1 [130-132]. UCP1 shares its tripartite structure and amino acid sequence with other family members, including UCP2 and UCP3. The binding domains of purine nucleotides, such as GDP, ADP, or ATP are conserved among UCP members. However, UCP1 is specific in that it has a central loop facing the matrix and its last part of the COOH terminus faces the cytosol [2, 133].These unique sequences and topology of UCP1 may contribute to its thermogenic function. Some studies have examined potential molecular mechanisms underlying FFA-mediated UCP1 activation. It has been shown that GDP inhibits proton permeability [130] and that the FFA derivatives acyl-CoAs compete with bound purine nucleotides [134]. Other studies also examine the role of FFAs in activating UCP1 [135, 136]. The current working models of how FFAs increase UCP1 activity include: an H+ channel is activated by allosteric binding of FFAs [137, 138]; an OH- channel is activated by allosteric binding of FFAs [132]; and the FFA cycling model. In the FFA cycling model, UCP1 catalyzes translocation of FFAs in anionic form, and the carboxylic group picks up a proton from the cytosolic side, so that the protonated FFAs flip-flop to the matrix side [139]. Although the molecular detail for UCP1 activation by FFAs remains elusive, it is commonly accepted that UCP1 activity depends on allosteric binding of long chain fatty acids (LCFAs) [132, 137, 139, 140]. Thus, FFA flow into mitochondria

is indispensable for generating a proton gradient via β-oxidation and for binding and activating UCP1.

IV. Intracellular Lipolysis and Thermogenesis

Excess energy is stored as TG-rich LDs in the cytosol of adipocytes. During starvation or increased energy demand, this stored energy is mobilized via a process called intracellular lipolysis (**Figure 4**) [11].

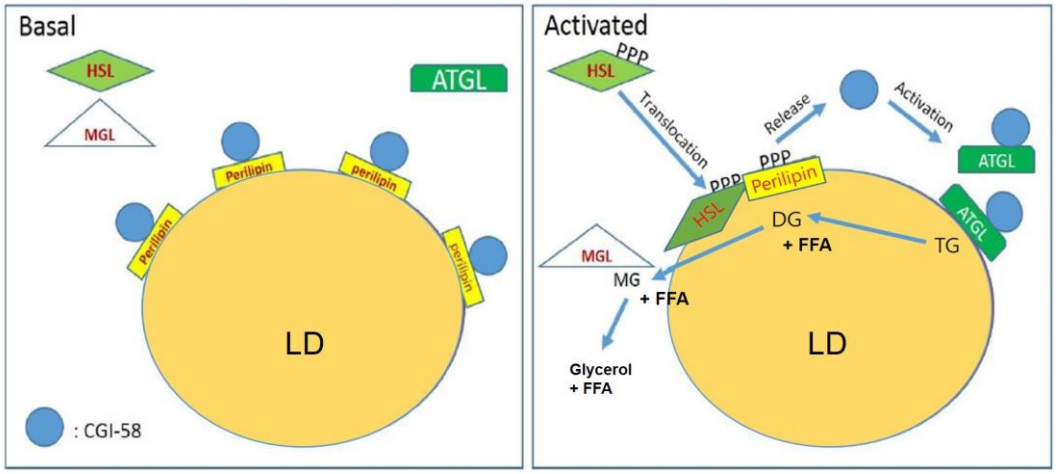

Figure 4. Intracellular Lipolysis. Under the basal condition, lipolytic enzymes adipose triglyceride lipase (ATGL), hormone-sensitive lipase (HSL) and monacylglycerol lipase (MGL) are not associated with lipid droplets (LDs). LDs are shielded by perilipin and its associated comparative gene identification-58 (CGI-58), a coactivator of ATGL. Under the stimulated condition, perilipin is phosphorylated, releasing CGI-58 to recruit ATGL onto LDs, which together with translocation of phosphorylated HSL initiates the lipolytic cascade. Adapted from [11].

Intracellular lipolysis is regulated by hormones and coordinated by many LD coat proteins and lipases [11, 141, 142]. ATGL is a cytosolic neutral lipase that initiates “Cytosolic/Neutral” Lipolysis by cleaving a fatty acyl chain from a triglyceride (TG) molecule [11, 143-146]. CGI-58 [147], also known as Abhd5, is

the fifth member of α/β-hydrolase fold protein family [148-150]. It is ubiquitously expressed with the highest expression in adipose tissues [151-155]. CGI-58 binds to cytosolic LDs via interactions with members of the PAT family [151, 153, 156-162]. It is the causative gene for Chanarin-Dorfman syndrome, a neutral-lipid storage disease [163, 164] associated with ichthyosis (scaly dry skin) and cytosolic accumulation of TG-rich LDs in most cell types. Purified CGI-58 promotes ATGL's activity *in vitro* by acting as a coactivator [152], though it clearly has ATGL-independent lipolytic functions [150, 152, 153, 158, 159, 165-169]. Since it is well established that CGI-58 limits LD deposition by promoting TG hydrolysis, not by inhibiting TG synthesis, CGI-58 may also activates other intracellular lipolytic pathways, one of which is the lipid-specific macroautophagy (lipophagy) that clears cytosolic LDs by delivering LD to lysosomes for degradation by lysosomal acidic lipase ("Lysosoma/Acidic" Lipolysis) [170].

Lipolysis in adipocytes is often triggered by catecholamine stimulation of $G_{\alpha s}$-coupled β-adrenergic receptors, which activates adenylyl cyclase to raise intracellular cAMP levels, leading to activation of PKA. Activated PKA phosphorylates HSL and Plin1. Under the basal condition, CGI-58 is bound to LDs by interacting with Plin1. This association may prevent ATGL from gaining access to LDs. Phosphorylation of Plin1 by PKA results in release of CGI-58 that subsequently recruits ATGL onto LDs to initiate TG hydrolysis. One study reported that CGI-58 Ser239 is also phosphorylated by PKA after lipolytic stimulation, which contributes to dispersion of CGI-58 from LDs and increases the co-activator function of CGI-58 [171].

Some lipolytic regulators or enzymes are implicated in thermoregulation. For example, the transcription regulator SERTA domain containing 2 (SERTA2, also known as TRIP-Br2) is involved in fat lipolysis, energy metabolism and thermogenesis [172-174]. TRIP-Br2 knockout mice are lean and show increased lipolytic activity. The increased lipolysis is HSL-dependent, whereas ATGL and CGI-58 activities remain normal in these animals [172].Ablation of TRIP-Br2 promotes transcription of β3-adrenergic receptors, energy expenditure, and FFA oxidation, which increases thermogenesis [172]. Mammalian target of rapamycin (mTOR) is a master regulator of many important metabolic processes, including energy expenditure, autophagy, protein synthesis, and lipogenesis [175, 176]. Inhibition of the mTORC1 signaling pathway *in vitro* promotes TG lipolysis to release FFAs [177]. Mice lacking raptor, a key component of mTOR complex 1 (mTORC1), display enhanced expression of UCP1, suggesting that mTORC1 may suppress thermogenesis [178]. The growth factor receptor-binding protein-10 (Grb10) was originally identified as a negative regulator of insulin and insulin-like growth factor-1 signaling pathways [179, 180]. A recent study identified Src homology 2 domain containing protein Grb10 as a direct substrate of mTORC1 [181, 182]. Liu et al. generated adipose-specific Grb10 knockout mice to study the role of Grb10 in adipocytes and found that these mice display reduced ATGL phosphorylation and total HSL protein, which is associated with increased fat mass [183]. G0/G1 switch gene 2 (G0S2), a negative regulator of cytosolic lipolysis [184], is also involved in thermogenesis in adipocytes [185]. Zandbergen et al. reported that G0S2 mRNA levels in adipose tissue are upregulated during

adipogenic differentiation [186]. G0S2 attenuates ATGL action both *in vivo* and *in vitro* [187]. Mice lacking G0S2 are lean due to increased ATGL-dependent lipolytic activity and they are cold tolerant [185, 188].

In addition to lipolysis regulators, lipolytic enzymes can also affect thermoregulation. Adipose-specific ATGL knockout mice show increased expression of WAT-enriched genes and decreased expression of BAT-associated genes in BAT [189]. Systemic deletion of ATGL impairs cold-tolerance in mice [190]. Controversy exists for HSL. HSL-null mice display increased energy expenditure, decreased insulin sensitivity, and increased uncoupling activity during cold adaptation [191]. In contrast, TRIP-Br2 KO mice show enhanced cold tolerance as a result of upregulated HSL [172]. Overall, the tissue-specific role of intracellular lipolysis on thermoregulation remains largely unknown.

2) Intravascular Lipolysis and Thermogenesis

Intravascular lipolysis is mainly referred to lipoprotein lipase (LPL)-mediated lipolysis occurring intravascularly, which releases FFAs from lipoprotein-TG particles for tissue uptake (**Figure 5**). It has been reported that LPL activity increases in BAT after a meal [192], when circulating chylomicrons are elevated. Cold-activated BAT is an important organ for the uptake of triglyceride-rich lipoproteins (TRLs) including chylomicrons and very low density lipoproteins (VLDLs), likely by increasing the endothelial permeability. It seems that both FFA uptake and TRL internalization into BAT are regulated by LPL activity. When LPL activity is inhibited by injecting the specific inhibitor tetrahydrolipstatin, the local

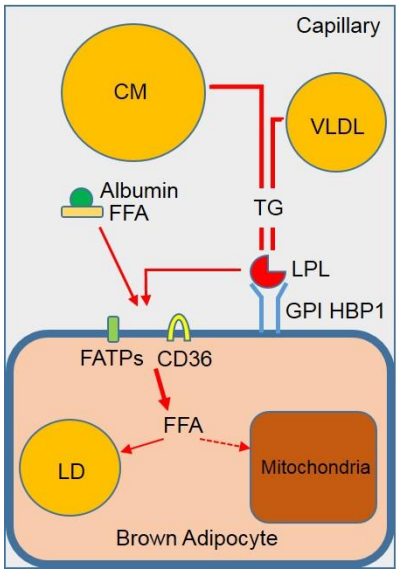

Figure 5. Schematic of Intravascular Lipolysis. Adapted from [11].

BAT FFA and TRL uptake is abolished [192]. Glycosylphosphatidylinositol-anchored high-density lipoprotein binding protein 1 (GPIHBP1) is responsible for anchoring LPL onto capillaries. GPIHBP1 KO mice show mislocalized LPL in various tissues including BAT, which decreases tissue TG content and limits lipolysis [193]. Following intravascular hydrolysis of TRLs, the released FFAs are transported into cells by various transporters. It has been shown that fatty acid transporter protein1 (FATP1) increases during brown adipocyte differentiation and facilitates FFA uptake in response to adrenergic stimulation [194]. FATP1 is highly expressed in adipose tissue and muscle [195]. It is involved in very long chain fatty acid (VLCFA) uptake [196, 197]. The muscle in FATP1 null mice has reduced FFA uptake in response to insulin stimulation [198]. Interestingly, FAPT1 knockout mice have impaired heat generation and reduced energy expenditure [199]. Cluster-of-differentiation 36 (CD36) is another fatty acid transporter [200-205]. Similar to glucose transporter (Glut) 4, upon the stimulation of insulin,

intracellular cytoplasmic CD36 is translocated to the extracellular side of the plasma membrane [206, 207]. Like FATP1 knockout mice, CD36 knockout mice show increased plasma FFA concentrations during cold exposure and impaired cold tolerance [192]. In particular, CD36 knockout mice display impaired thermogenic capacity under the conditions of fasting and cold stress, and they are cold sensitive when food is absent during cold exposure [208]. Taken together, intravascular lipolysis seems to play an important role in BAT thermogenesis.

V. Glucose Uptake and Thermogenesis

The existence of brown fat-like depots in humans was established by PET-CT using a glucose tracer whose uptake is substantially increased in individuals exposed to cold [12-16]. Glucose uptake in brown adipocytes upon catecholamine stimulation is more dependent on Glut1 activity than on insulin-dependent Glut4 activity [209]. One report suggested that Glut1 translocation in BAT is mTORC2-dependent [210]. However, FGF21 interplays with insulin to regulate glucose uptake [211]. It has been shown that there is a 110-fold increase in glucose uptake in BAT under the cold [212]. Deletion of insulin receptor in BAT causes reduced BAT mass and FFA synthesis, suggesting the importance of insulin action in BAT fat accumulation [213]. Collectively, it seems that both Glut1 and Glut4 in BAT may be implicated in cold adaptation.

During cold adaptation, glucose tolerance is improved and Glut1/Glut4 mRNA levels are increased, implying that activation of BAT thermogenesis may

promote glucose disposal [214]. Mice lacking lipocalin prostaglandin D synthase (L-PGDS) show elevated glucose uptake in BAT and increased reliance on carbohydrate as a fuel for thermogenesis [215]. It is currently unknown whether glucose is directly utilized in brown/beige adipocytes for UCP1-dependent thermogenesis or is first converted to fatty acids via de novo lipogenesis and then used for heat production. However, it is clear that brown/beige adipocytes are major organs for clearing glucose under cold conditions.

VI. Challenges and Hypotheses

Despite some studies linking ATGL and HSL to thermogenesis, it is currently unknown if CGI-58-medaited adipose lipolysis regulates cold-induced thermogenesis. Although brown adipocyte LD lipolysis was predicted to be central for thermoregulation [2], this prediction has not been tested directly *in vivo*, due to lack of appropriate animal models. It was known that multiple substrates can be used for BAT thermogenesis, but several outstanding questions exist about regulation of thermogenic substrates selection by BAT. For example, how do multiple substrates or different origins of the same substrates (*e.g.*, fatty acids from blood versus those from cytosolic LDs) communicate with each other in brown adipocytes for thermogenesis? Does intracellular LD lipolysis, a cellular process robustly regulated by nutritional, hormonal and neuronal signals, play any roles in regulating selection of thermogenic substrates or their origins by brown adipocytes? If it does, what is the thermogenic/energetic/metabolic consequences when inhibited? Intracellular LD

lipolysis is just one (perhaps not a quantitatively critical one) of multiple thermogenic substrate sources upstream of the mitochondrial thermogenic machinery.

The major goal of this project was to establish the role of BAT and WAT lipolysis in cold-induced thermogenesis in vivo and in metabolic health using BAT-specific CGI-58 knockout (BAT-KO) mice and whole fat CGI-58 knockout (FAT-KO) mice. We mainly tested two hypotheses: 1) BAT lipolysis is required for cold-induced thermogenesis; and 2) WAT lipolysis is critical in cold-induced thermogenesis during fasting.

MATERIALS and METHODS

Materials

Tris hydroxymethyl amino methane (Tris), sodium dodecyl sulphate (SDS), ammonium persulphate (APS), N,N,N',N' tetramethylethylenediamine (TEMED), Bovine serum albumin (BSA), acrylamide, N,N' methylenebisacrylamide, Bicinchoninic acid (BCA), Pierce Modified Lowry protein assay reagents, 3,3'-diaminobenzidine tetrahydrochloride (DAB), and Tween-20 were obtained from Thermo Fisher Scientific (Waltham, MA). Goat anti-(rabbit-IgG or mouse-IgG) conjugated to horse-radish peroxidase, chromatography columns, and nitrocellulose membrane were obtained from Bio-Rad Laboratories (Hercules, CA). SuperSignal West Pico PLUS Chemiluminescent western blotting detection substrates was obtained from Pierce (Rockford, IL). A rabbit polyclonal CD36 and mouse monoclonal ABHD5 (CGI-58) antibodies were obtained from Abnova (Jhongli, Taiwan). A rabbit polyclonal tyrosine hydroxylase (TH) antibody was obtained from Novus Biologicals, LLC. (Littleton, CO). A polyclonal UCP1 antibody was obtained from Abcam Biotechnology Company (Cambridge, United Kingdom). A polyclonal glyceraldehyde 3-phosphate dehydrogenase (GAPDH) antibody, isoproterenol, 4-methylumbelliferyl heptanoate (4-MUH), free glycerol reagent, and triglyceride reagent were purchased from Sigma-aldrich (St. Louis, MO). Half Micro Test Kit for free fatty acid assay was obtained from Roche Pharmaceutics Company (Basel, Switzerland). Contour glucose test kit and test strips were purchased from Bayer Pharmaceutics Company (Leverkusen, Germany). Enzymatic assay kits for total cholesterol, free cholesterol, and

phospholipids were obtained from Wako (Richmond, VA). CL-243,316 was purchased from Tocris Bioscience (Bristol, United Kingdom). C^{14}-2-Deoxyglucose and H^3-2-Deoxyglucose were obtained from PerkinElmer (Waltham, MA). VECTASSTAIN Elite ABC HRP Kit (Peroxidase, Rabbit IgG) was obtained from Vector Laboratories (Burlingame, CA). Hematoxylin Stain Gill 2 was obtained from Ricca Chemical Company (Arlington, TX). Quanti-iT™ dsDNA Assay Kit was obtained from Invitrogen (Eugene, Oregon).

Table 1. Primers used to amplify mRNAs encoding targeted mouse genes.

Name	Forward (5' to 3')	Reverse (5' to 3')
ANP	CAAGAACCTGCTAGACCACC	AGCTGTTGCAGCCTAGTCC
BNP	CCAGAGACAGCTCTTGAAGG	TCCGATCCGGRCTATCTTG
CD36	GGAACTGTGGGCTCATTGC	CATGAGAATGCCTCCAAACAC
CPT1α	TGAGTGGCGTCCTCTTTGG	CATGAGAATGCCTCCAAACAC
Dio2	GTCCGCAAATGACCCCTTT	CCCACCCACTCTCTGACTTTC
FATP1	CCGTATCCTCACGCATGTGT	CTCCATCGTGTCCTCAATGAC
Glut1	GGTGTGCAGCAGCCTGTGTA	CAACAAACAGCGACACCACAGT
Glut4	CCGGCAGCCTCTGATCAT	CCGACTCGAAGATGCTGGTT
LPL	ACTCTGTGTCTAACTGCCACTTCAA	ATACATTCCCGTTACCGTCCAT
PGC1α	GACTCAGTGTCACCACCGAAA	TGAACGAGAGCGCATCCTT
PRDM16	CAGCACGGTGAAGCCATTC	GCGTGCATTCGCTTGTG
PPAR-α	GCCTGTCTGTCGGGATGT	GGCTTCGTGGATTCTCTTG
PPAR-γ	GCCCTTTGGTGACTTTATGGA	GCAGCAGGTTGTCTTGGATG
UCP1	AAGCTGTGCGATGTCCATGT	AAGCCACAAACCCTTTGAAAA

SCD1	CCGGAGACCCCTTAGATCGA	TAGCCTGTAAAAGATTTCTGCAAACC
SirT1	GATGACGATGACAGAACGTCACA	GGATCGGTGCCAATCATGAG
GAPDH	ACCACAGTCCATGCCATCAC	CACCACCCTGTTGCTGTAGCC
18s RNA	GGGAGCCTGAGAAACGGC	GGGTCGGGAGTGGGTAATTT

Methods

Animals and Diets

Brown adipose-specific CGI-58 knockout (BAT-KO) mice were produced by crossing CGI-58-floxed mice generated in our lab previously [216] with B6.FVB-Tg (Ucp1-cre) 1 Evdr/J mice (The Jackson Laboratory, Stock #: 024670) generated by Dr. Evan Rosen's lab at Harvard Medical School. The Ucp1-cre mice specifically express cre recombinase in UCP1 positive cells, leading to selective inactivation of gene expression in brown and beige adipocytes [217]. Homozygous CGI-58 floxed mice without Ucp1-cre transgene were used as controls for all experiments.

Whole adipose tissue CGI-58 knockout (FAT-KO) mice were generated by crossing our CGI-58-floxed mice with adiponectin-cre mice [B6;FVB-Tg(Adipoq-cre)1Evdr/J mice, The Jackson Laboratory, Stock #: 010803] generated by Dr. Evan Rosen [218]. The adiponectin-cre mice express cre recombinase in all adipose tissues, thus inactivating gene expression in whole adipose tissue. Homozygous CGI-58 floxed mice without adiponectin-cre transgene were as controls for all experiments.

Mice were housed in a pathogen-free animal facility at 22^{o}C with a 12h light/dark cycle from 6AM to 6PM and fed *ad libitum* a standard chow diet

(LabDiet) or a high fat diet (HFD) containing 60% energy from fat, 20% energy from carbohydrate, and 20% energy from protein (D12492, Research Diets Inc.). Diet treatments and weight measurements were started at 6 weeks of age. All animal experiments were performed with male mice and approved by the Institutional Animal Care and Use Committees (IACUC) at the University of Maryland at College Park and at Georgia State University.

Body Weight and Food Intake

Body weight was monitored weekly on Wednesday at 10 AM from the beginning of diet treatment (6 weeks of age) until 17-18 week of diet treatment. On the 5th week of diet treatment, mice were individually caged and measured food intake daily for 7 days.

Metabolic Phenotyping and Telemetry

Indirect Calorimetry (Oxymax/ CLAMS, Columbus Instruments, Columbus, OH) was used to measure energy expenditure, respiratory exchange ratio (RER), and physical activity in mice at 22^{o}C, 30^{o}C, or 30^{o}C combined with intraperitoneal (*i.p.*) injections of β3 agonist CL-316,243 at 0.1 mg/kg body weight. The core body temperature was continuously monitored by Telemetry (Mini Mitter/Philips Respironics, Bend, OR; ER4000 energizer/receivers, G2 E-mitters implanted intraperitoneally). Rectal temperature was monitored in some mice subjected to acute cold exposure using Thermalert TH-5 device (Physitemp). Food intake was measured in metabolic chambers. Body composition was determined by using by EchoMRI-100H Body Composition Analyzer (EchoMRI LLC.). For chronic cold

exposure, we allowed 2-4 days of acclimation to different housing environment to finally mice to adapt 4^{o}C.

CL-316,243 and Saline Injection for mimicking chronic cold

CL-316,243 (1 mg/kg body weight) or saline were administered *i.p.* to 14-week-old HFD-fed mice (8 weeks on HFD). Injection was performed at 10 AM daily for 4 days. Following consecutive injection, mice, on day 5, were sacrificed without additional injection.

***In vivo* Lipolysis Assays**

The mice were injected *i.p.* with isoproterenol at 10 mg/kg body weight around 10AM. Blood samples were collected before and 15 min after isoproterenol injection. Collected blood were centrifuged for 15 min at 2500 RPM. Plasma concentrations of FFA and glycerol were analyzed by enzymatic assay.

BAT Hydrolysis Assays

Snap-frozen brown adipose tissues were quickly weighed, homogenized in ice-cold Tris-HCl homogenization buffer (50 mM, pH 7.4, 250 mM sucrose, 1 mM EDTA), and sonicated briefly. Protein contents in homogenates were analyzed using BCA assay. Hydrolytic activity were assessed by mixing 20 µl of 2 µg total protein containing homogenates, 20 µl of 5 µM 4-MUH in reaction buffer (20 mM Tris-HCl, pH 8.0, 1mM EDTA, 300 µM taurodeoxycholate), and 60 µl of the reaction buffer in 96-well plates and incubating at room temperature with shaking for 5 min. The fluorescence was continuously recorded over a 10 min period at 355 nm as excitation and 460 nm as emission wavelengths at 22^{o}C [219].

Immunohistochemistry of Tissues

The iWAT was fixed in 10% formalin solution, paraffin-embedded, and then sectioned at 5 μm thickness. The sections were deparaffinized and rehydrated, followed by antigen retrieval using 10 mM sodium citrate (pH 6.0) for 20 min. After antigen retrieval, non-specific sites were blocked by incubating the sections in TBS containing 10% normal goat serum and 0.2% Tween 20 for 40 min. The sections were then incubated with the primary antibody against UCP1 (1:200) or TH (1:200) for overnight at 4ºC, followed by three washes, 5 min each, with TBS-Tween 20 solution and incubation for 1h with a biotinylated secondary antibody (1:200). After three washes, the sections were incubated with the reagents in VECTASSTAIN Elite ABC HRP Kit for 30 min and then with DAB for 5-10 min. After three washes, cell nuclei were stained with hematoxylin. The sections were dehydrated, sealed, and examined under a microscope.

Glucose Tolerance and Insulin Tolerance Tests

For glucose tolerance test (GTT), the mice were fasted overnight (16h) and then injected *i.p.* with glucose solution at 1.5 g/kg body weight. Blood glucose concentrations were measured at 0, 15, 30, 60, and 120 min after glucose injection. For insulin tolerance test (ITT), the mice were fasted for 6h during the daytime cycle, followed by an intraperitoneal injection of recombinant human insulin in saline at a dose of 0.75 U/kg body weight. Blood glucose levels were monitored at 0, 15, 30, 60 and 120 min after insulin injection.

Analysis of Adipocyte Size

The adipose tissue cell sizing was done in osmium-fixed urea-isolated adipocytes as described previously [220] with some modifications. Briefly, the adipose

tissues from different fat depots of the mice on HFD for 17 weeks were excised aseptically, sliced to ~50 mg in size and rinsed twice in 0.154M NaCl at 37^{o}C to wash off free lipids on the tissues. The tissue slices were transferred to scintillation vials containing 1.2 mL of 50mM Colloidine HCl buffer and 2 mL of 3% osmium tetroxide in 0.05 M Colloidine HCl buffer (pH 7.4 at 37^{o}C). The sample vials were kept in a ventilated fume hood at room temperature for 72h. The osmium-colloidine buffer was removed and replaced by 10 mL of 0.154M NaCl for 24h. Subsequently, 10mL 8M Urea in 0.154M NaCl was added to the sample vials and the vials were intermittently swirled by hand and kept in room temperature for 48h. This solubilized the connective tissue in the adipose tissue slices resulting in a suspension of adipocyte cells. The adipocyte cell suspension was passed through 250µM nylon membrane to remove any of the remaining tissue debris. The cells were rinsed with 0.01% Triton-X in distilled water and then used to profile cell size distribution using Multisizer® Coulter Counter (Beckman coulter Ireland Inc.).

Tissue Lipid Analysis

Total lipids were extracted as described previously [221]. To determine tissue lipid concentrations, about 40~50 mg of liver piece or 20~30 mg of adipose tissues were sliced and extracted with 1:1 $CHCl_3$/MeOH. The organic phase was analyzed for lipid species. Samples were allowed to stay at room temperature overnight to ensure extraction of lipid until the tissue sink at the bottom of the tube. Extractions were centrifuged at 2,000 x*g* for 15 min at room temperature. The lipid phase was transferred into a new tube, leaving the delipidated tissue

behind for protein determination. Delipidation process was repeated with additional $CHCl_3$/MeOH. Lipid extraction was dried down under N_2 at 60^oC. Additional $CHCl_3$/MeOH was added and sit on heating blocks at 60^oC for 5 min to solubilize the lipid. To split the phases, 0.6ml of 0.05% H2SO4 was then added. Samples were centrifuged at 2,000 x*g* for 15 min at room temperature. Bottom phase was transferred to new glass tube, mixed with 1% TritonX-100, and dried down under N_2 gas. 0.5ml dH2O was added and tubes were placed on heating block for 5 min. Samples went vortex until solution appeared clear. Concentrations of TC, FC, and TG in each sample were used to determine by enzymatic assay kit described in the material section. Protein concentrations in the delipidated samples were determined using a Lowry assay [222].

Glucose Uptake Assays

To measure insulin-stimulated glucose uptake, the mice were fasted overnight (16h), and then injected with human insulin at 0.75 mU/Kg and 10 µCi of C^{14}-2-Deoxyglucose (2-DG). Forty-five minutes after 2-DG injection, the mice were sacrificed and tissues collected. For cold-induced glucose uptake, overnight fasted mice were exposed to cold (4^oC) for 30 min before injection of 10 µCi of [^{3}H]-2-DG as a tracer and then sacrificed for tissue collection after additional 45 min cold exposure. DG is transported into tissues and phosphorylated to 2-deoxyglucose 6-phosphate (2-DGP). Tissue contents of 2-DGP were used to reflect their glucose uptake efficiency. To determine tissue 2-DGP content, samples were homogenized and 2-DGP was separated from 2-DG using ion exchange column, and then 2-DGP was counted.

Protein Extraction and Immunoblotting

The tissues were homogenized and lysed for 30 min in RIPA buffer containing 0.1% SDS with a protease and phosphatase inhibitor cocktail, followed by sonication and centrifugation. To avoid fat contamination, a $26G_{1/2}$ syringe was used to collect the supernatant. The protein concentration of the supernatant was determined using a bicinchoninic acid (BCA) kit. For immunoblotting, proteins in the supernatant were denatured by heating, separated by SDS-PAGE, and then transferred onto a nitrocellulose membrane. The membrane was incubated in a 5% non-fat milk blocking buffer (TBS-Tween 20) for 1h, followed by incubation with a primary antibody in TBS-Tween 20 containing 5% BSA for overnight at $4^{o}C$. After 3 washes with TBS-Tween 20, the membrane was incubated with a goat-anti-rabbit or goat-anti-mouse IgG conjugated horse radish-peroxidase secondary antibody in a 5% non-fat milk TBS-Tween 20 for 1h, washed three times with TBS-Tween 20, and developed with Enhanced Chemiluminescence Detection Reagents. The protein signals were imaged using a Bio-Rad ChemiDoc System.

Quantitative Real-Time Polymerase Chain Reaction (qPCR)

Total RNAs were isolated using TRIzol® Reagents. RNAs were reverse transcribed into cDNA using TaqMan® Reverse Transcription Reagents (Applied Biosystems) and tissue mRNA levels were determined by qPCR using Stratagene Mx3005p PCR machine (Agilent Technologies). Reactions were done in duplicate for each biological sample using SYBR® Green Real-Time PCR Master Mix (Invitrogen). The relative mRNA expression level for each gene was

calculated by the $2^{(-DDCt)}$ method and normalized to GAPDH or 18s rRNA, which was arbitrarily set to 1. Primer sequences are listed in table 1.

Statistical Analysis

Data are expressed as Mean ± SEM, and were tested for statistical significance by Two-way ANOVA with Bonferroni *post hoc* tests when both genotypes and treatments were considered, or by Student *t*-tests when the two genotypes were compared. The *p* value less than 0.05 was considered statistically significant. Data were analyzed using Grad Pad software and SAS version 9.2 (SAS Institute, Inc.).

Objective 1.

Manuscript was submitted on Jan 26, 2017 to Cell Metabolism. Revision was invited on Feb 23, 2017. In Process.

Brown Adipocyte Lipid Droplet Lipolysis Is Not Essential for Cold-Induced Thermogenesis in Mice

Hyunsu Shin[1,2], Yinyan Ma[1,3], Tanya Chanturiya[3], Youlin Wang[1,2], Anil K.G. Kadegowda[1], Rachel Jackson[1], Dominic Rumore[1], Bingzhong Xue[4], Hang Shi[4], Oksana Gavrilova[3], Liqing Yu[1,2,*]

[1]Department of Animal and Avian Sciences, University of Maryland, College Park, MD 20742; [2]Center for Molecular and Translational Medicine, Institute for Biomedical Sciences, Georgia State University, Georgia, Atlanta, GA 30303; [3]The National Institute of Diabetes and Digestive and Kidney Diseases, National Institutes of Health, Bethesda, MD 20892; [4]Department of Biology, Center for Obesity Reversal, Georgia State University, Atlanta, GA 30303

***To whom correspondence should be addressed:**

Liqing Yu, M.D., Ph.D.

Email: Lyu68@gsu.edu

In Brief

Shin et al. show that mice lacking BAT CGI-58, an ATGL coactivator critically implicated in cytosolic lipid droplet lipolysis, are not cold sensitive due to increased combustion of circulating thermogenic fuels and WAT browning. WAT lipolysis is essential to fuel thermogenesis during fasting.

Highlights

- BAT lipolysis is not essential for cold-induced thermogenesis regardless of food availability
- Mice with defective lipolysis in both BAT and WAT are not cold sensitive when food is present
- WAT lipolysis is essential to defend body temperature during fasting
- Lipolysis deficiency in BAT induces WAT browning

Summary

Brown adipose tissue (BAT) lipid droplet (LD) lipolysis was believed to play a central role in non-shivering thermogenesis, but this concept has not been tested *in vivo*. Here we show that mice lacking BAT Comparative Gene Identification-58 (CGI-58), a coactivator of Adipose Triglyceride Lipase (ATGL), are not cold sensitive. When CGI-58 is inactivated in both BAT and white adipose tissue (WAT), mice become cold sensitive only in the fasted, but not fed state. BAT-specific knockout (BAT-KO) mice versus controls display higher body temperature when food is present during cold exposure, which is associated with increases in BAT glucose uptake, WAT browning, total energy expenditure, and adipose sympathetic innervation. Thus, BAT LD lipolysis is not essential for cold-induced thermogenesis *in vivo*. Our data uncover a key role of BAT lipolysis in regulating compensatory cold adaptation mechanisms and suggest a critical role of WAT lipolysis in provision of thermogenic fuels during fasting.

Introduction

Adipose tissues can be broadly divided into two types, brown adipose tissue (BAT) and white adipose tissue (WAT). While rodents and human infants have visible classical BAT depots, it was once thought adult humans lack BAT. Recent re-discovery of BAT-like tissues in adult humans through the use of positron emission tomography (PET)-scanning technology has revitalized interest in basic and clinical research of BAT biology (Cypess et al., 2009; van Marken Lichtenbelt et al., 2009; Virtanen et al., 2009). A major function of BAT is to defend against cold in a nonshivering manner by generating heat from free fatty acids (FFAs), glucose and perhaps other chemicals (Cannon and Nedergaard, 2004; Kazak et al., 2015; Ozaki et al., 2011; Shabalina et al., 2013). Uncoupling protein 1 (UCP1) plays a key role in this adaptive thermogenesis by uncoupling mitochondrial oxidation of substrates from ATP synthesis (Cannon and Nedergaard, 2004).

Recently a distinct population of adipocytes that exist in WAT contain multiple lipid droplets (LDs) and express UCP1 were named brown-like (beige) or brown-in-white (brite) adipocytes (Petrovic et al., 2010; Wu et al., 2012). Although origins of beige adipocytes are under debate, they are functionally thermogenic (Shabalina et al., 2013). The process of beige adipocyte recruitment to WAT is called WAT browning, which is often induced by cold exposure or stimulation with a sympathetic agonist (Nedergaard and Cannon, 2014; Rosen and Spiegelman, 2014). Rodents clearly have “classical” brown adipocytes and beige/brite adipocytes. Humans may possess both brown and beige adipocytes

(Jespersen et al., 2013), or largely beige adipocytes (Sidossis and Kajimura, 2015). Besides their endocrine functions, brown/beige and white adipocytes mainly function to dissipate and store energy, respectively, in response to environmental and nutritional fluctuations.

BAT activity is mainly controlled by the sympathetic nervous system (SNS) (Cannon and Nedergaard, 2004). Stimulation of SNS releases norepinephrine (NE) to increase intracellular cyclic AMP (cAMP) by activating adenylyl cyclase in the adrenergic signaling pathway. In mature brown adipocytes, NE-induced formation of cAMP seems to be fully mediated via β3-adrenergic receptor (Zhao et al., 1994). Thus, a selective β3-adrenoreceptor agonist CL-316,243 is often used to mimic cold exposure to activate BAT activity. Increases in cellular cAMP activate protein kinase A (PKA) that phosphorylates a transcriptional factor cAMP-response-element binding protein (CREB) (Thonberg et al., 2002), resulting in transcriptional activation of thermogenic genes including UCP1 (Kozak et al., 1994). Activation of PKA promotes intracellular lipolysis (Honnor et al., 1985) that supposedly provides FFAs for brown adipocytes to produce heat. It was assumed that cytosolic LD lipolysis is central to understanding the control of nonshivering thermogenesis (Cannon and Nedergaard, 2004), but this assumption has not been directly tested *in vivo* due to lack of appropriate animal models.

To address this long outstanding question, we created BAT-specific Comparative Gene Identification-58 (CGI-58) knockout (BAT-KO) mice. CGI-58, also known as Abhd5 (the fifth member of α/β-hydrolase fold protein family), is a

LD-associated protein that is critically implicated in cytosolic LD lipolysis through interacting with LD coat proteins (Liu et al., 2004; Subramanian et al., 2004; Yamaguchi et al., 2004) and serving as a coactivator of Adipose Triglyceride Lipase (ATGL) (Lass et al., 2006). Like ATGL, CGI-58 is ubiquitously expressed with the highest expression in adipose tissues (Lass et al., 2006; Subramanian et al., 2004). In this study, we found that BAT-KO mice are not cold sensitive even in the fasted state. They display unaltered expression of UCP1 mRNA/protein and increased expression of fatty acid and glucose transporters in the interscapular BAT (iBAT) as well as increased subcutaneous WAT browning. We also found that mice lacking CGI-58 in all adipose tissues (FAT-KO mice) are cold sensitive only in the fasted, but not fed state, which is different from a previous study that concluded that intracellular lipolysis is essential for cold-induced thermogenesis and brown phenotypes (Ahmadian et al., 2011). Comparison of cold tolerance between mice lacking CGI-58 in BAT only and those lacking CGI-58 in all adipose tissues reveals an important role of WAT lipolysis in cold adaptation during fasting. Thus, our studies establish a new paradigm that LD lipolysis in brown adipocytes is not required for sustaining whole-body thermogenesis, but rather plays a critical role in regulating compensatory thermogenic mechanisms during cold adaptation.

Results

BAT-Specific Deletion of CGI-58 Induces BAT Steatotic Hypertrophy and Hyperplasia

To identify the role of brown adipocyte LD lipolysis in thermogenesis and metabolic health, we generated BAT-KO mice by crossing CGI-58-floxed mice (Guo et al., 2013) with Ucp1-cre transgenic mice (Kong et al., 2014) as described in Methods. As reported by others using the same Cre mouse line (Kong et al., 2014), BAT-specific deletion was achieved (Figure S1A). BAT-KO versus control mice on chow or HFD gained weight similarly and had similar energy intake (Figure 1A and 1B). They appeared grossly normal except a visible hump on the upper back, which was caused by enlarged iBAT that appeared like WAT (Figure 1C). The white fat appearance was attributable to large cytosolic LD accumulation resulting in a ~2-fold increase in average adipocyte size (steatotic hypertrophy) (Figure 1D and 1E). In addition, the total amount of DNA in CGI-58-deficient iBAT relative to controls was increased by 2.1 folds (Figure 1F), though the DNA amount per mg BAT was decreased by 56% (Figure S1B). Similar changes were observed for BAT proteins (Figure 1G and S1C). These changes are consistent with the increased total cell number (hyperplasia) in CGI-58-deficient iBAT. Steatotic hypertrophy and hyperplasia of CGI-58-deficient iBAT together resulted in a 4.3-fold increase of its weight on average (Figure 1H). Increased BAT did not cause changes in body composition in BAT-KO mice (Figure S1D), which may largely attribute to significant decreases in weights of other fat depots, including iWAT, eWAT and mesenteric WAT (mWAT), though not peri-renal WAT (pWAT) (Figure 1H). As expected, the TG content was increased by 2.4 folds in CGI-58-deficient iBAT (Figure 1I). It has been well established that CGI-58 deficiency causes cytosolic TG-rich LD accumulation by

inhibiting intracellular lipolysis (Brown et al., 2007; Lass et al., 2006). Consistently CGI-58-deficient iBAT had significantly reduced lipase activity (Figure 1J). The lipase activity left in CGI-58-deficient BAT may reflect that from hormone-sensitive lipase (HSL), which is capable of hydrolyzing TG *in vitro* to some extent (Sztalryd et al., 1995), and that from cell types other than brown adipocytes, which constitutes about 50% of BAT (Rosenwald et al., 2013). Nonetheless, BAT CGI-58 deficiency suffices to cause cytosolic LD accumulation demonstrating its crucial role in cytosolic LD dynamics. Interestingly, the TG content was decreased in iWAT and mWAT (Figure 1I) suggesting a compositional change of these white fat depots in BAT-KO mice. Decreased WAT mass and TG content may contribute to reduced capacity of these animals to release FFA and glycerol following lipolytic stimulation by isoproterenol (Figure 1K), but fold increases in FFA and glycerol release after isoproterenol injection were similar between the two genotypes (Figure 1K), suggesting that WAT's responsiveness to lipolytic stimulation is reserved in BAT-KO mice.

A major function of BAT is to dissipate energy as heat. To determine if CGI-58 deletion in thermogenic BAT influences whole-body energy balance and body temperature, we performed metabolic phenotyping using Indirect Calorimetry and Telemetry. BAT-KO mice showed a moderate, but significant reduction in total energy expenditure at room temperature (22^{o}C), but not thermoneutrality (30^{o}C) (Figure S1E). There were no significant changes in oxygen consumption, respiratory exchange ratio (indicative of metabolic substrate preference), total physical activity, food intake, and core body

temperature between BAT-KO and control mice housed at either room or thermoneutral temperature (Figure S1E). As expected, thermoneutrality reduced total energy expenditure, oxygen consumption and increased respiratory exchange ratio in normal mice. Similar responses were reserved in BAT-KO mice (Figure S1E). These findings demonstrate that BAT lipolysis has limited impact on whole-body energy balance and thermogenesis at room temperature (a mild cold condition) and thermoneutrality.

BAT CGI-58 Deficiency Does Not Cause Cold Intolerance

To determine whether defective LD lipolysis in BAT influences cold-induced thermogenesis, we subjected chow-fed BAT-KO mice to acute cold exposure (4^{o}C) and monitored their intra-rectal temperature changes. We found that BAT-KO mice were not cold sensitive even when food was absent during cold exposure (Figure 2A). Interestingly BAT-KO mice versus controls on chow displayed higher body temperature when food was present during acute cold exposure (Figure 2B). Similar responses were observed in HFD-fed mice when the core body temperature was continuously measured by Telemetry (Figure 2D and 2E). During chronic cold exposure when mice had free access to food and water, the core body temperature was significantly higher in BAT-KO than control mice in the first 2 days (Figure 2F). It stayed higher from Day 3 to Day 7 of cold exposure, though the level did not reach statistical significance (Figure 2F). In addition to their normal or better cold tolerance, BAT-KO mice also showed no changes in total energy expenditure during acute cold exposure regardless of

food availability, or higher total energy expenditure during chronic cold exposure (Figure S2A). The maintenance of body temperature and energy expenditure in cold-exposed BAT-KO mice was not a result of increased physical activity (Figure S2B).

UCP1 Protein Is Not Reduced in CGI-58-Deficient BAT

BAT thermogenesis is mainly governed by UCP1 (Cannon and Nedergaard, 2004). It was reported that iBAT UCP1 expression was reduced in adipose lipolysis-deficient mice (*i.e.*, mice lacking ATGL in all adipose tissues) and this reduction in UCP1 expression was used to explain cold-sensitive phenotypes in these animals (Ahmadian et al., 2011). However, we did not observe a significant reduction of UCP1 protein expression in the iBAT of BAT-KO mice on chow diet (Figure 3A). Considering a ~50% increase of the total proteins in the CGI-58-deficient relative to control iBAT (Figure 1G), the total amount of UCP1 protein was actually increased. To gain additional information about why mice deficient in BAT lipolysis are not cold sensitive, we measured iBAT expression levels of UCP1 and other genes related to thermogenesis in mice treated with the β3 agonist CL-316,243 for 4 days or cold for 7 days. Under the basal condition, *i.e.*, mice housed at room temperature without β3 agonist or cold treatment, iBAT UPC1 mRNA and protein levels did not differ between the two genotypes (Figure 3B-3E). Interestingly, the protein expression of tyrosine hydroxylase (TH), a marker of sympathetic innervation (Foster and Bartness, 2006), was substantially increased in CGI-58-deficient iBAT (Figure 3D)

suggesting augmented sympathetic drive under this condition, which may explain its hyperplasic phenotype (Figure 1F) and reserved UCP1 expression. CGI-58 deficiency also had no effects on iBAT expression of mRNA for peroxisome proliferator-activated receptor (PPAR)-α (Figure 3B), a gene critical in regulation of mitochondrial fatty acid oxidation and functions, and mRNA for PR domain-containing 16 (PRDM16) (Figure 3B), a transcription coregulator that controls brown adipocyte development and adipocyte thermogenic program (Seale et al., 2008; Seale et al., 2011). Interestingly, the mRNAs for PPAR-γ coactivator (PGC)-1α and type II iodothyronine deiodinase (Dio2), two genes relevant to thermogenesis (de Jesus et al., 2001; Wu et al., 2012), were significantly elevated in CGI-58-deficient iBATs (Figure 3B). These results, together with normal cold tolerance of BAT-KO mice, imply that the thermogenic machinery is intact in CGI-58-deficient iBAT. Despite this, UCP1 protein expression in the CGI-58-deficient iBAT did show a blunted response to β3 agonist (Figure 3C) or cold (Figure 3D). However, the total amount of UCP1 protein in the CGI-58-deficient iBAT remained largely unchanged due to a ~50% increase of the total protein content in this iBAT relative to controls (Figure 1G). Overall, our results indicate that BAT CGI-58 deficiency does not reduce its total amount of UCP1 protein.

CGI-58-Deficient BAT Increases Combustion of Blood Substrates for Cold-Induced Thermogenesis

Brown adipocytes may directly use FFA, glucose and other chemicals derived from the blood circulation as thermogenic substrates without firstly storing them in cytosolic LDs, though it was reported that utilization of TG stored in cytosolic LDs of brown adipocytes plays a predominant role in acute cold-induced thermogenesis (Ma and Foster, 1986; Ouellet et al., 2012). In the fed state, diet is obviously a major source of energetic substrates present in the blood. BAT-KO mice had increased calorie intake during cold exposure (Figure 4A), which may be a compensatory mechanism when LD lipolysis is inhibited in brown adipocytes. The respiratory exchange ratio (RER) was significantly higher in BAT-KO mice during the first 5 days of cold exposure (Figure 4B), indicating increased combustion of carbohydrates during this period. To provide direct evidence in support of increased carbohydrate utilization for cold-induced thermogenesis in BAT-KO mice, we examined glucose-initiated thermogenesis during acute cold exposure. After a bolus of glucose, blood glucose levels remained remarkably lower and the intra-rectal temperature was significantly higher in BAT-KO mice than controls (Figure 4C and 4D). These observations are consistent with increased glucose uptake by iBAT as an organ during acute cold exposure (Figure 4E) as well as augmented expression of iBAT mRNA for glucose transporter 1 (Glut1) (Figure 4F). The mRNA for glucose transporter 4 (Glut4), which is responsible for insulin-stimulated glucose uptake, was decreased in the CGI-58-deficient iBAT (Figure 4F). The insulin-stimulated glucose uptake per mg wet tissue was not significantly altered in adipose and muscle tissues (Figure S3), except CGI-58-deficient iBAT whose total glucose

uptake should be considered elevated because of its increased wet weight (Figure 1H).

Compared to glucose, FFAs are energy-rich molecules and normally the major fuels for thermogenesis (Cannon and Nedergaard, 2004). CD36, lipoprotein lipase (LPL) and fatty acid transporter 1 (FATP1) play important roles in iBAT uptake and transport of FFAs (Bartelt et al., 2011; Wu et al., 2006). We observed that iBAT levels of mRNAs for CD36 and LPL, tbut not FATP1, were significantly increased in BAT-KO mice (Figure 4G). The iBAT expression level of CD36 protein, a fatty acid transporter critically implicated in cold-induced thermogenesis (Bartelt et al., 2011), was substantially higher in BAT-KO mice than controls during cold exposure or after CL-316,243 treatment (Figure 4H). These findings imply that CGI-58-deficient BAT may have increased FFA uptake from the blood, especially during cold adaptation. Collectively our results suggest that CGI-58-deficient BAT reprograms its metabolism to increase combustion of blood fuels including glucose and perhaps FFAs for thermogenesis.

WAT Lipolysis Is Essential for Thermogenesis During Fasting

When BAT-KO mice can use dietary nutrients to fuel thermogenesis in the fed state, they must use endogenous fuels during fasting. Fasting mobilizes energy stores mainly by inducing hepatic glycogenolysis and WAT lipolysis. It has been shown that mice lacking ATGL globally or in all adipose tissues are cold sensitive (Ahmadian et al., 2011; Haemmerle et al., 2006) suggesting a critical role of adipose lipolysis in cold-induced thermogenesis. Given the normal

cold tolerance of mice lacking CGI-58 selectively in BAT during fasting (Figure 2), we hypothesized that WAT lipolysis is essential to fuel thermogenesis during fasting. To test this hypothesis, we created a mouse line with CGI-58 inactivation in both BAT and WAT (FAT-KO mice) (Figure S4A). FAT-KO mice showed no alterations in weight gain and food intake despite increased fat mass and weights of all adipose depots (Figure 5A-D). Like BAT-KO mice, FAT-KO mice also showed an enlarged white fat-looking iBAT (Figure 5E) and large LD deposition in iBAT adipocytes (Figure 5F) resulting in increased brown adipocyte size (Figure 5G). Their iBAT relative to controls also had higher total amounts of DNAs and proteins, though the DNA and protein contents per mg iBAT were decreased (Figure S4B). As expected, FAT-KO mice were completely resistant to lipolysis stimulation (Figure 5H). The failure of an adrenergic agonist to stimulate lipolysis in FAT-KO mice highlights the essential role of CGI-58 in mediating cytosolic LD lipolysis. Like mice lacking ATGL globally (Haemmerle et al., 2006), FAT-KO mice housed at ambient temperature also developed hypothermia during fasting (Figure 5I). They were cold sensitive when food was removed during cold exposure (Figure 5J). Since mice lacking CGI-58 in BAT only are not cold sensitive during fasting, our results indicate that it is WAT lipolysis that fuels thermogenesis in these animals in the fasted state.

Despite cold intolerance during fasting, FAT-KO mice were able to tolerate cold when food was present (Figure 5J), suggesting that inhibiting adipose lipolysis causes cold intolerance by limiting thermogenic substrates, not by impairing thermogenic machinery (brown phenotypes). Consistently, iBAT UCP1

protein and mRNA levels normalized to GAPDH were not changed in FAT-KO mice fed a HFD (Figure 5K and 5L), a chow diet, or a chow diet coupled with β3 agonist treatment (Figure S4C). Considering the increased total DNA and protein contents in CGI-58-deficient iBAT relative to control iBAT (Figure S4B), the total amounts of UCP1 protein and mRNA were actually elevated in this organ. When the HFD-fed mice were treated with the β3 agonist CL-316,243, we did see a lower UCP1 protein expression level in the CGI-58-deficient iBAT after normalization to the amount of GAPDH protein (Figure S4D). Again, given the increased relative protein content, the total amount of UCP1 protein in CGI-58-deficient iBAT was largely unchanged. Taken together, our results indicate that adipose lipolysis deficiency does not reduce the total amount of UCP1 protein in BAT, which may explain why adipose lipolysis-deficient mice including our FAT-KO mice and adipose tissue-specific ATGL knockout mice (the manuscript submitted to *Cell Metabolism* by Drs. Renate Schreiber and Rudolf Zechner) are not cold sensitive in the fed state.

CGI-58 Deletion in BAT Enhances WAT Browning

Cold-exposed BAT-KO mice exhibit higher body temperature when food is available (Figure 2). This phenomenon seems to suggest a higher setting point of whole-body thermogenesis in BAT-KO mice, which may be achieved through chronic activation of multiple compensatory thermogenic mechanisms. WAT browning is an important cold adaptive mechanism (Nedergaard and Cannon, 2014; Rosen and Spiegelman, 2014). To examine this possibility, we examined

the morphology of iWAT, a fat pad sensitive to browning factors. Indeed, BAT-KO versus control mice housed at room temperature (a moderate cold condition compared to thermoneutrality), exposed to cold, or treated with the β3 agonist CL-316,243 for 4 days all showed augmented browning as evidenced by increased emergence of adipocytes containing multilocular LDs (Figure 6A) and enhanced UCP1 immunohistochemical staining (Figure 6B) in the iWAT. Increased browning of BAT-KO mice was further supported by elevated UCP1 mRNA and protein levels in the iWAT after chronic cold exposure or β3 agonist treatment (Figure 6C and 6D). Under the basal condition (22^{o}C and saline treatment), iWAT UCP1 mRNA expression was also significantly increased in BAT-KO mice when Student-*t*-test not Two-way ANOVA was used for statistical analysis (Figure 6C).

Adipose browning can be induced by increased sympathetic innervation and/or direct actions of humoral and hormonal factors on adipocytes (Cannon and Nedergaard, 2004; Wu et al., 2013). We observed that TH protein expression was substantially increased in the iWAT of BAT-KO mice housed at room temperature or exposed to cold for 7 days (Figure 6E), suggesting that lipolysis deficiency in BAT enhances WAT browning, at least in part, by increasing sympathetic drive.

BAT CGI-58 Deficiency Improves Metabolic Profiles in Mice on HFD

Both brown and beige adipocytes contribute to handling of fatty acids and glucose in humans (Orava et al., 2011; Ouellet et al., 2012). It was recently

demonstrated that BAT plays a critical role in triglyceride clearance from the blood circulation in mice during cold exposure (Bartelt et al., 2011). To examine whether inhibition of LD lipolysis selectively in BAT, a major energy-dissipating organ, has any effects on overnutrition-induced metabolic disorders such as glucose tolerance, insulin resistance and hepatic steatosis, we fed BAT-KO and control mice a HFD. It was found that BAT-KO mice tolerated glucose better (Figure 7A), had reduced fasting HOMA insulin resistance index [(glucose at mg/dL x insulin at μIU/mL)/22.5] (Figure 7B) due to significantly reduced plasma insulin and a trend toward reduction of plasma glucose (Figure 7C). Although no significant changes were observed for serum concentrations of triglycerides (TG), total cholesterol (TC), and FFA (Figure 7D and 7E) between the two genotypes, the serum concentration of leptin was significantly reduced (Figure 7F) likely due to reduced WAT mass (Figure 1H). Adipose tissue energy homeostasis plays an important role in regulating fat deposition in non-adipose tissues such as liver. Overnutrition often induces hepatic steatosis. We found that inhibition of LD lipolysis in BAT reduced liver weight (Figure 7G) and hepatic contents of lipids, including triglycerides and cholesterol in HFD-fed mice (Figure 7H). Our results collectively suggest a healthier metabolic profile in BAT-KO mice relative to their controls.

Discussion

Brown adipocyte LD lipolysis is situated at the crossroad of cold-induced thermogenesis (Cannon and Nedergaard, 2004), but its *in vivo* significance has

not been examined in whole animals. In this study, we demonstrate that CGI-58-dependent LD lipolysis in brown adipocytes is not essential for sustaining BAT UCP1 expression and for cold-induced thermogenesis in mice regardless of food availability. Instead, we show that mice with defective BAT lipolysis (BAT-KO mice) relative to control mice display higher body temperature when food is present during acute and chronic cold exposure. Inhibition of BAT lipolysis reprograms BAT to use more glucose and perhaps FFAs from the blood circulation and markedly enhances WAT browning. Our studies indicate that BAT LD lipolysis is not energetically critical in fueling thermogenesis, but plays a key role in regulating body's multiple thermogenic mechanisms during cold adaptation.

ATGL knockout mice are cold sensitive (Haemmerle et al., 2006), but the reason remains unclear given its severe cardiac phenotype. Mice lacking ATGL in both BAT and WAT are also cold sensitive (Ahmadian et al., 2011). These studies seem to suggest that adipose lipolysis is required for mice to defend against cold. However, Ahmadian et al. did not report cold sensitivity of their mice in the fed state. We found that mice lacking CGI-58 in both BAT and WAT (FAT-KO mice) are cold sensitive only when food is not available. When food is left in the cage during cold exposure, FAT-KO mice are able to defend body temperature. Dr. Rudolf Zechner and associates had similar observations in their mice lacking ATGL in all adipose tissues (a manuscript recently submitted to *Cell Metabolism*). A recent human study using nicotinic acid, a pharmacological inhibitor of intracellular TG hydrolysis, shows that inhibition of intracellular TG

lipolysis in the whole-body abolishes cold-stimulated BAT thermogenesis, which is compensated by increased muscle shivering (Blondin et al., 2017). We did not measure muscle shivering in our mice due to technical challenges, but we acclimated our mice for a week to minimizing shivering prior to housing them at 4oC for 7 days and we did not observe reduced thermogenesis during this chronic cold exposure (Figure 2) implying limited impact of muscle shivering on heat production in our animals. Nonetheless, it may be difficult to compare this short-term human study with studies using genetically altered animals because of its acute and broad nature of lipolysis inhibition. A previous study suggests a role of ATGL-mediated lipolysis of cytosolic LDs in UCP1 activation (Li et al., 2014). Although we did not directly measure UCP1 activation in CGI-58-deficient mature brown adipocytes, Dr. Zechner and associates compared the mitochondrial respiration (oxygen consumption) of tissue slices and mitochondria between ATGL-deficient BAT and control BAT, and did not observe any differences between the two genotypes (Schreiber's manuscript submitted to *Cell Metabolism*). Additionally, both Dr. Zechner's group and ours did not observe a significant reduction of iBAT UCP1 protein expression in lipolysis-deficient mice (*i.e.*, mice lacking ATGL or CGI-58 in all adipose tissues) housed at room temperature. Mice lacking ATGL or CGI-58 in BAT only also did not show reduced iBAT UCP1 expression (Schreiber's manuscript and Figure 3) under the normal housing condition. Although UCP1's responsiveness to cold or □□3 adrenergic stimulation is attenuated in the iBAT of our HFD-fed BAT-KO mice (Figure 3), we estimate that the total UCP1 protein is increased in the CGI-5-

deficient iBAT given that it has increased total amounts of proteins and DNAs (indicative of BAT recruitment). One explanation for attenuated responsiveness of UCP1 to cold or β3 agonist could be that UCP1 expression is already recruited to the highest level possible in the CGI-58-deficient BAT and there is no space for further upregulation. Increased sympathetic innervation to CGI-58-deficient BAT as evidenced by elevated expression of tyrosine hydroxylase (Figure 3D) and/or potentially augmented uptake of circulating FFAs via elevated CD36 protein (Figure 4H) may contribute to maximal induction of UCP1 expression under this condition. Alternatively, the increased recruitment of beige adipocytes in the WAT of BAT-KO mice may reduce the need to upregulate UCP1 expression in the classical BAT during cold exposure. Collectively, the findings from us and Dr. Zechner's group suggest that lipolysis deficiency in adipose tissues does not impair thermogenic machinery in mice. Our comparative studies using BAT-KO and FAT-KO mice instead support a key role of WAT lipolysis in providing thermogenic substrates for cold adaptation during fasting. This conclusion is in total agreement with the finding from adipose ATGL knockout mice by Drs. Schreiber and Zechner (Schreiber's manuscript).

An interesting finding in this study is that BAT-KO mice display profound WAT browning. Mice with BAT paucity (Schulz et al., 2013) or hamsters with iBAT sympathetic denervation (Nguyen et al., 2016) also exhibit WAT browning, but this may be due to a general loss of BAT function or thermogenic stimulation. Here we show that selective inhibition of BAT lipolysis is sufficient to induce WAT browning suggesting a critical role of BAT lipolysis in whole-body

thermoregulation, though it is dispensable for cold-induced thermogenesis. It is currently unclear how this occurs at the molecular level and the origin of beige adipocytes. We observed that the protein level of tyrosine hydroxylase (TH), a marker of sympathetic innervation (Foster and Bartness, 2006), is elevated in both iBAT (Figure 3D) and inguinal fat (Figure 6E) suggesting a role of neural signals. BAT-derived adipokines (Batokines) are also critically implicated in BAT recruitment and WAT browning in response to cold exposure (Kajimura et al., 2015; Wu et al., 2013). Future studies are needed to determine the origin of beige adipocytes in our mice and whether CGI-58-deficient BAT secretes more and specific browning batokines to directly stimulate WAT browning.

Blondin et al. showed that nicotinic acid-induced inhibition of whole-body intracellular TG lipolysis reduced BAT uptake of ^{11}C-acetate and ^{18}F-fluorodeoxyglucose tracers in cold-exposed humans (Blondin et al., 2017), which may not represent a direct effect of BAT lipolysis inhibition on its lipid and glucose uptake because other vital organs such as heart may compete with BAT to take up more of these tracers in the absence of intracellular lipolysis, particularly when WAT lipolysis is also inhibited and there is no enough to increase BAT mass (recruitment). We show in the present study that CGI-58-deficient iBAT takes up more glucose. Although the underlying molecular mechanism remains to be delineated, CGI-58-deficient iBAT expresses increased mRNA for glucose transporter 1 (Glut1). Increased mRNA and protein expression of Glut1 was also observed in CGI-58-deficient muscle, macrophages and cultured cancer cells (Miao et al., 2014; Ou et al., 2014; Xie et al., 2015), and

thus may reflect a cell autonomous metabolic adaptation when energy stores in cytosolic LDs cannot be mobilized for utilization. While increased Glut1 mRNA seems to be inconsistent with unaltered glucose uptake per mg iBAT (wet weight) (Figure 4E), CGI-58-deficient iBAT shows a ~50% reduction in protein content per mg wet weight due to a ~2-fold increase in average cell size and TG content (Figure 1E and 1I). When normalized by iBAT protein content, glucose uptake is increased by ~2 fold in CGI-58-deficient iBAT. Considering iBAT as an organ, CGI-58-deficeint iBAT displays a 3-8-fold increase in wet weight depending on animal age, diet, and feeding duration. The increased wet weight of CGI-58-deficient iBAT can be fully accounted by steatotic hypertrophy and hyperplasia (indicative of BAT recruitment). Recruited BAT, together with recruited beige adipocytes, is expected to increase whole-body's glucose disposal capacity during fasting, which may explain why a bolus of glucose only induces a modest rise in blood glucose in BAT-KO mice under cold (Figure 4C).

CGI-58 deficiency in BAT seems to promote metabolic benefits as evidenced by improvement of glucose tolerance and decreases in plasma insulin, HOMA index, and hepatic steatosis after HFD feeding (Figure 7). It was reported that BAT critically regulates glucose homeostasis, insulin sensitivity and circulating lipids disposal (Bartelt et al., 2011; Stanford et al., 2013). A simple explanation is that more circulating nutrients, such as triglycerides, FFAs and glucose, are channeled to CGI-58-deficient BAT to produce heat, resulting in less nutrients flowing to other tissues including liver. Improved insulin sensitivity may also protect liver from steatosis as insulin-resistant liver shows augmented

lipogenesis (Brown and Goldstein, 2008). It was shown that BAT-derived neuregulin 4 protects liver against fat deposition by suppressing hepatic lipogenesis (Wang et al., 2014). It is possible that CGI-58-deficient BAT releases specific batokines to directly act on target tissues including liver, thereby preventing HFD-induced glucose intolerance and hepatic steatosis.

References

Ahmadian, M., Abbott, M.J., Tang, T., Hudak, C.S., Kim, Y., Bruss, M., Hellerstein, M.K., Lee, H.Y., Samuel, V.T., Shulman, G.I.*, et al.* (2011). Desnutrin/ATGL is regulated by AMPK and is required for a brown adipose phenotype. Cell metabolism *13*, 739-748.

Bartelt, A., Bruns, O.T., Reimer, R., Hohenberg, H., Ittrich, H., Peldschus, K., Kaul, M.G., Tromsdorf, U.I., Weller, H., Waurisch, C.*, et al.* (2011). Brown adipose tissue activity controls triglyceride clearance. Nature medicine *17*, 200-205.

Blondin, D.P., Frisch, F., Phoenix, S., Guerin, B., Turcotte, E.E., Haman, F., Richard, D., and Carpentier, A.C. (2017). Inhibition of Intracellular Triglyceride Lipolysis Suppresses Cold-Induced Brown Adipose Tissue Metabolism and Increases Shivering in Humans. Cell metabolism.

Brown, J.M., Chung, S., Das, A., Shelness, G.S., Rudel, L.L., and Yu, L. (2007). CGI-58 facilitates the mobilization of cytoplasmic triglyceride for lipoprotein secretion in hepatoma cells. Journal of lipid research *48*, 2295-2305.

Brown, M.S., and Goldstein, J.L. (2008). Selective versus total insulin resistance: a pathogenic paradox. Cell metabolism *7*, 95-96.

Cannon, B., and Nedergaard, J. (2004). Brown adipose tissue: function and physiological significance. Physiological reviews *84*, 277-359.

Cypess, A.M., Lehman, S., Williams, G., Tal, I., Rodman, D., Goldfine, A.B., Kuo, F.C., Palmer, E.L., Tseng, Y.H., Doria, A.*, et al.* (2009). Identification and importance of brown adipose tissue in adult humans. The New England journal of medicine *360*, 1509-1517.

de Jesus, L.A., Carvalho, S.D., Ribeiro, M.O., Schneider, M., Kim, S.W., Harney, J.W., Larsen, P.R., and Bianco, A.C. (2001). The type 2 iodothyronine deiodinase is essential for adaptive thermogenesis in brown adipose tissue. The Journal of clinical investigation *108*, 1379-1385.

Eguchi, J., Wang, X., Yu, S., Kershaw, E.E., Chiu, P.C., Dushay, J., Estall, J.L., Klein, U., Maratos-Flier, E., and Rosen, E.D. (2011). Transcriptional control of adipose lipid handling by IRF4. Cell metabolism *13*, 249-259.

Etherton, T., Thompson, E., and Allen, C. (1977). Improved techniques for studies of adipocyte cellularity and metabolism. Journal of lipid research *18*, 552-557.

Foster, M.T., and Bartness, T.J. (2006). Sympathetic but not sensory denervation stimulates white adipocyte proliferation. American journal of physiology Regulatory, integrative and comparative physiology *291*, R1630-1637.

Guo, F., Ma, Y., Kadegowda, A.K., Xie, P., Liu, G., Liu, X., Miao, H., Ou, J., Su, X., Zheng, Z.*, et al.* (2013). Deficiency of liver Comparative Gene Identification-

58 causes steatohepatitis and fibrosis in mice. Journal of lipid research *54*, 2109-2120.

Haemmerle, G., Lass, A., Zimmermann, R., Gorkiewicz, G., Meyer, C., Rozman, J., Heldmaier, G., Maier, R., Theussl, C., Eder, S.*, et al.* (2006). Defective lipolysis and altered energy metabolism in mice lacking adipose triglyceride lipase. Science *312*, 734-737.

Honnor, R.C., Dhillon, G.S., and Londos, C. (1985). cAMP-dependent protein kinase and lipolysis in rat adipocytes. II. Definition of steady-state relationship with lipolytic and antilipolytic modulators. The Journal of biological chemistry *260*, 15130-15138.

Jespersen, N.Z., Larsen, T.J., Peijs, L., Daugaard, S., Homoe, P., Loft, A., de Jong, J., Mathur, N., Cannon, B., Nedergaard, J.*, et al.* (2013). A classical brown adipose tissue mRNA signature partly overlaps with brite in the supraclavicular region of adult humans. Cell metabolism *17*, 798-805.

Kajimura, S., Spiegelman, B.M., and Seale, P. (2015). Brown and Beige Fat: Physiological Roles beyond Heat Generation. Cell metabolism *22*, 546-559.

Kazak, L., Chouchani, E.T., Jedrychowski, M.P., Erickson, B.K., Shinoda, K., Cohen, P., Vetrivelan, R., Lu, G.Z., Laznik-Bogoslavski, D., Hasenfuss, S.C.*, et al.* (2015). A creatine-driven substrate cycle enhances energy expenditure and thermogenesis in beige fat. Cell *163*, 643-655.

Kong, X., Banks, A., Liu, T., Kazak, L., Rao, R.R., Cohen, P., Wang, X., Yu, S., Lo, J.C., Tseng, Y.H.*, et al.* (2014). IRF4 is a key thermogenic transcriptional partner of PGC-1alpha. Cell *158*, 69-83.

Kozak, U.C., Kopecky, J., Teisinger, J., Enerback, S., Boyer, B., and Kozak, L.P. (1994). An upstream enhancer regulating brown-fat-specific expression of the mitochondrial uncoupling protein gene. Molecular and cellular biology *14*, 59-67.

Lass, A., Zimmermann, R., Haemmerle, G., Riederer, M., Schoiswohl, G., Schweiger, M., Kienesberger, P., Strauss, J.G., Gorkiewicz, G., and Zechner, R. (2006). Adipose triglyceride lipase-mediated lipolysis of cellular fat stores is activated by CGI-58 and defective in Chanarin-Dorfman Syndrome. Cell metabolism *3*, 309-319.

Li, Y., Fromme, T., Schweizer, S., Schottl, T., and Klingenspor, M. (2014). Taking control over intracellular fatty acid levels is essential for the analysis of thermogenic function in cultured primary brown and brite/beige adipocytes. EMBO reports *15*, 1069-1076.

Liu, P., Ying, Y., Zhao, Y., Mundy, D.I., Zhu, M., and Anderson, R.G. (2004). Chinese hamster ovary K2 cell lipid droplets appear to be metabolic organelles involved in membrane traffic. The Journal of biological chemistry *279*, 3787-3792.

Ma, S.W., and Foster, D.O. (1986). Uptake of glucose and release of fatty acids and glycerol by rat brown adipose tissue in vivo. Canadian journal of physiology and pharmacology *64*, 609-614.

Miao, H., Ou, J., Ma, Y., Guo, F., Yang, Z., Wiggins, M., Liu, C., Song, W., Han, X., Wang, M.*, et al.* (2014). Macrophage CGI-58 Deficiency Activates ROS-Inflammasome Pathway to Promote Insulin Resistance in Mice. Cell reports *7*, 223-235.

Nedergaard, J., and Cannon, B. (2014). The browning of white adipose tissue: some burning issues. Cell metabolism *20*, 396-407.

Nguyen, N.L., Barr, C.L., Ryu, V., Cao, Q., Xue, B., and Bartness, T.J. (2016). Separate and shared sympathetic outflow to white and brown fat coordinately regulate thermoregulation and beige adipocyte recruitment. American journal of physiology Regulatory, integrative and comparative physiology, ajpregu 00344 02016.

Orava, J., Nuutila, P., Lidell, M.E., Oikonen, V., Noponen, T., Viljanen, T., Scheinin, M., Taittonen, M., Niemi, T., Enerback, S.*, et al.* (2011). Different metabolic responses of human brown adipose tissue to activation by cold and insulin. Cell metabolism *14*, 272-279.

Ou, J., Miao, H., Ma, Y., Guo, F., Deng, J., Wei, X., Zhou, J., Xie, G., Shi, H., Xue, B.*, et al.* (2014). Loss of abhd5 promotes colorectal tumor development and progression by inducing aerobic glycolysis and epithelial-mesenchymal transition. Cell reports *9*, 1798-1811.

Ouellet, V., Labbe, S.M., Blondin, D.P., Phoenix, S., Guerin, B., Haman, F., Turcotte, E.E., Richard, D., and Carpentier, A.C. (2012). Brown adipose tissue oxidative metabolism contributes to energy expenditure during acute cold exposure in humans. The Journal of clinical investigation *122*, 545-552.

Ozaki, K., Sano, T., Tsuji, N., Matsuura, T., and Narama, I. (2011). Carnitine is necessary to maintain the phenotype and function of brown adipose tissue. Laboratory investigation; a journal of technical methods and pathology *91*, 704-710.

Petrovic, N., Walden, T.B., Shabalina, I.G., Timmons, J.A., Cannon, B., and Nedergaard, J. (2010). Chronic peroxisome proliferator-activated receptor gamma (PPARgamma) activation of epididymally derived white adipocyte cultures reveals a population of thermogenically competent, UCP1-containing adipocytes molecularly distinct from classic brown adipocytes. The Journal of biological chemistry *285*, 7153-7164.

Rosen, E.D., and Spiegelman, B.M. (2014). What we talk about when we talk about fat. Cell *156*, 20-44.

Rosenwald, M., Perdikari, A., Rulicke, T., and Wolfrum, C. (2013). Bi-directional interconversion of brite and white adipocytes. Nature cell biology *15*, 659-667.

Schulz, T.J., Huang, P., Huang, T.L., Xue, R., McDougall, L.E., Townsend, K.L., Cypess, A.M., Mishina, Y., Gussoni, E., and Tseng, Y.H. (2013). Brown-fat paucity due to impaired BMP signalling induces compensatory browning of white fat. Nature *495*, 379-383.

Seale, P., Bjork, B., Yang, W., Kajimura, S., Chin, S., Kuang, S., Scime, A., Devarakonda, S., Conroe, H.M., Erdjument-Bromage, H.*, et al.* (2008). PRDM16 controls a brown fat/skeletal muscle switch. Nature *454*, 961-967.

Seale, P., Conroe, H.M., Estall, J., Kajimura, S., Frontini, A., Ishibashi, J., Cohen, P., Cinti, S., and Spiegelman, B.M. (2011). Prdm16 determines the thermogenic program of subcutaneous white adipose tissue in mice. The Journal of clinical investigation *121*, 96-105.

Shabalina, I.G., Petrovic, N., de Jong, J.M., Kalinovich, A.V., Cannon, B., and Nedergaard, J. (2013). UCP1 in brite/beige adipose tissue mitochondria is functionally thermogenic. Cell reports *5*, 1196-1203.

Sidossis, L., and Kajimura, S. (2015). Brown and beige fat in humans: thermogenic adipocytes that control energy and glucose homeostasis. The Journal of clinical investigation *125*, 478-486.

Stanford, K.I., Middelbeek, R.J., Townsend, K.L., An, D., Nygaard, E.B., Hitchcox, K.M., Markan, K.R., Nakano, K., Hirshman, M.F., Tseng, Y.H.*, et al.* (2013). Brown adipose tissue regulates glucose homeostasis and insulin sensitivity. The Journal of clinical investigation *123*, 215-223.

Subramanian, V., Rothenberg, A., Gomez, C., Cohen, A.W., Garcia, A., Bhattacharyya, S., Shapiro, L., Dolios, G., Wang, R., Lisanti, M.P.*, et al.* (2004). Perilipin A mediates the reversible binding of CGI-58 to lipid droplets in 3T3-L1 adipocytes. The Journal of biological chemistry *279*, 42062-42071.

Sztalryd, C., Komaromy, M.C., and Kraemer, F.B. (1995). Overexpression of hormone-sensitive lipase prevents triglyceride accumulation in adipocytes. The Journal of clinical investigation *95*, 2652-2661.

Thonberg, H., Fredriksson, J.M., Nedergaard, J., and Cannon, B. (2002). A novel pathway for adrenergic stimulation of cAMP-response-element-binding protein (CREB) phosphorylation: mediation via alpha1-adrenoceptors and protein kinase C activation. The Biochemical journal *364*, 73-79.

van Marken Lichtenbelt, W.D., Vanhommerig, J.W., Smulders, N.M., Drossaerts, J.M., Kemerink, G.J., Bouvy, N.D., Schrauwen, P., and Teule, G.J. (2009). Cold-

activated brown adipose tissue in healthy men. The New England journal of medicine *360*, 1500-1508.

Virtanen, K.A., Lidell, M.E., Orava, J., Heglind, M., Westergren, R., Niemi, T., Taittonen, M., Laine, J., Savisto, N.J., Enerback, S.*, et al.* (2009). Functional brown adipose tissue in healthy adults. The New England journal of medicine *360*, 1518-1525.

Wang, G.X., Zhao, X.Y., Meng, Z.X., Kern, M., Dietrich, A., Chen, Z., Cozacov, Z., Zhou, D., Okunade, A.L., Su, X.*, et al.* (2014). The brown fat-enriched secreted factor Nrg4 preserves metabolic homeostasis through attenuation of hepatic lipogenesis. Nature medicine *20*, 1436-1443.

Wei, E., Gao, W., and Lehner, R. (2007). Attenuation of adipocyte triacylglycerol hydrolase activity decreases basal fatty acid efflux. The Journal of biological chemistry *282*, 8027-8035.

Wu, J., Bostrom, P., Sparks, L.M., Ye, L., Choi, J.H., Giang, A.H., Khandekar, M., Virtanen, K.A., Nuutila, P., Schaart, G.*, et al.* (2012). Beige adipocytes are a distinct type of thermogenic fat cell in mouse and human. Cell *150*, 366-376.

Wu, J., Cohen, P., and Spiegelman, B.M. (2013). Adaptive thermogenesis in adipocytes: is beige the new brown? Genes & development *27*, 234-250.

Wu, Q., Kazantzis, M., Doege, H., Ortegon, A.M., Tsang, B., Falcon, A., and Stahl, A. (2006). Fatty acid transport protein 1 is required for nonshivering thermogenesis in brown adipose tissue. Diabetes *55*, 3229-3237.

Xie, P., Kadegowda, A.K., Ma, Y., Guo, F., Han, X., Wang, M., Groban, L., Xue, B., Shi, H., Li, H.*, et al.* (2015). Muscle-Specific Deletion of Comparative Gene

Identification-58 (CGI-58) Causes Muscle Steatosis but Improves Insulin Sensitivity in Male Mice. Endocrinology *156*, 1648-1658.

Yamaguchi, T., Omatsu, N., Matsushita, S., and Osumi, T. (2004). CGI-58 interacts with perilipin and is localized to lipid droplets. Possible involvement of CGI-58 mislocalization in Chanarin-Dorfman syndrome. The Journal of biological chemistry *279*, 30490-30497.

Zhao, J., Unelius, L., Bengtsson, T., Cannon, B., and Nedergaard, J. (1994). Coexisting beta-adrenoceptor subtypes: significance for thermogenic process in brown fat cells. The American journal of physiology *267*, C969-979.

EXPERIMENTAL PROCEDURES

Extended experimental procedures were included in the Supplemental Materials.

Animals and Diets

BAT-KO mice were produced by crossing CGI-58-floxed mice (Guo et al., 2013) with UCP1-Cre mice (Kong et al., 2014). FAT-KO mice were generated by crossing CGI-58-floxed mice with Adiponectin-Cre mice (Eguchi et al., 2011). Homozygous CGI-58 floxed mice without Cre transgene were as controls for all experiments. Mice housed at different temperatures were allowed 2-4 days of acclimation to different housing environment and temperatures. Mice were fed *ad libitum* a standard chow diet (LabDiet) or a HFD (D12492, Research Diets Inc.). Diet treatments and weight measurements were started at 6 weeks of age. All animal experiments were performed with male mice and approved by the Institutional Animal Care and Use Committees (IACUC) at the University of Maryland at College Park and at Georgia State University.

Metabolic Phenotyping

Indirect Calorimetry was used to measure energy expenditure, respiratory exchange ratio (RER), and physical activity. The core body temperature was continuously monitored by Telemetry. Rectal temperature was monitored using Thermalert TH-5 device (Physitemp). Food intake was measured in metabolic chambers. Body composition was determined by using by EchoMRI-100H Body Composition Analyzer (EchoMRI LLC.).

Lipase Activity Assays

Tissue lipase activity was assayed as described previously (Wei et al., 2007).

***In vivo* Lipolysis Assays**

The mice were injected intraperitoneally with isoproterenol and plasma concentrations of FFAs and glycerol analyzed using commercial available kits.

Immunohistochemistry, Glucose and Insulin Tolerance Tests, Glucose Uptake Assays, Tissue Lipid Analyses, Immunoblotting

These standard procedures were described in details in the Supplemental Materials.

Analyses of Adipocyte Size

The adipose tissue cell sizing was done in osmium-fixed urea-isolated adipocytes as described previously (Etherton et al., 1977).

Statistical Analysis

Data are expressed as Mean ± SEM, and were tested for statistical significance by Two-way ANOVA with Bonferroni *post hoc* tests when both genotypes and treatments were considered, or by Student *t*-tests when the two genotypes were compared. The *p* value less than 0.05 was considered statistically significant. Data were analyzed using Grad Pad software and SAS version 9.2 (SAS Institute, Inc.). For all Figures, $*p < 0.05$ and $**p < 0.01$ vs. genotype on the same diet; $\#p < 0.05$ vs. treatment of the same genotype.

Author Contributions

H.S. and L.Y. designed the study and wrote the manuscript. H.S. did most of the experiments and data analyses. Y.M., Y.W., A.K.G.K., and R.J. contributed to

experiments and data acquisition. Y.M., T.C., and O.G. performed metabolic cage studies. D.R. helped with the manuscript writing. O.G., B.X. and H.S. helped with the experimental design and data interpretations.

Acknowledgements

This work was supported in part by Award Numbers R01DK085176 (L.Y.), R01DK111052-01 (L.Y.), R01DK107544 (B.X.), and R01HL107500 (B.X.) from the National Institute of Diabetes and Digestive and Kidney Diseases, 15GRNT25710256 (H.S.) from AHA, and ADA 7-13-BS-159 (H.S.).

Legends to Figures

Figure 1. CGI-58 Deletion in BAT Causes iBAT Steatosis, Hypertrophy and Hyperplasia (A) Weight gain of 6-week-old (Week 0) BAT-KO (KO) and control (Con) mice subjected to chow (n = 10/group) or HFD (n = 11/group).

(B) Food intake of mice on the fifth week of chow (n = 6/group) or HFD (n = 11/group).

(C) Gross appearance of iBATs in 24-week-old mice on chow diet.

(D) H&E staining of iBATs from 14-week-old chow-fed mice.

(E) Average brown adipocyte sizes in iBATs of mice on HFD for 18 weeks. For each mouse, 5,000 cells were measured. n = 5/group.

(F, G) Relative DNA and protein amounts of whole iBAT in 14-week-old mice on chow. n = 5/group.

(H) Adipose depot/body weight ratios (%) of mice on HFD for 5 weeks. n =7/group.

(I) TG content in individual adipose depots of mice on HFD for 18 weeks. n = 5-7/group.

(J) Lipase activity of iBATs from 14-week-old chow-fed mice. n = 5/group.

(K) *In vivo* lipolysis capacity of mice on HFD for 4 weeks. n = 5/group.

Figure 2. Mice Lacking CGI-58 in UCP1-Positive Cells Are Not Cold Sensitive

(A) Rectal temperatures of 20-week-old HFD-fed BAT-KO (KO) and control (Con) mice at 22oC. n = 4-5/group.

(B, C) Rectal temperatures of 10-11-week-old chow-fed mice exposed 4oC in the absence or presence of diet. n = 5/group.

(D) Core body temperatures of 28-week-old HFD-fed mice exposed to 4oC in the absence of food. n = 5-6/group.

(E) Core body temperatures of 24-week-old HFD-fed mice exposed to 4oC in the presence of food. n = 5-6/group. (F) Core body temperatures of 18-week-old HFD-fed mice during 7 days of cold exposure. n = 6/group.

Figure 3. UCP1 Expression Is Not Reduced in CGI-58-Deficient iBAT

(A) Western blots and densitometry of iBAT UCP1 protein in 14-week-old chow-fed mice.

(B) Relative iBAT expression levels of thermogenesis-related genes from the mice injected with CL-316,243 for 4 days (CL) or vehicle (Saline). n = 5/group.

(C) Western blots and densitometry of iBAT UCP1 in the same mice described under 3B.

(D) Western blots and densitometry analyses of iBAT UCP1 and TH proteins in 18-week-old HFD-fed mice at 22^{o}C (Basal) or 4oC for 7 days (Cold).

(E) iBAT mRNA levels in the mice described under 3D. n = 4-5/group.

Figure 4. BAT-KO Mice Show Increased Capacity to Use Circulating Substrates for Heat Generation

(A and B) Average daily calorie intake (A) and respiratory exchange ratio (RER) (B) of 18-week-old HFD-fed BAT-KO (KO) and control (Con) mice during 7 days of cold exposure. n = 5-6/group.

(C and D) Blood glucose levels (C) and body temperature (D) changes of 12-week-old HFD-fed mice after a bolus of glucose injection (*i.p.*, at 1.5 g/kg body weight). The mice were fasted for 7h (4h at room temperature and 3h at cold) prior to glucose injection. n = 4-5/group.

(E) Tissue glucose uptake in 20-week-old HFD-fed mice during acute cold exposure. The total glucose uptake of iBAT was calculated based on the total iBAT weight. n = 4-5/group.

(F) iBAT mRNAs for glucose transporter 1 (Glut1) and glucose transporter 4 (Glut4) in mice at 22^{o}C (Basal) or 4^{o}C for 7 days (Cold). n = 5/group.

(G) iBAT mRNAs for CD36, lipoprotein lipase (LPL), fatty acid transporter protein 1 (FATP1) in 14-week-old HFD-fed mice at 22^{o}C. n = 5/group.

(G) Immunoblots and densitometry analyses of iBAT CD36 protein in mice exposed to cold for 7 days or injected daily with CL-316,243 for 4 days.

Figure 5. Lipolysis-Deficient FAT-KO Mice Are Not Cold Sensitive When Food Is Available

(A) Weight gain of FAT-KO and Control mice on chow (n = 9-12) or HFD (n = 10-13. Mice were 6 weeks old at Week 0.

(B) Calorie intake on the fifth week of chow (n = 5-6/group) or HFD (n = 5-6/group) treatment.

(C) Body composition of 12-week-old HFD-fed mice. n = 6/group.

(D) Adipose depot/body weight ratios in 24-week-old HFD-fed mice. n = 7/group.

(E) Gross appearance of iBATs from 24-week-old HFD-fed mice.

(F) H&E staining of iBATs from 14-week-old HFD-fed mice.

(G) Adipocyte size of iBATs from 24-week-old HFD-fed mice. For each sample, 5,000 cells were measured. n = 5/group.

(H) *In vivo* lipolysis capacity of 10-week-old HFD-fed mice.

(I) Core body temperatures of 26-week-old HFD-fed mice during cold exposure in the absence of food. n = 5-6/group.

(J) Core body temperatures of 23-week-old HFD-fed mice during cold exposure in the presence of food. n = 5-6/group.

(K) Western blots and densitometry of iBAT UCP1 protein in 22-week-old HFD-fed mice.

(L) iBAT UCP1 mRNA levels in 22-week-old HFD-fed mice. n = 4/group.

Figure 6. CGI-58 Deletion in BAT Enhances WAT Browning

(A) H&E staining of iWATs from 14-week-old chow-fed BAT-KO (KO) and control (Con) mice (top), 18-week-old HFD-fed mice (middle), and 18-week-old HFD-fed mice exposed to cold for 7 days (bottom).

(B) Immunohistochemical staining of iWAT UCP1 protein in 18-week-old HFD-fed mice or 18-week-old HFD-fed mice exposed to cold for 7 days.

(C, D) iWAT UCP1 mRNA (C) and protein (D) levels in 18-week-old HFD-fed mice at 22oC (B) or 4oC for 7 days (C) (n = 4-5/group), or 14-week-old HFD-fed mice injected with CL-316,243 for 4 days (CL) or saline (S) (n = 5/group).

(E) Western blots and densitometry of iWAT tyrosine hydroxylase (TH) in 18-week-old HFD-fed mice exposed to cold for 7 days.

Figure 7. CGI-58 Deletion in BAT Improves Metabolic Profiles in Mice on HFD

(A) Glucose tolerance test (GTT) and insulin tolerance test (ITT) in BAT-KO (KO) and control (Con) mice on HFD. n = 9-11/group.

(B) HOMA-insulin resistance (IR) index in overnight-fasted 17-week-old HFD-fed mice. n = 6/group.

(C) Plasma concentrations of insulin and glucose in 17-week-old HFD-fed mice fasted overnight. n = 6/group.

(D and E) Serum concentrations of triglycerides (TG) and total cholesterol (TC) in the fed or overnight-fasted

Figure 1

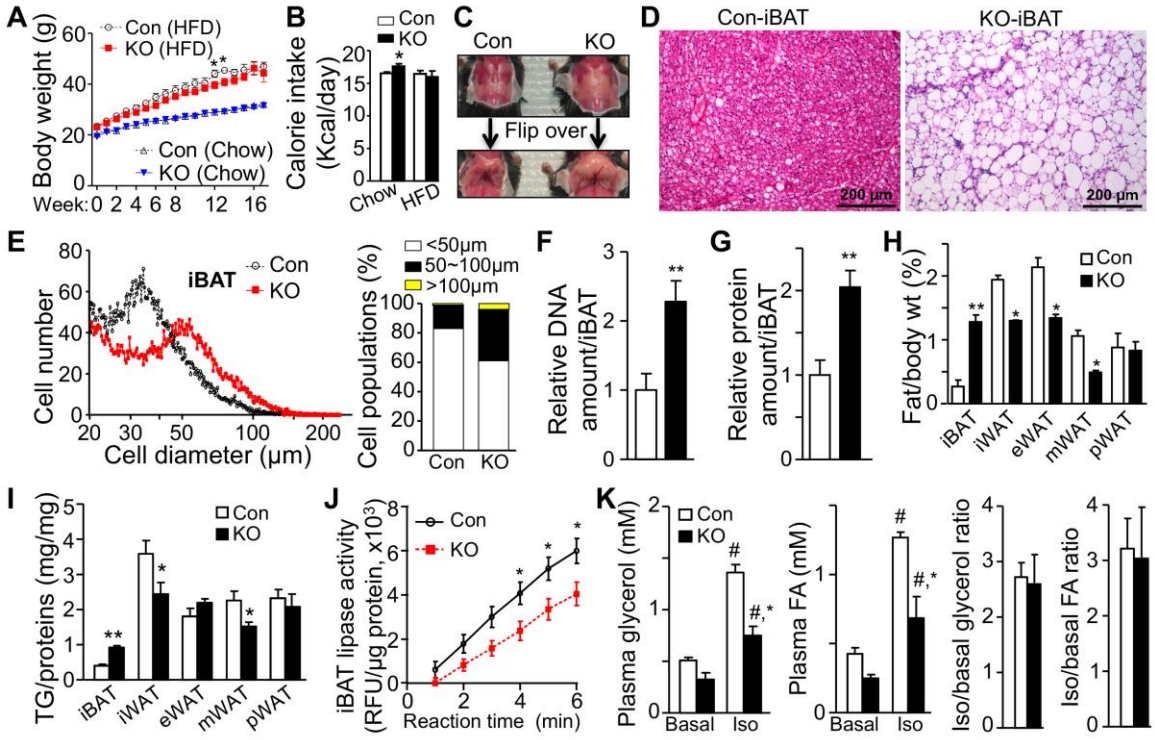
A
Body weight (g)
Con (HFD)
KO (HFD)
Con (Chow)
KO (Chow)
Week: 0 2 4 6 8 12 16
B
Calorie intake (Kcal/day)
Con
KO
Chow
HFD
C
Con
KO
Flip over
D
Con-iBAT
KO-iBAT
200 μm
E
Cell number
iBAT
Con
KO
Cell diameter (μm)
Cell populations (%)
<50μm
50~100μm
>100μm
F
Relative DNA amount/iBAT
G
Relative protein amount/iBAT
H
Fat/body wt (%)
iBAT
iWAT
eWAT
mWAT
pWAT
I
TG/proteins (mg/mg)
J
iBAT lipase activity (RFU/μg protein, x10³)
Reaction time (min)
K
Plasma glycerol (mM)
Basal
Iso
Plasma FA (mM)
Iso/basal glycerol ratio
Iso/basal FA ratio

Figure 2

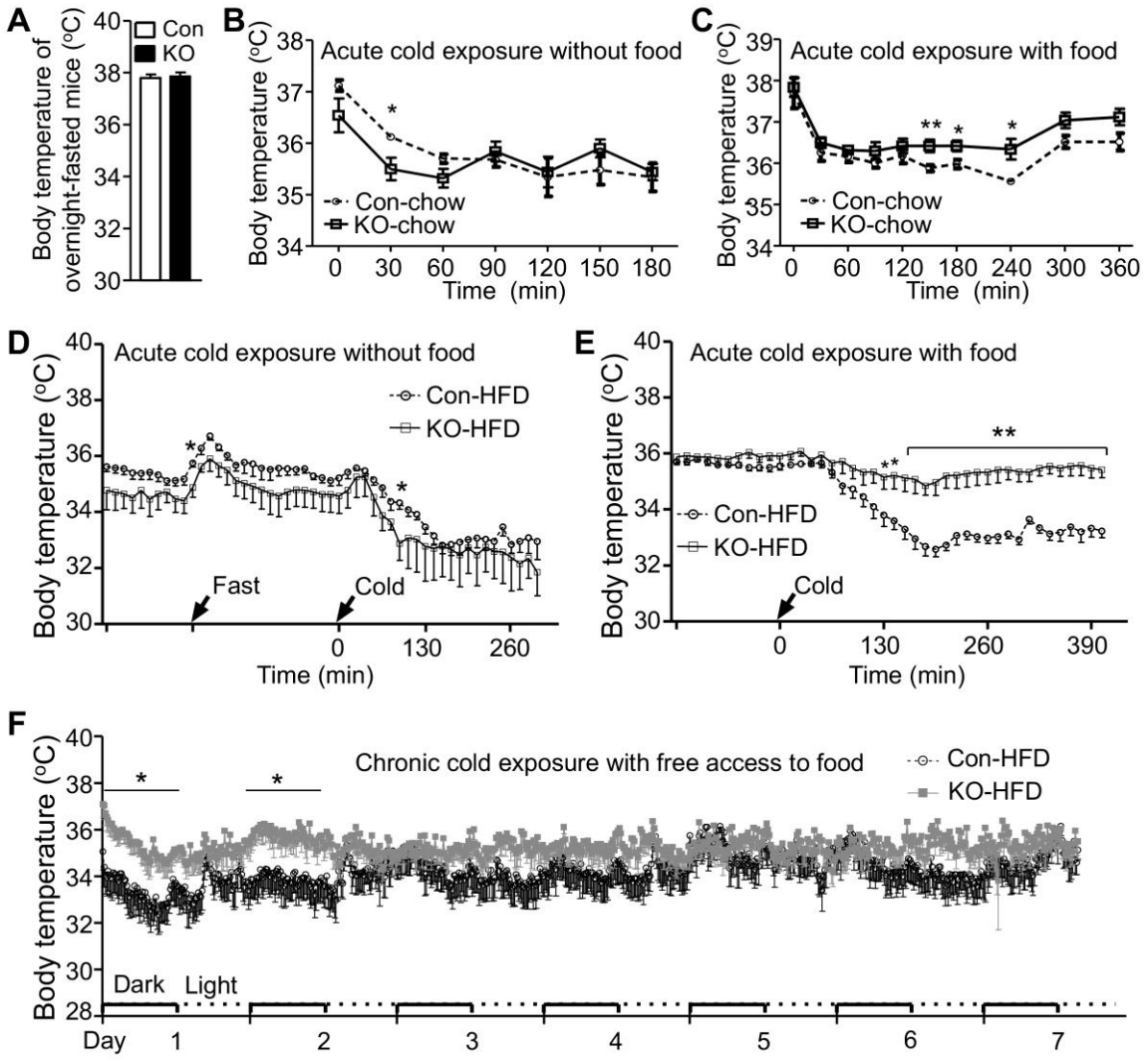
A
Body temperature of overnight-fasted mice (°C)
Con
KO
B
Acute cold exposure without food
Body temperature (°C)
Con-chow
KO-chow
Time (min)
C
Acute cold exposure with food
Body temperature (°C)
Con-chow
KO-chow
Time (min)
D
Acute cold exposure without food
Body temperature (°C)
Con-HFD
KO-HFD
Fast
Cold
Time (min)
E
Acute cold exposure with food
Body temperature (°C)
Con-HFD
KO-HFD
Cold
Time (min)
F
Chronic cold exposure with free access to food
Body temperature (°C)
Con-HFD
KO-HFD
Dark
Light
Day

Figure 3

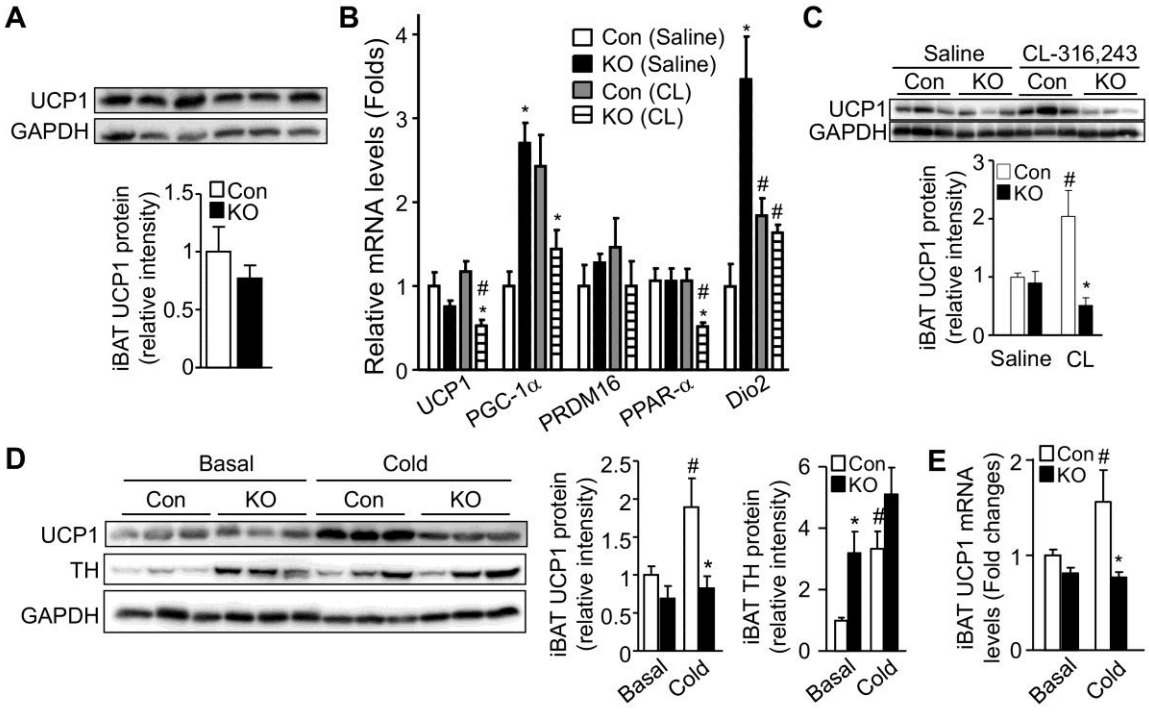
A
UCP1
GAPDH
iBAT UCP1 protein (relative intensity)
Con
KO
B
Relative mRNA levels (Folds)
Con (Saline)
KO (Saline)
Con (CL)
KO (CL)
UCP1
PGC-1α
PRDM16
PPAR-α
Dio2
C
Saline
CL-316,243
Con
KO
UCP1
GAPDH
iBAT UCP1 protein (relative intensity)
Saline
CL
D
Basal
Cold
Con
KO
UCP1
TH
GAPDH
iBAT UCP1 protein (relative intensity)
iBAT TH protein (relative intensity)
E
iBAT UCP1 mRNA levels (Fold changes)

Figure 4

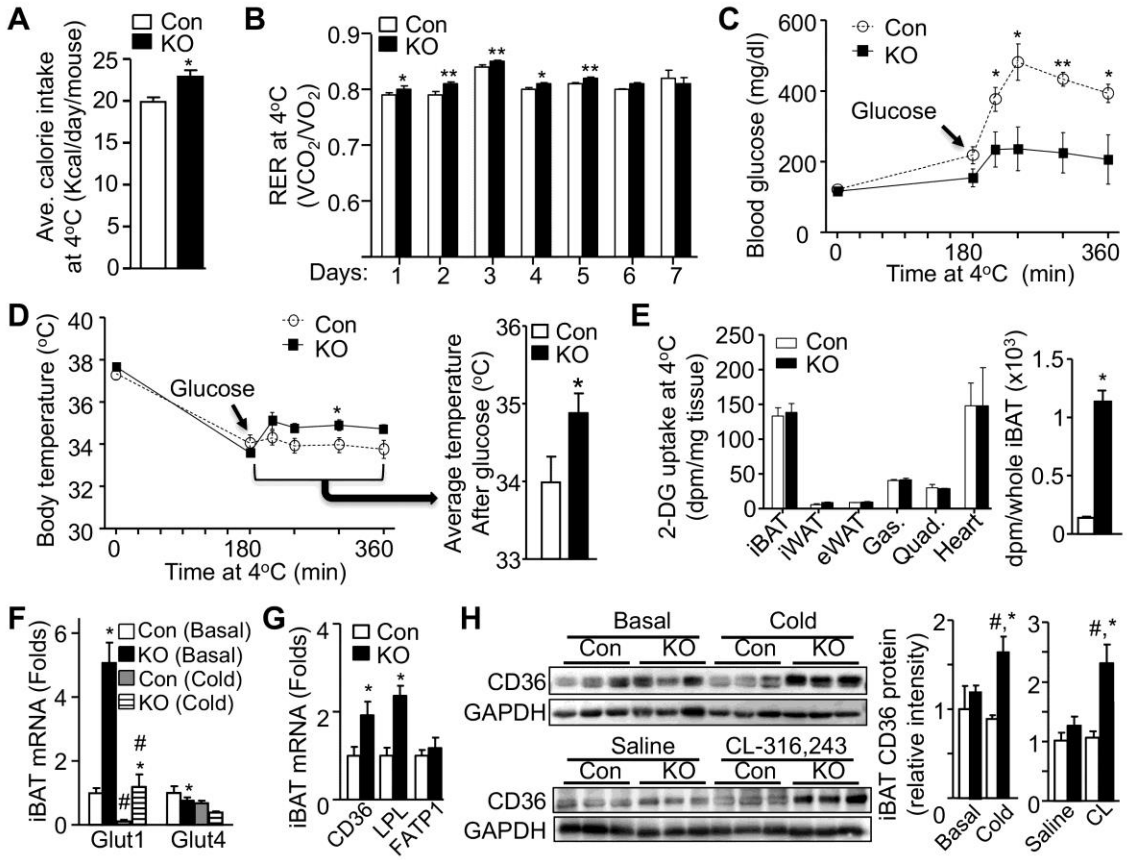
A
Ave. calorie intake at 4°C (Kcal/day/mouse)
Con
KO
B
RER at 4°C (VCO_2/VO_2)
Days: 1 2 3 4 5 6 7
C
Blood glucose (mg/dl)
Glucose
Time at 4°C (min)
D
Body temperature (°C)
Glucose
Time at 4°C (min)
Average temperature After glucose (°C)
E
2-DG uptake at 4°C (dpm/mg tissue)
iBAT
iWAT
eWAT
Gas.
Quad.
Heart
dpm/whole iBAT (x10³)
F
iBAT mRNA (Folds)
Con (Basal)
KO (Basal)
Con (Cold)
KO (Cold)
Glut1
Glut4
G
iBAT mRNA (Folds)
CD36
LPL
FATP1
H
Basal
Cold
Saline
CL-316,243
CD36
GAPDH
iBAT CD36 protein (relative intensity)
Basal
Cold
Saline
CL

Figure 5

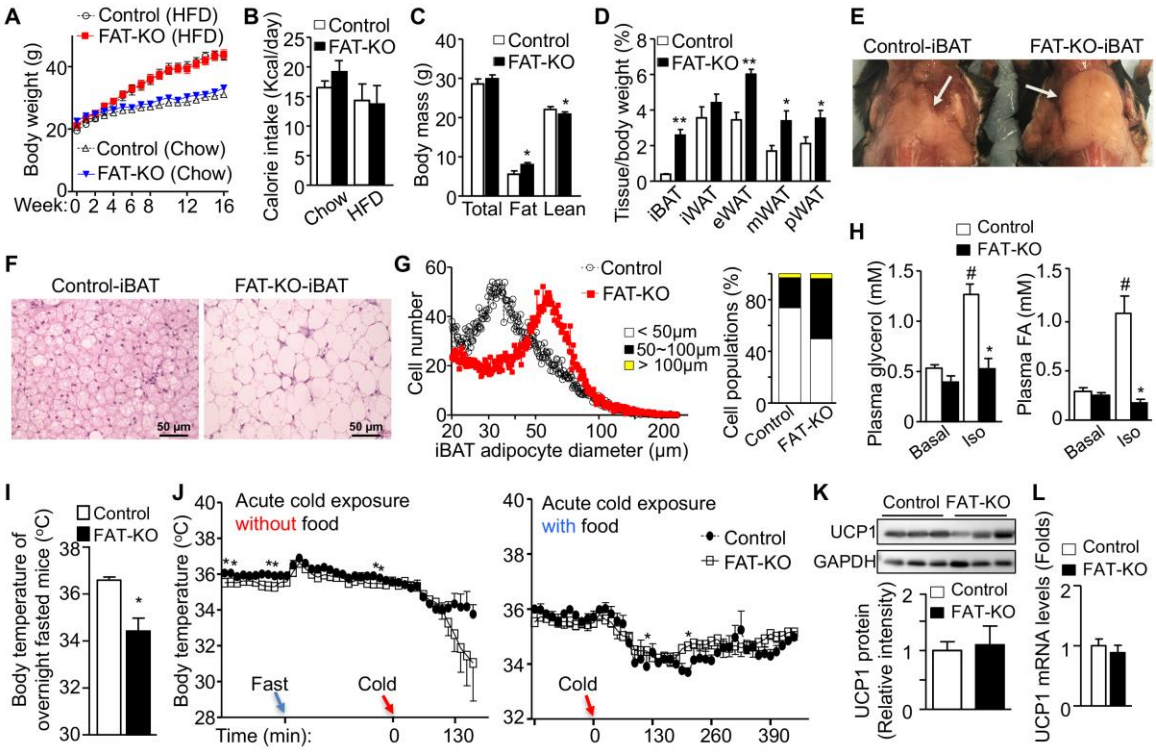
A
Control (HFD)
FAT-KO (HFD)
Control (Chow)
FAT-KO (Chow)
Body weight (g)
Week: 0 2 4 6 8 12 16
B
Control
FAT-KO
Calorie intake (Kcal/day)
Chow
HFD
C
Control
FAT-KO
Body mass (g)
Total Fat Lean
D
Control
FAT-KO
Tissue/body weight (%)
iBAT iWAT eWAT mWAT pWAT
E
Control-iBAT
FAT-KO-iBAT
F
Control-iBAT
FAT-KO-iBAT
50 μm
G
Control
FAT-KO
< 50μm
50~100μm
> 100μm
Cell number
iBAT adipocyte diameter (μm)
Cell populations (%)
H
Control
FAT-KO
Plasma glycerol (mM)
Plasma FA (mM)
Basal Iso
I
Control
FAT-KO
Body temperature of overnight fasted mice (°C)
J
Acute cold exposure without food
Acute cold exposure with food
Body temperature (°C)
Fast
Cold
Time (min):
Control
FAT-KO
K
Control FAT-KO
UCP1
GAPDH
UCP1 protein (Relative intensity)
L
Control
FAT-KO
UCP1 mRNA levels (Folds)

Figure 6

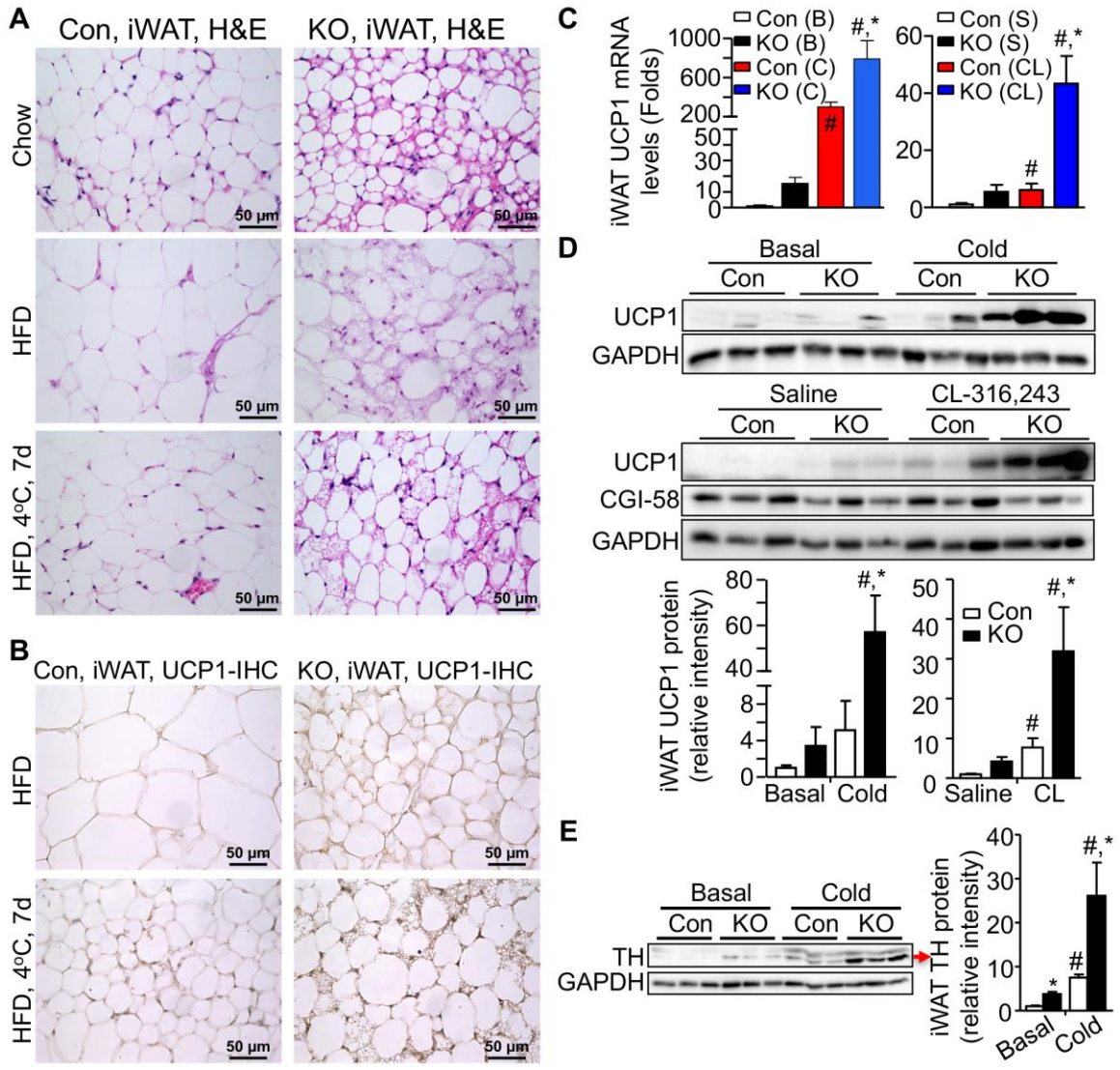
A
Con, iWAT, H&E
KO, iWAT, H&E
Chow
HFD
HFD, 4°C, 7d
50 μm
B
Con, iWAT, UCP1-IHC
KO, iWAT, UCP1-IHC
HFD
HFD, 4°C, 7d
C
iWAT UCP1 mRNA levels (Folds)
Con (B)
KO (B)
Con (C)
KO (C)
Con (S)
KO (S)
Con (CL)
KO (CL)
D
Basal
Cold
Saline
CL-316,243
Con
KO
UCP1
GAPDH
CGI-58
iWAT UCP1 protein (relative intensity)
Basal
Cold
Saline
CL
E
TH
GAPDH
iWAT TH protein (relative intensity)

Figure 7

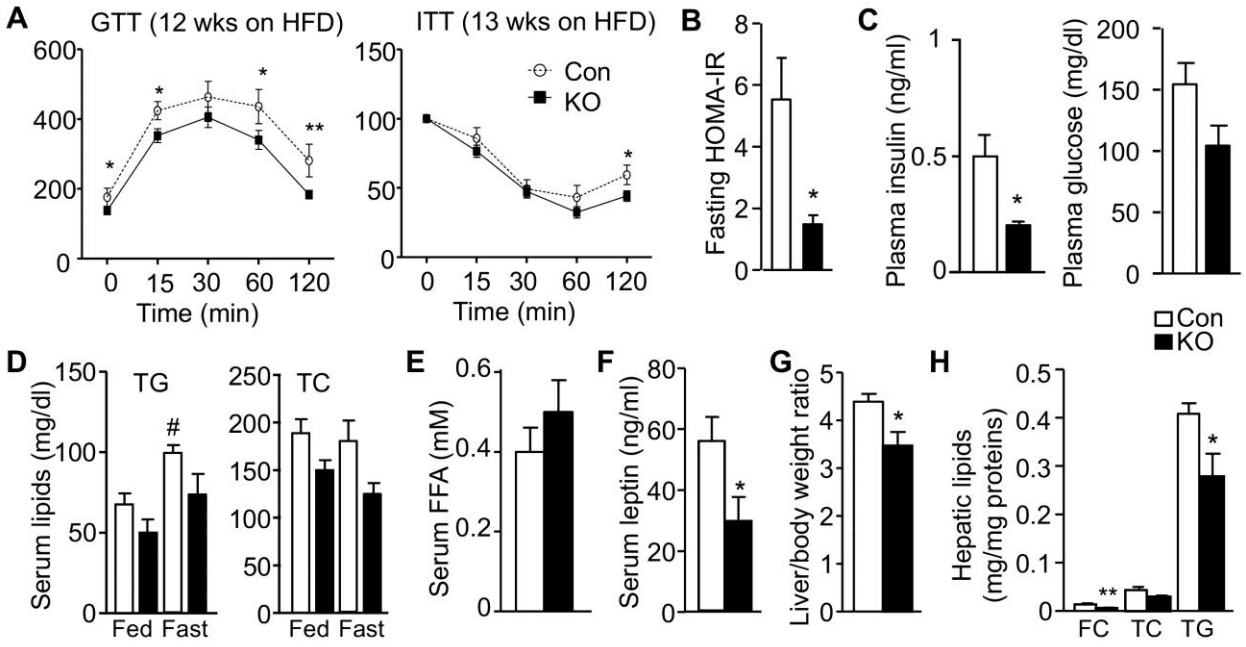
A
GTT (12 wks on HFD)
ITT (13 wks on HFD)
Con
KO
Time (min)
B
Fasting HOMA-IR
C
Plasma insulin (ng/ml)
Plasma glucose (mg/dl)
D
TG
TC
Serum lipids (mg/dl)
Fed Fast
E
Serum FFA (mM)
F
Serum leptin (ng/ml)
G
Liver/body weight ratio
H
Hepatic lipids (mg/mg proteins)
FC TC TG

Supplemental Figures and Figure Legends

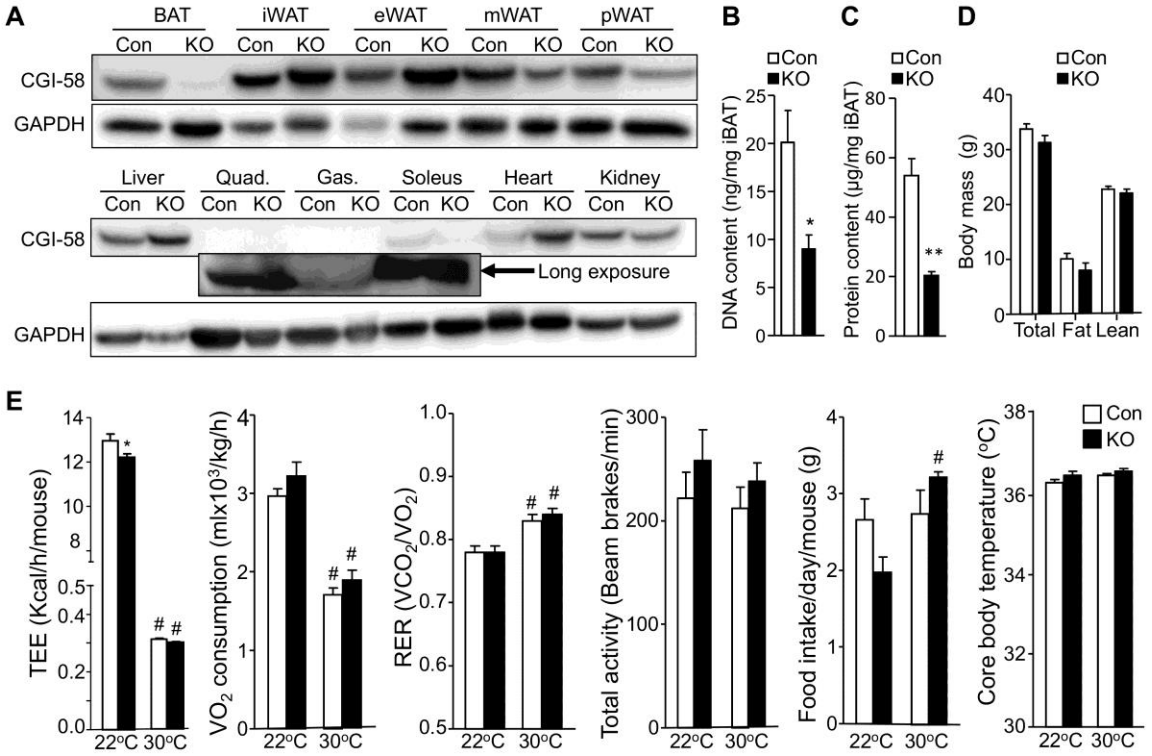

Figure S1. Effects of BAT CGI-58 Deficiency on iBAT DNA and Protein Contents, Body Composition and Metabolic Phenotypes (linked to Figure 1)

(A) Immunoblots of CGI-58 in adipose depots and other tissues of 24-week-old HFD-fed BAT-KO (KO) and control (Con) mice. GAPDH was used as a loading control. Quad., quadriceps; Gas., gastrocnemius.

(B, C) DNA and protein contents of the iBAT from 14-week-old mice on chow. n = 5/group.

(D) Fat and lean body mass of mice on HFD for 9 weeks. n = 6/group.

(E) Metabolic phenotypes of 23-week-old HFD-fed BAT-KO (KO) and control (Con) mice housed at room temperature (22°C) or thermoneutrality (30°C). n = 6/group. *$p < 0.05$ vs. genotype; #$p < 0.05$ vs. temperature treatment of the same genotype.

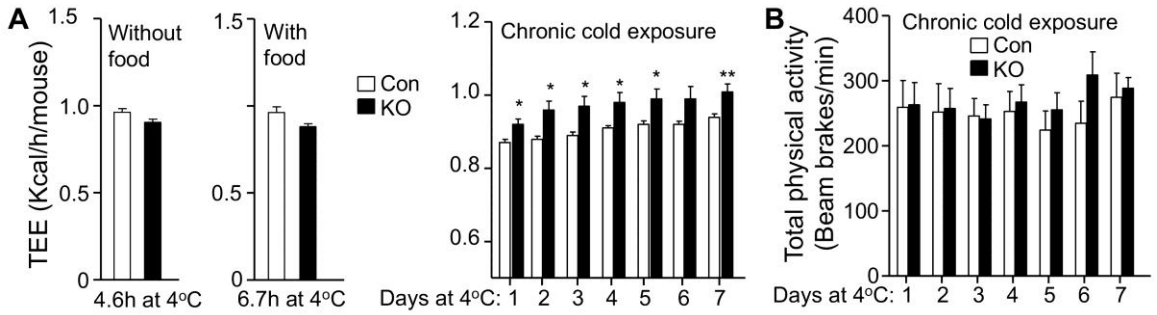

Figure S2. Mice Lacking CGI-58 in UCP1-Positive Cells Display Increased Energy Expenditure During Chronic Cold Exposure (linked to Figure 2)

(A) Total energy expenditure (TEE) of 28-week-old HFD-fed BAT-KO (KO) and control (Con) mice during acute cold without food, of 24-week-old HFD-fed mice during acute cold with food, and of 18-week-old HFD-fed mice during 7 days of cold exposure. n = 5-6/group.

(B) Total physical activity of 18-week-old HFD-fed mice during 7 days of cold exposure. n = 5-6/group.

*p < 0.05 and **p <0.01 vs. genotype.

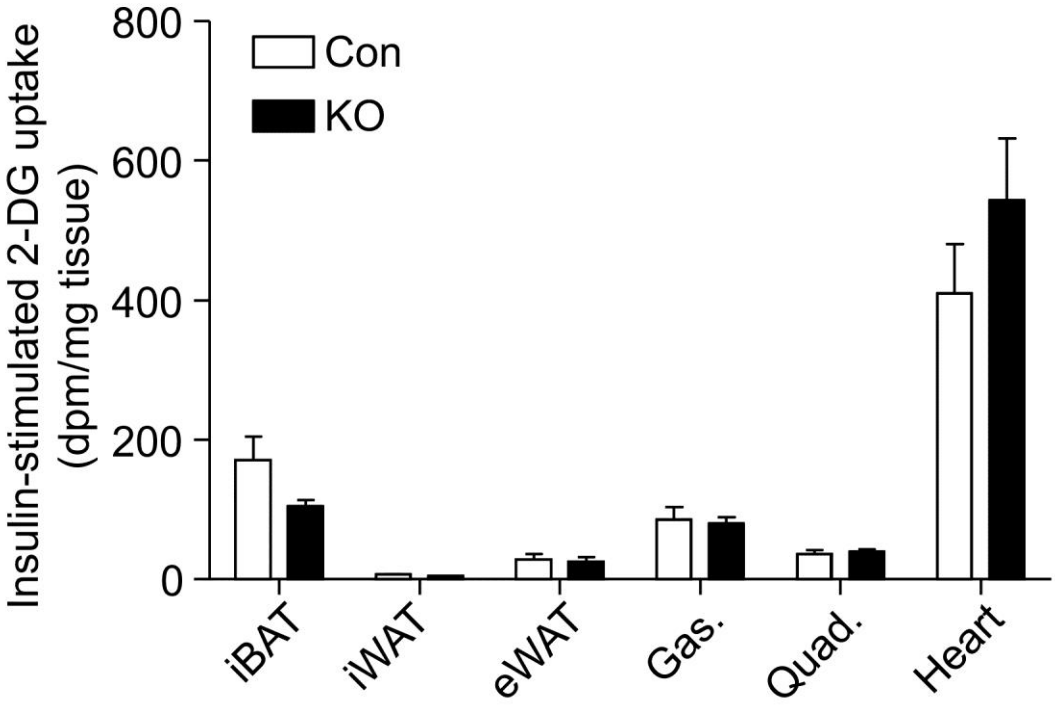

Figure S3 (linked to Figure 4). Insulin-stimulated glucose uptake in the adipose and muscle tissues of 29-week-old HFD-fed BAT-KO (KO) and control (Con) mice. n = 5-6/group.

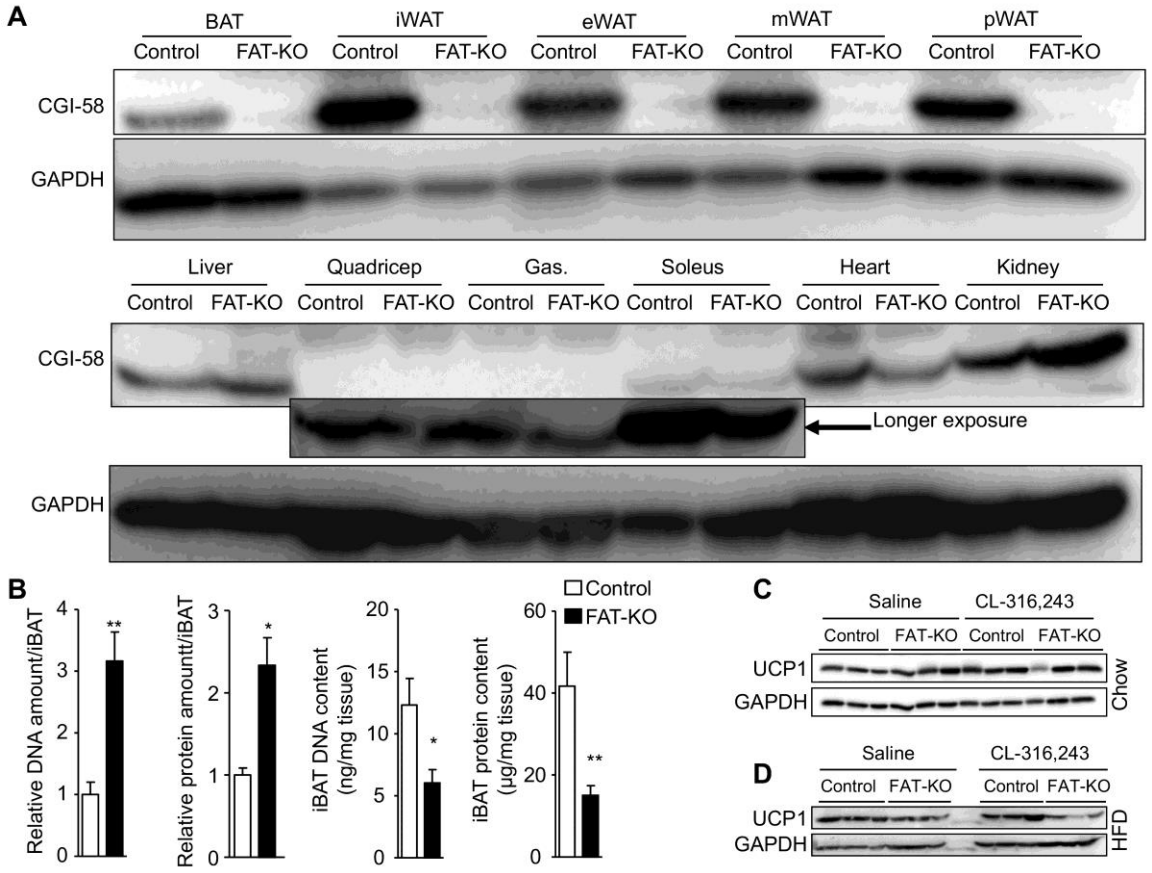

Figure S4. Adipose-Specific Deletion of CGI-58 in FAT-KO Mice (linked to Figure 5)

(A) Immunoblots of CGI-58 protein in tissues from FAT-KO and control mice. GAPDH was used as a loading control. Gas., gastrocnemius.

(B) DNA and protein amounts and contents of the iBATs from 14-week-old mice on chow. n = 5/group.

(C) Immunoblots of UCP1 protein in the iBATs of 14-week-old chow-fed mice.

(D) Immunoblots of UCP1 protein in the iBATs of 14-week-old HFD-fed mice.

Objective 2.

Rationale

In Objective 1, we mainly focused on the role of BAT lipolysis in cold-induced thermogenesis. In contrast to our working hypothesis, BAT-KO mice showed normal to higher body temperature during cold exposure. The lipolysis-deficient BAT as an organ had normal UCP1 expression, increased sympathetic innervation, and elevated glucose uptake and CD36 expression. In addition, selective ablation of CGI-58 in BAT increased the sympathetic innervation in iWAT resulting in increased recruitment of beige adipoctyes. Therefore, we concluded in Objective 1 that BAT lipolysis is not required for whole-body thermoregulation, but has a critical role in activation of compensatory thermogenic mechanisms such as BAT uptake of thermogenic substrates and WAT browning. In Objective 2, our goal was to identify the role of WAT lipolysis in cold-induced thermogenesis and metabolic health. Given that there are no genetic manipulations specific for WAT, we employed an indirect approach to achieve our goal. We characterized mice lacking CGI-58 in both BAT and WAT (FAT-KO mice). We reasoned that comparison of phenotypes from FAT-KO mice with those from the mice lacking CGI-58 in BAT only (BAT-KO mice) would reveal some effects specific for WAT lipolysis.

Fat-Specific CGI-58 Deletion Abolishes Adipose Lipolysis

We have shown under Objective 1 that FAT-KO mice have increased fat mass and adipose depot weights (Figure 1C and 1D of Objective 1). Morphological

examinations of iWAT by H&E staining showed that white adipoctyes in the iWAT of FAT-KO mice were enlarged (Figure 6A). The average diameter of iWAT white adipoctyes in FAT-KO mice was increased, and the population of enlarged adipocytes was also increased (Figure 6B), which likely resulted from inhibition of CGI-58-mediated lipolysis (see Objective 1). Consistently, *ex vivo* lipolysis assays showed that iWAT explants had an impaired response to a β-adrenergic agonist in glycerol release (Figure 6C).

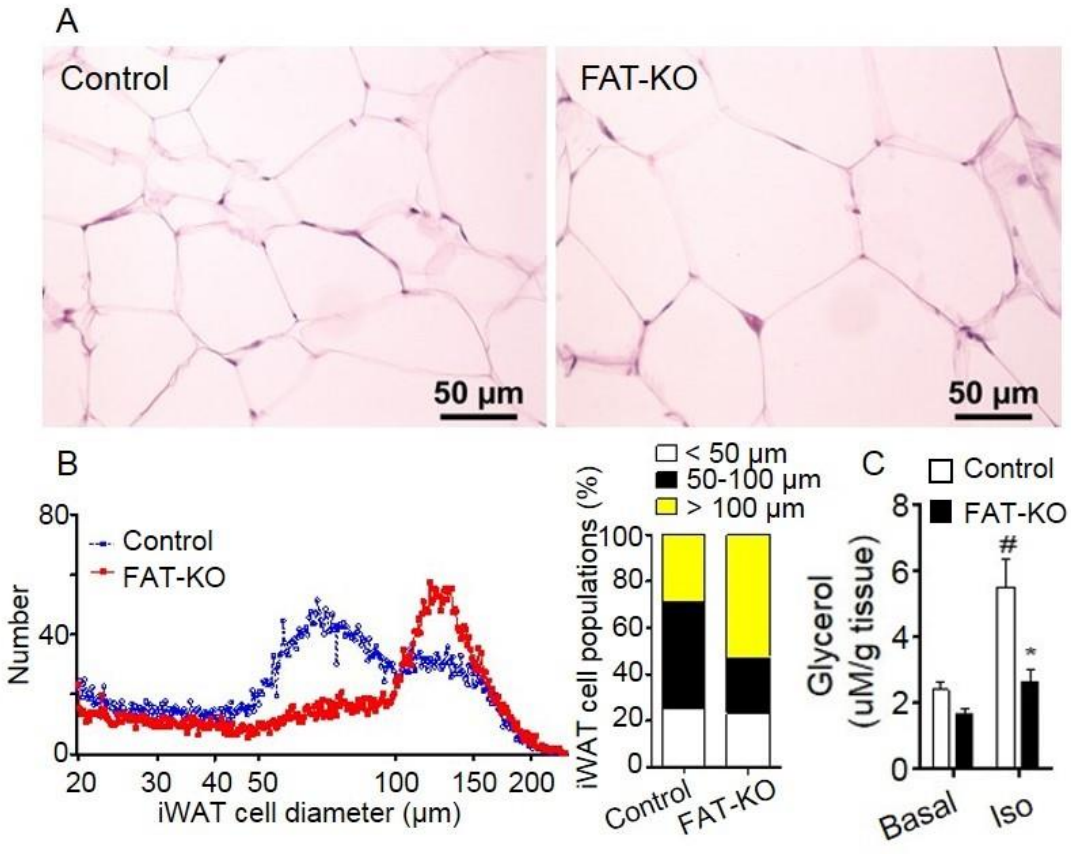

Figure 6. Inactivation of CGI-58 in Adipose Tissues Causes WAT Hypertrophy and Abolishment of Lipolysis Stimulated by an Adrenergic Receptor Agonist.

(A) H&E staining of the iWAT from 18-week-old HFD-fed control and FAT-KO mice.

(B) Average white adipocyte sizes in iWAT of mice on HFD for 18 weeks. For each mouse, 5,000 cells were measured (left panel) and categorized into different size group (right panel).

(C) *Ex vivo* lipolysis of iWAT from 14-week-old chow-fed mice. Glycerol release into tissue culture media was measured after a 2h incubation at 37^{o}C in the

absence (Basal) or presence of isoproterenol (Iso). n = 5 per group. *$p < 0.05$ vs. genotype; #$p < 0.05$ vs. treatment.

Fat-Specific Deletion of CGI-58 Down-regualtes Whole-Body Thermogenic Capacity

In Objective 1, we have shown that FAT-KO mice on HFD are cold sensitive only when food is not available during cold exposure (Figure 5J in Objective 1). Similar results were obtained when the rectal temperature was measured during acute cold exposure in mice on chow or HFD (Figure 7).

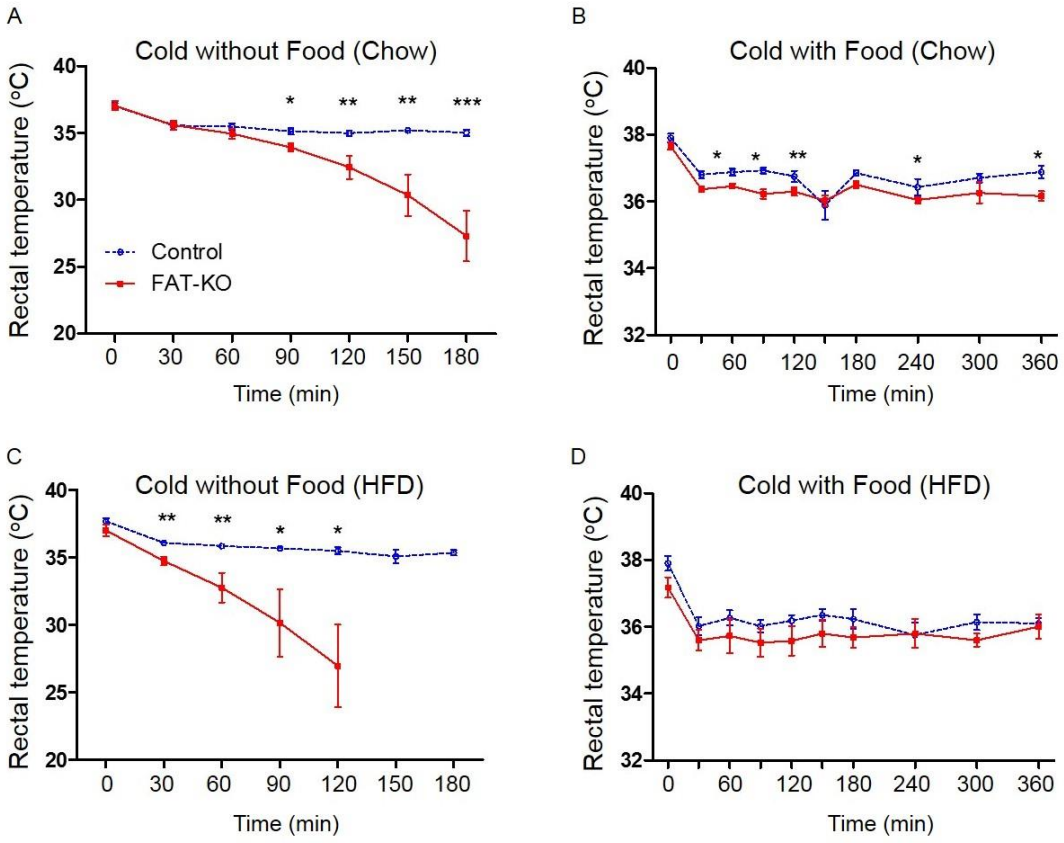

Figure 7. FAT-KO Mice on Chow or HFD Are Not Cold Sensitive When Food Is Available During Cold Exposure.

(A,B) Cold-induced rectal temperature changes of 10-week-old chow-fed mice in the absence of food (A), or 11-week-old chow-fed mice in the presence of food (B). n = 4-6.

(C) Cold-induced rectal temperature changes of 11-week-old HFD-fed mice in the absence of food (C), or 12-week-old HFD-fed mice in the presence of food. n = 4-6.

*p < 0.05, **p < 0.01 vs. genotype.

To determine if CGI-58 deletion in whole-body fat affects whole-body energy balance and body temperature under different environmental conditions, we performed metabolic phenotyping using Indirect Calorimetry and Telemetry (Figure 8). FAT-KO mice displayed no significant changes in TEE, core body temperature, RER, food intake, and total activity when housed at either room or thermoneutral temperature, though their oxygen consumption waslower at room temperature (Figure 8A-F). To measure the capacity of NST, we administered thermoneutrally housed mice with CL-316,243 at 0.1 kg/body weight (Figure 8G-H). FAT-KO mice showed blunted responses to the β-adrenergic agonist stimulation in heat production (Figure 8G), oxygen consumption (Figure 8H), and RER reduction (Figure 8I).

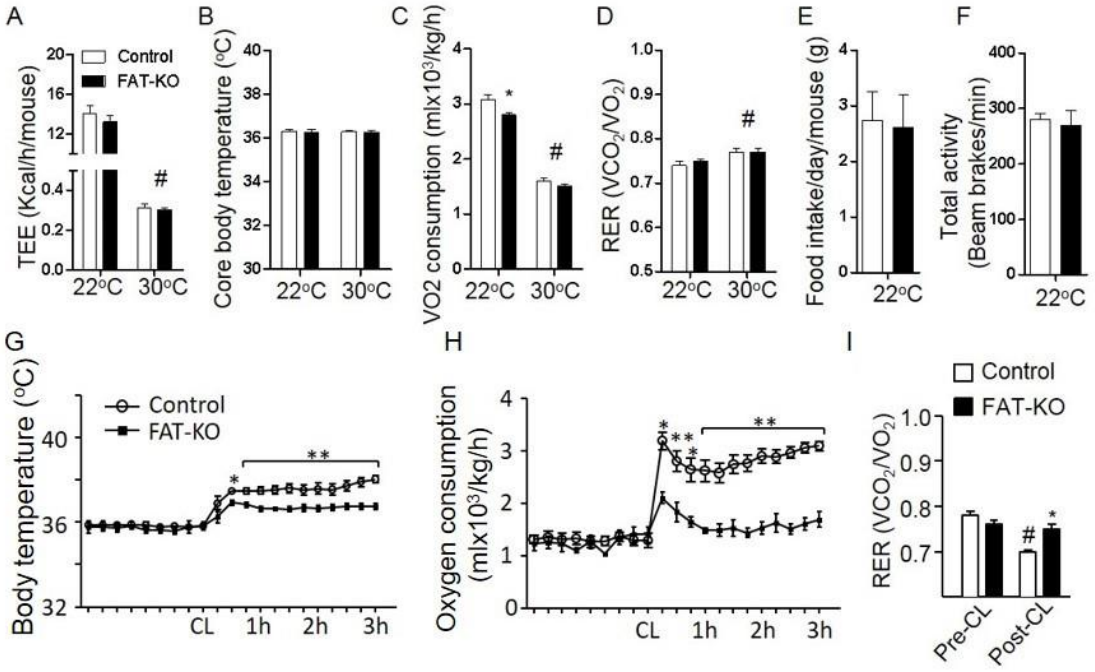

Figure 8. Mice Lacking Adipose Lipolysis Are Resistant to β-Adrenergic Agonist-Induced Increases in Body Temperature and Oxygen Consumption.

(A-F) Metabolic phenotypes of 22-week-old HFD-fed FAT-KO and control mice housed at room temperature (22 ^{o}C) or thermoneutrality (30 ^{o}C).

(G-I) Core body temperature changes (G), oxygen consumption (H), and Respiratory Exchange Ratio (RER) (I) in 22-week-old HFD-fed FAT-KO and control mice before and after CL-316,243 injections at thermoneutrality (30 ^{o}C). n = 5-6/group.

*p < 0.05, **p<0.01 vs. genotype; #p < 0.05 vs. temperature treatment.

To determine how FAT-KO mice respond to cold in energy metabolism, we performed metabolic phenotyping during cold exposure. It was found that FAT-KO mice relative to controls displayed higher RER during cold exposure and this higher RER level stayed longer when food was present than absent (Figure 9A and 9B). Cold-exposed FAT-KO mice showed reduced TEE only in the absence of food and no changes in physical activities (Figure 9C and 9D).

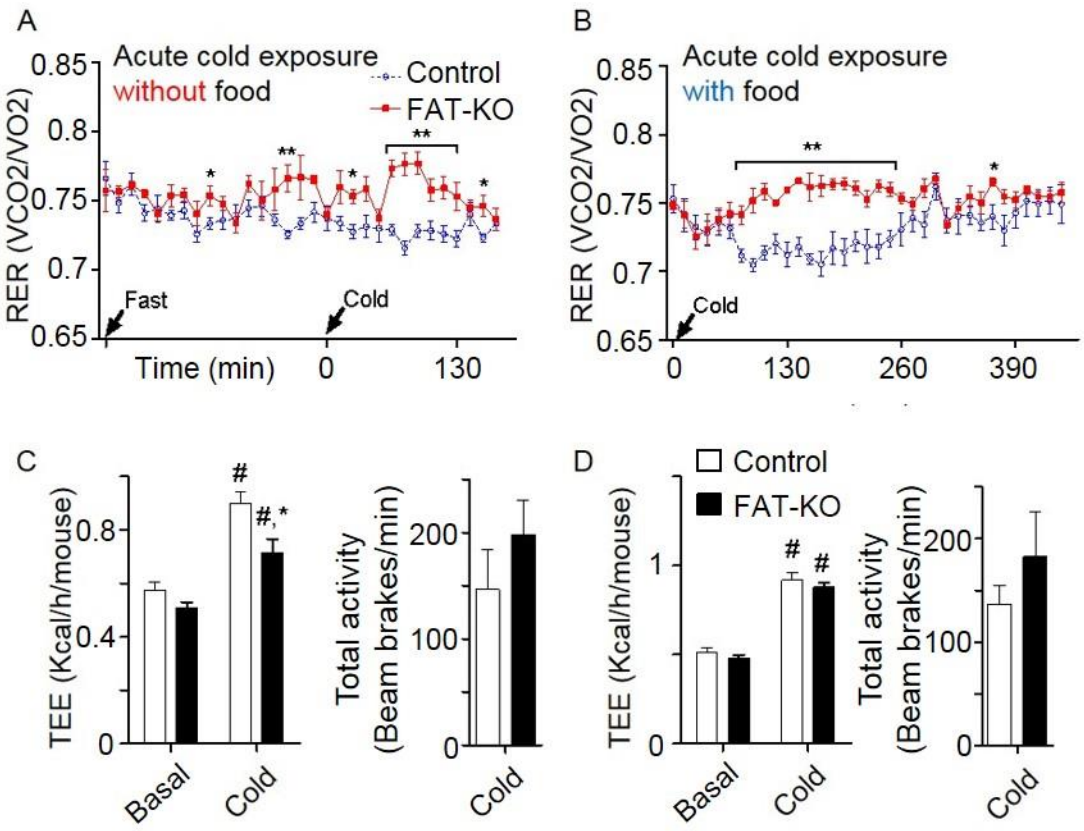

Figure 9. FAT-KO Mice Display Increased Glucose Utilization During Cold Exposure and Reduced Energy Expenditure Only When Food Was Absent During Cold Exposure.

(A) Cold-induced changes of RER in 26-week-old HFD-fed mice in the absence of food.

(B) Cold-induced RER changes in 23-week-old HFD-fed mice in the presence of food.

(C) Total energy expenditure and total activity of the cold-exposed mice described above in the absence of food.

(D) Total energy expenditure and total activity of the cold-exposed mice described above in the presence of food.

n = 5/group; *p < 0.05, **p < 0.01 vs. genotype; #p < 0.05 vs. temperature treatment.

FAT-KO Mice Are Resistant to β-Adrenergic Agonist-Induced Increases of UCP1 Expression in iBAT

To examine whether the thermogenic machinery of lipolysis-deficient BAT respond normally to activation of β3-adrenergic receptor, we treated FAT-KO and control mice with CL-316,243 (1 mg/kg body weight once daily for 4 days), and measured protein and mRNA levels of genes relevant to thermogenesis in the iBAT (Figure 10). While UCP1 protein and mRNA levels were not significantly different between the two genotypes under the saline-injected (basal) condition, they were not increased in FAT-KO mice as the controls did in response to CL-316,243 injections (Figure 10A-C). Dio2 and PGC1-α, two genes implicated in BAT thermogenesis, were significantly increased in FAT-KO mice under the basal conditions, though these increases were attenuated after CL-316-243 stimulation (Figure 10C). Considering a dramatic increase in iBAT hyperplasia (see Objective 1), the total amounts of UCP1, Dio2 and PGC-1α in the iBAT were actually increased or at lest stayed unchanged. Thus, lipolysis-deficient BAT has intact thermogenic machinery, at least in vivo. While this BAT cannot mobilize cytosolic LDs as thermogenic fuels, it has increased expression of glucose transporter 1 (Glut1) that mediates a cell's basal glucose uptake, as well as CD36 that mediates FFA uptake (Figure 10C), implying that lipolysis-deficient BAT may use more circulating fuels.

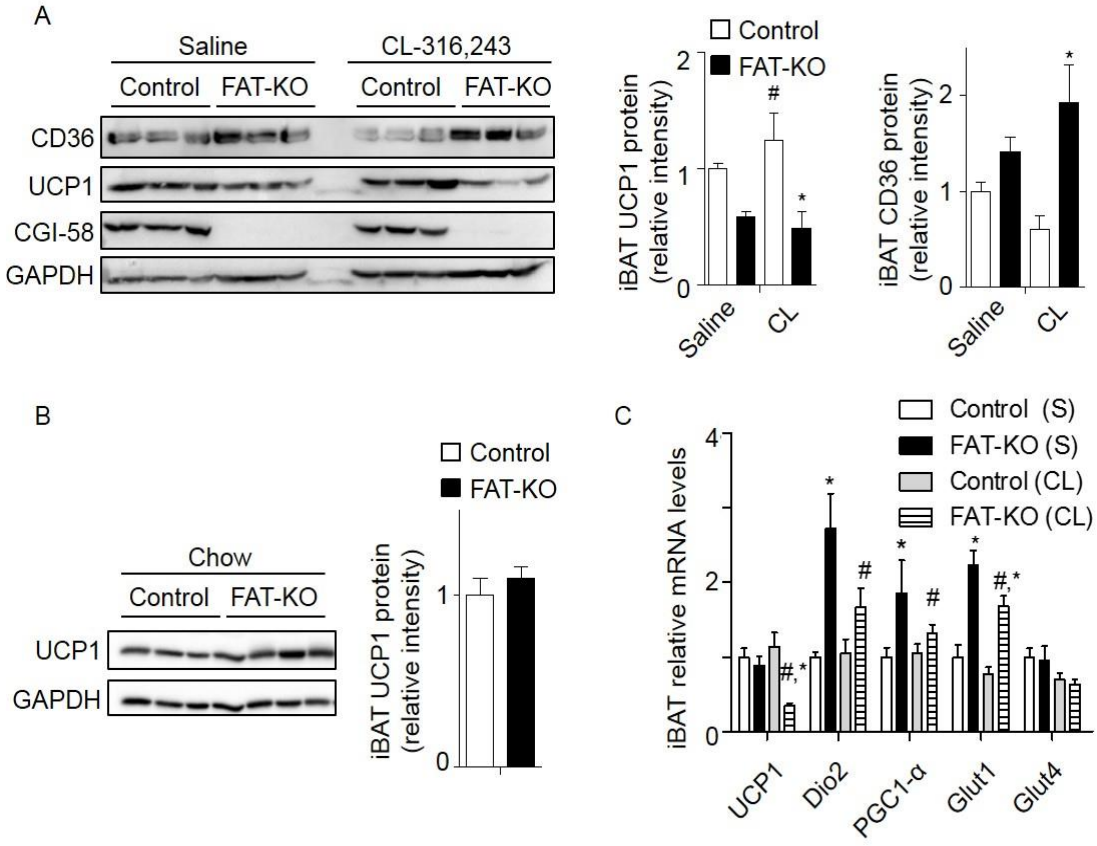

Figure 10. Mice Lacking Adipose Lipolysis Are Resistant to β-Adrenergic Agonist-Induced Increases of UCP1 Expression in iBAT.

(A) iBAT UCP1 and CD36 protein expression and densitometry of 14-week-old HFD-fed mice housed at room temperature and treated with or without the β–adrenergic agonist CL-316,243 for 4 days.

(B) iBAT UCP1 protein expression and densitometry of 14-week-old chow-fed mice housed at room temperature.

(C) mRNA expression levels in the iBAT of 14-week-old HFD-fed mice administered consecutively with vehicle (Saline) or CL-316,243 for 4 days.

n = 5/group; *$p < 0.05$ vs. genotype; #$p < 0.05$ vs. temperature treatment.

Mice Deficient in Adipose Lipolysis Utilize More Glucose as a Thermogenic Substrate During Cold Exposure

To test whether FAT-KO mice uses more glucose for thermogenesis during cold exposure, we measured blood glucose levels of the mice exposed to cold and adminitrated with a bolus of glucose. Consitently with increased glucose utilization in FAT-KO mice during cold exposure, a bolus of glucose injection cannot raise blood glucose levels in these animals as it did in the controls (Figure 11A). Although the body temperature of FAT-KO mice was still lower than the controls after glucose injection, it was higher than FAT-KO mice without glucose (Figure 11B), implying that glucose was used for heat produtction. To identify tissues with increased glucose use during cold exposure, we measured tissue glucose uptake during acute cold exposure without insulin administration. Strikingly, there was a ~12-fold increase of cardiac glucose uptake in FAT-KO mice versus controls (Figure 11C). Although iBAT glucose uptake was significantly reduced when expressed as glucose uptake per mg wet tissue, BAT from FAT-KO mice showed significantly increased glucose uptake as an organ (Figure 11D) due to the increased iBAT weight (see Objective 1).

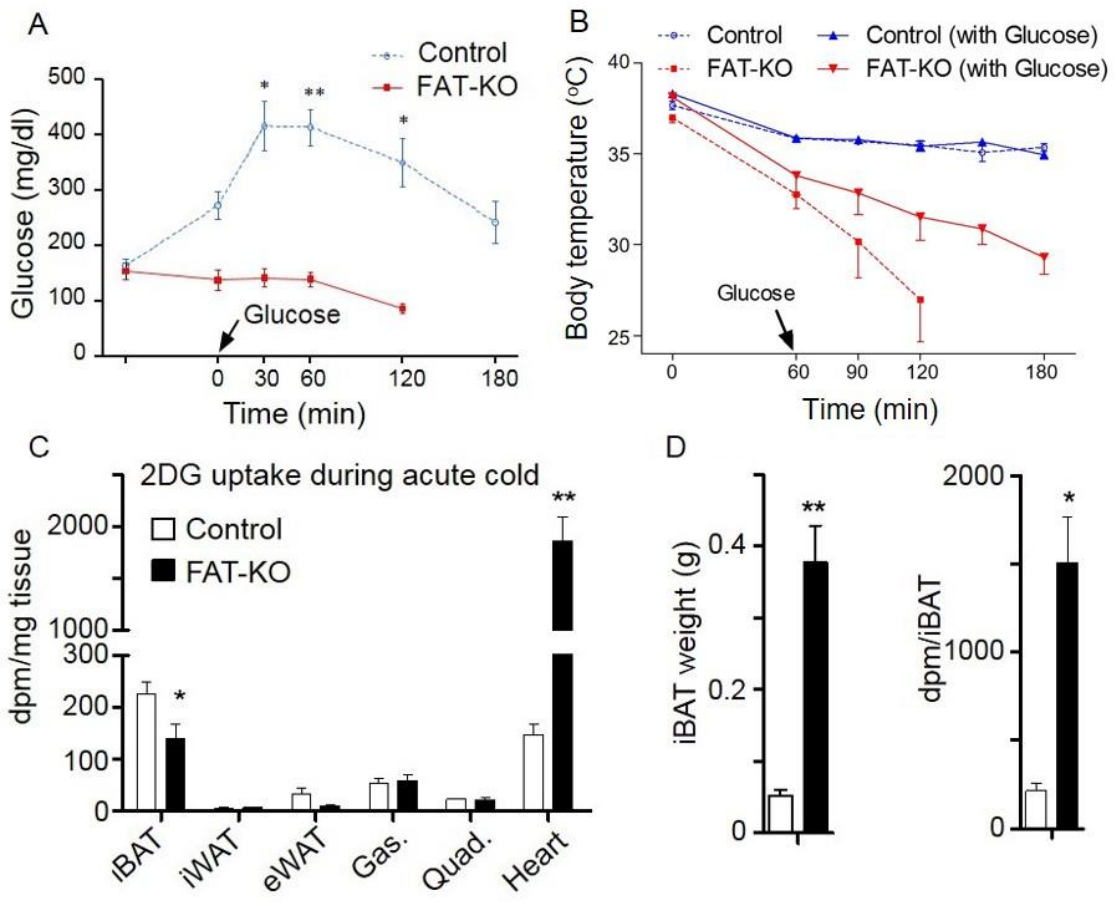

Figure 11. Mice Lacking Adipose Lipolysis Are Resistant to Glucose-Induced Increases in Blood Glucose During Cold Exposure and Display a Dramatically Increased Glucose Uptake in the Heart and the iBAT as an Organ.

(A) Blood glucose levels of 11-week-old HFD-fed mice during acute cold exposure 60 min before and 180 min after a bolus of glucose (*i.p.*, at 1.5 g/kg body weight). n = 4 - 5/group.

(B) Body temperature changes in the mice described in (A). Reference body temperature without glucose injection is from Figure 7C.

(C) Tissue glucose uptake in 20-week-old HFD-fed mice during acute cold exposure.

(D) Glucose uptake of whole iBAT. n = 4 - 5/group.

*p < 0.05, **p < 0.01 vs. genotype.

Although Glut4 mRNA levels remain unaltered in the iBAT of FAT-KO mice (Figure 10C), insulin stimulates Glut4 protein translocation from intraceuular compartments to the cell surface to mediate glucose uptake in the fed state. To examine whether lipolysis-deficient BAT has increased glucose uptake in the fed state, we measured insulin-stimulated glucose uptake in FAT-KO mice. It was found that iBAT glucose uptake under this condition was reduced when normalized by mg wet weight (Figure 12A) and only slightly increased when normalized by the total iBAT weight (not shown). Interestingly, while epididymal fat glucose uptake was reduced, there was a significant increase in insulin-stimulated glucose uptake in the gastrocnemius muscle and heart of FAT-KO mice (Figure 12A).

Normally, heart uses FFAs as fuels. When it is forced to use more glucose due to lipolysis deficiency, its functions are likely changed due to glucose-induced cardiac remodeling. Indeed, the mRNAs for BNP and ANP, two cardiac hormones sensitive to cardiac functional alterations, especially heart failure, were significantly increased in the heart of FAT-KO mice (Figure 12B).

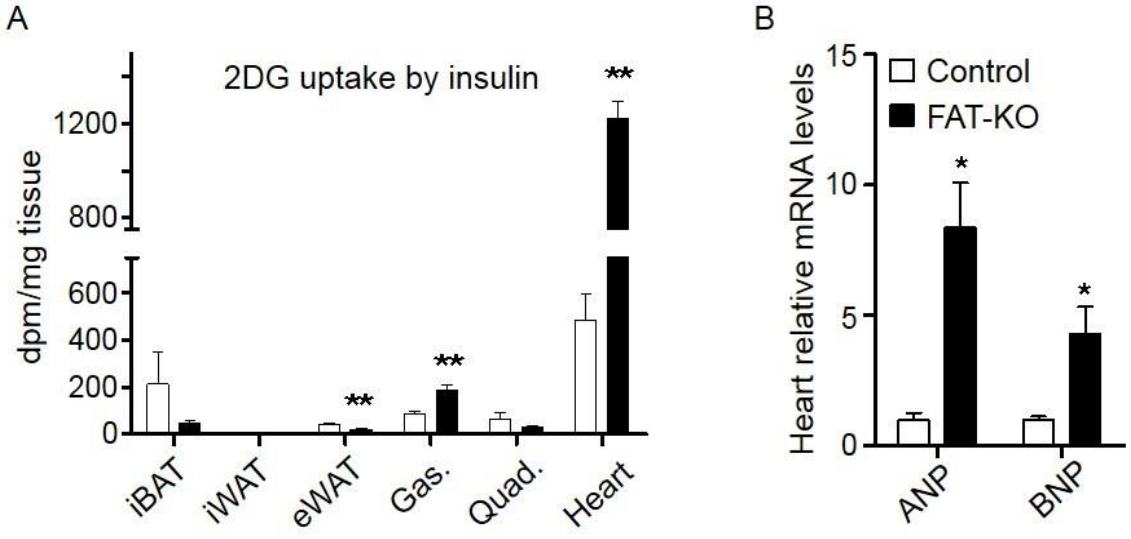

Figure 12. Insulin-Induced Glucose Uptake Is Dramatically Increased in the Heart of FAT-KO Mice.

(A) Tissue glucose uptake induced by insulin in 28-week-old HFD-fed mice housed at room temperature. n = 5 - 6/group.

(B) ANP and BNP mRNA expression levels in the hearts of 14-week-old HFD-fed mice housed at room temperature. n = 4 - 5/group.

*$p < 0.05$, **$p < 0.01$ vs. genotype.

β_3-Adrenergic Stimulation Cannot, But Cold Can Induces WAT Browning in FAT-KO Mice

We have shown in BAT-KO mice that BAT lipolysis deficiency induces WAT browning (Figure 6 of Objective 1). To test if this is WAT lipolysis-dependent, we first stimulated iWAT browning using CL-316,243. As expected, the adipocyte size in the iWAT was reduced in the control mice after CL-316-243 stimulation (Figure 13A), which was associated with increased mRNAs for UCP1, PGC-1α, and PPAR-α (Figure 13B) as well as increased UCP1 protein expression as evidenced by immunohistochemistry (Figure 13C) and immunoblotting (Figure 13D). These changes did not happen or even suppressed after β3-adrenergic stimulation (Figure 13A-D).

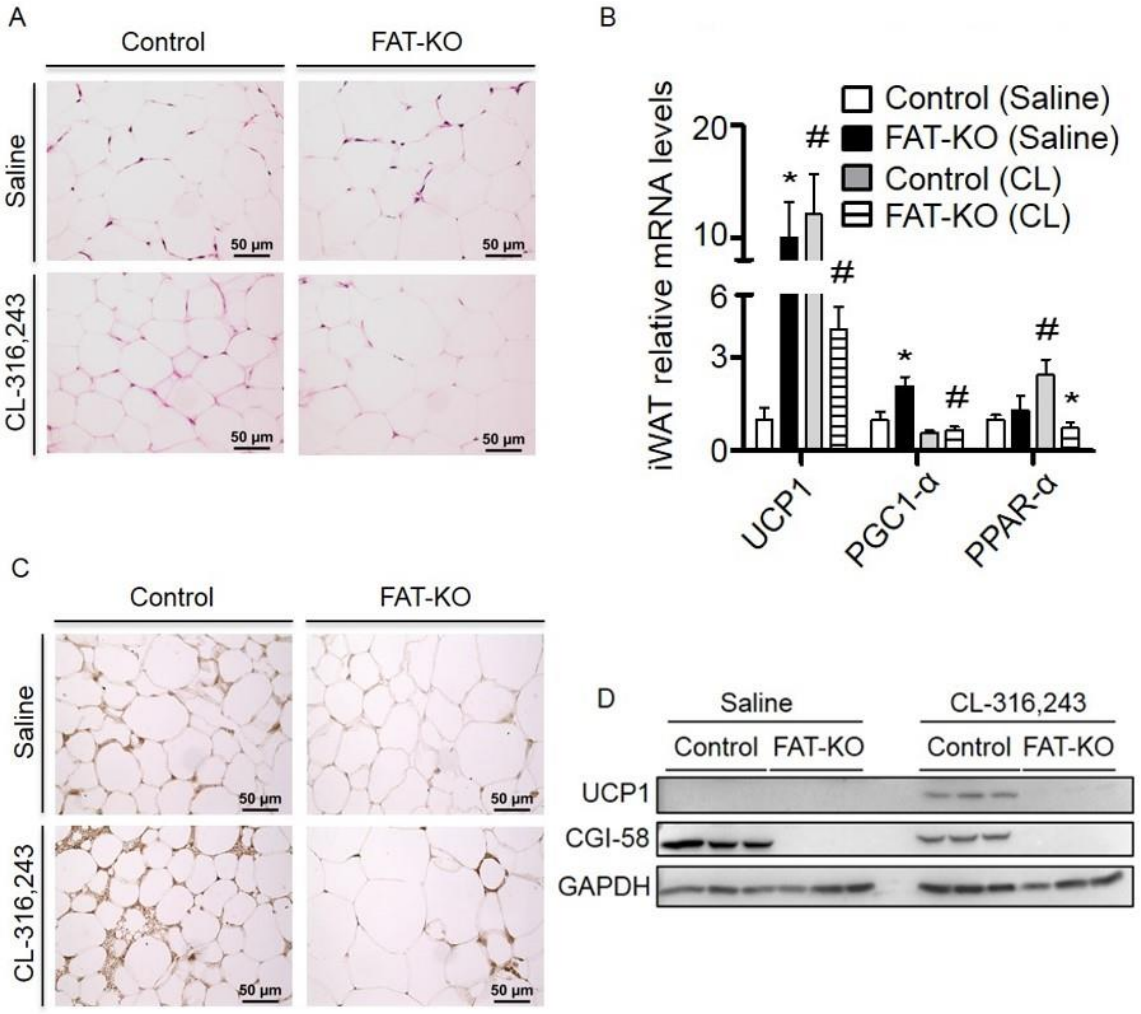

Figure 13. Mice Deficient in Adipose Lipolysis Are Resistant to β_3-Adrenergic Agonist-Induced Increases of UCP1 Expression in iWAT.

(A) Representative H&E staining of iWAT.

(B) mRNA levels of UCP1, PGC-1α and PPAR-α in the iWAT. n = 5/group.

(C) Immunohistochemical staining of UCP1 protein in the iWAT.

(D) Immunoblotting of UCP1 protein in the iWAT.

All experiments were done with the 14-week-old HFD-fed mice injected consecutively with vehicle (Saline) or CL-316,243 for 4 days. *$p < 0.05$ vs. genotype; #$p < 0.05$ vs. CL treatment.

To determine whether FAT-KO mice respond to cold similarly in terms of WAT browning, we exposed our mice to cold for 3 days after a 7 day acclimation period. Interestingly, adipose lipolysis deficiency did not impair cold-induced increases of UCP1 protein expression (indicative of increased iWAT browning) (Figure 14A and 14B), though it did to the β_3-adrenergic receptor stimulation-induced WAT browning. In addition to UCP1, TH (a marker of sympathetic innervation) was also similarly increased in the two genotypes during cold exposure (Figure 14A and 14B).

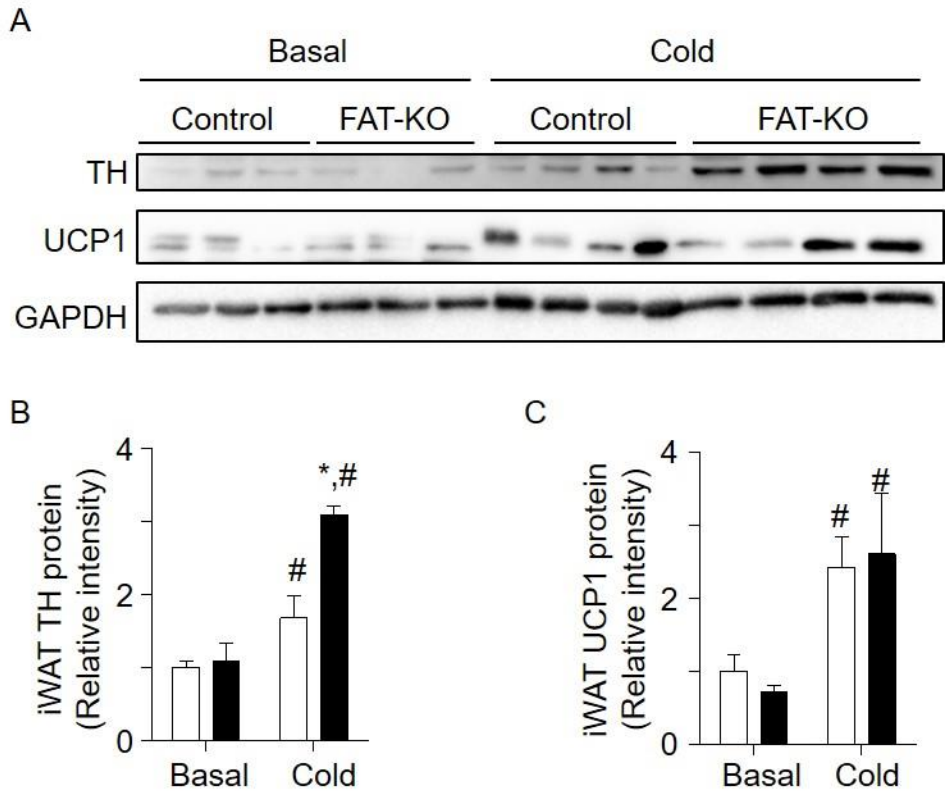

Figure 14. Adipocyte Lipolysis Deficiency Does Not Affect Cold-Induced iWAT Browning.

(A) Immunoblotting of TH and UCP1 protein in the iWAT

(B and C) Densitometry of TH and UCP1 protein in the iWAT

All experiments were done with the 22-week-old HFD-fed mice with basal or 3 days of cold. *$p < 0.05$ vs. genotype; #$p < 0.05$ vs. Cold treatment.

Metabolic Benefits of CGI-58 Deletion in Fat.

Under Objective 1, we have seen several metabolic benefits of BAT lipolysis suppression in mice on an HFD (Figure 7 of Objective 1). We hypothesized that these benefits may be amplified due to simultaneous inhibition of lipolysis in both BAT and WAT. Indeed, adipose lipolysis deficiency induced by fat-specific inactivation largely protected mice against HFD-induced glucose intolerance and insulin resistance (Figure 15A). HOMA-IR index was also reduced in FAT-KO mice, though it did not reach statistical significance due to large variations of the values (Figure 15B). Serum levels of leptin were unaffected in FAT-KO mice (Figure 15C), though fat mass was increased (see Objective 1). As expected, fasting failed to raise serum FFAs due to lipolysis inhibition in FAT-KO mice (Figure 15D). Interestingly, FAT-KO mice displayed a significant reduction in serum TG levels during fasting, but not in the fed state (Figure 15E). No changes in serum total cholesterol (TC) were observed in FAT-KO mice in both fed and fasted states (Figure 15E). In addition, liver weight was significantly lower due to reduced accumulation of TG in the liver of FAT-KO mice (Figure 15F). Hepatic contents of free cholesterol (FC) and total cholesterol (TC) did not differ between the two genotypes (Figure 15F), suggesting that FAT-KO mice on HFD are protected from developing hepatic steatosis. Collectively, the results demonstrated that suppression of fat lipolysis improves metabolic health in mice presumably by preventing FFA overloads and by improving glucose disposal.

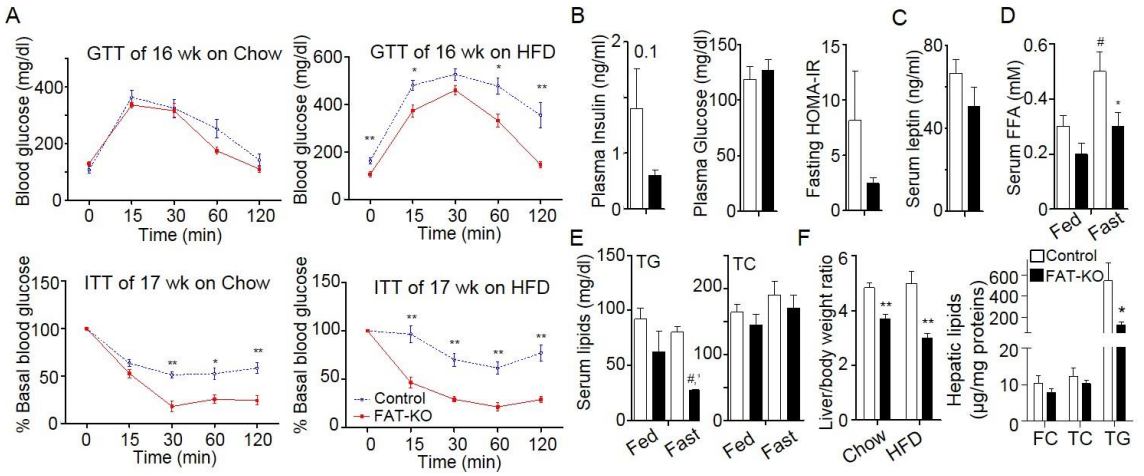

Figure 15. Mice Deficient in Adipose Lipolysis Exhibit Increased Glucose Tolerance and Insulin Sensitivity and Are Protected Against HFD-Induced Hepatic Steatosis.

(A) GTT and ITT of the mice on chow for 16 or 17 weeks or HFD for 16 or 17 weeks. n = 5 - 6/group in chow-fed mice; n = 7 - 8/group in HFD-fed mice.

(B) Fasting plasma levels of insulin and glucose as well as HOMA-IR in 17-week-old HFD-fed mice. n = 5 - 6/group.

(C) Serum leptin levels of 15-week-old HFD-fed mice in the fed state. n = 5 - 6/group.

(D) Serum FFA levels of 15-week-old HFD-fed mice in the fed and of 17-week-old HFD-fed mice in the fasted state. n = 5 - 6/group.

(E) Serum levels of triglycerides (TG) and total cholesterol (TC). n = 5 - 6/group.

(F) Liver-to-body weight ratios of 24-week-old mice on chow or HFD as well as hepatic contents of free cholesterol (FC), TC and TG in 24-week-old HFD-fed mice. n = 5/group.

*p < 0.05, **p <0.01 vs. genotype; #p < 0.05 vs. fed or fasted state.

Discussion

The major findings with FAT-KO mice are 1) adipose lipolysis is required for cold-induced thermogenesis only during fasting; 2) In the fed state, dietary nutrients can substitute for adipose lipolysis deficiency to maintain cold-induced thermogenesis, at least for a few days in mice; 3) Mice deficient in adipose lipolysis utilize more circulating glucose, especially during cold exposure; 4) Mice deficient in adipose lipolysis are protected against overnutrition-induced glucose intolerance and insulin resistance; and 5) Adipose lipolysis deficiency likely impairs cardiac functions by forcing the heart to use more glucose for oxidation driving cardiac remodeling.

It has been reported that cold stimulates BAT to use glucose for thermogenesis in addition to FFAs in both insulin-dependent and independent manners [210, 223-228]. Our findings with FAT-KO mice indicate that cold-induced glucose utilization is further upregulated in the absence of adipose lipolysis. Although the underlying mechanisms may reflect an integrated whole-body response that may involve altered secretion of batokines and activation of the sympathetic nervous system [229, 230], the cell autonomous adaptation may also play a part. We have previously shown in cultured cells that CGI-58 deficiency promotes glucose uptake [154, 231, 232]. Thus, cells may program its metabolism to take up more exogenous fuels when cytosolic LD cannot be mobilized for use as substrates. It is currently unclear whether glucose in lipolysis-deficient BAT is used directly or after conversion to FFAs via *de novo* lipogenesis for heat production.

Based on RER (indicative of substrate preference) and body temperature changes during chronic cold exposure, glucose-mediated thermogenesis may not be sustainable. Lipolysis-deficient BAT showed increased CD36 protein expression after chronic CL-316,243 treatment or cold exposure. CD36 has been implicated in FFA uptake from the circulation [214] and upregulation of HSL-mediated LD lipolysis activity [233] in adipocytes. In addition, the BAT of CD36-null mice had blunted glucose uptake during cold exposure [208], suggesting that there is a CD36-dependent crosstalk between FFA and glucose utilization in BAT. Increased BAT CD36 expression in both BAT-KO and FAT-KO mice after chronic cold or CL-316,243 treatment could provide more sustainable thermogenic fuels for BAT to combust in the absence of lipolysis.

In addition to increasing BAT uptake of thermogenic substrates, beige adipocyte attainment in iWAT (iWAT browning) is another compensatory mechanism for BAT lipolysis-deficient mice to boost whole-body thermogenic capacity in BAT-KO mice (Objective 1). Beige adipocytes, like brown adipocytes, may combust FFAs and glucose. It seems that the glucose uptake in beige adipocytes is insulin-independent, largely relying on Glut1 [234]. We observed that the β_3 agonist CL-316,243-induced iWAT browning is WAT lipolysis-dependent because it occurs only in BAT-KO mice, but not in FAT-KO mice. Interestingly, the iWAT of FAT-KO mice can be browned to the same extent as the control mice in response to the cold as evidenced by increased UCP1 expression (Figure 14). Expression of TH protein, a marker of sympathetic innervation, was also increased in the iWAT of FAT-KO mice after cold exposure

(Figure 14). Although β_3 is the predominant form of β-adrenergic receptors in WAT [81] and its activation by CL-316-243 does not increase UCP1 expression in the iWAT of FAT-KO mice, the increased sympathetic innervation may activate other forms of β-adrenergic receptors to promote thermogenesis, or simply reflect an augmented response to the cold on the face of adipose lipolysis deficiency, which may not lead to activation of downstream receptors. Alternatively cold may have triggered other browning mechanisms in addition to the sympathetic activity, which may result in iWAT browning.

One potential β_3-adrenoceptor-independent thermogenic mechanisms noted in our study is ANP and BNP whose expression levels are significantly increased the heart of FAT-KO mice. This increase in ANP and BNP could result from increased glucose uptake. It has been shown that heart-specific overexpression of Glut1 in mice results in contractile dysfunction due to increased oxidative stress [235]. In general, ANP and BNP are elevated in heart as a result of failed natriuretic and vasodilating actions [236]. As mentioned in the Introduction section, ANP and BNP can activate thermogenesis via cAMP-independent but p38 MAPK-dependent signaling in iWAT [237, 238]. It is tempting to speculate that FAT-KO mice may release increased amounts of ANP and BNP during chronic cold exposure as a result of increased cardiac glucose uptake, thereby inducing iWAT browning. Future studies are warranted to investigate how adipose lipolysis deficiency alters cardiac functions and how this alteration regulates metabolism and pathophysiology of other organs via ANP and BNP in FAT-KO mice.

BAT glucose uptake is reduced in humans and mice when adipose lipolysis is inhibited by niacin [228, 239]. This might be a result of re-distribution of glucose uptake when adipose lipolysis is deficient as seen in our FAT-KO mice when glucose uptake is expressed as mg BAT wet weight. When lipolysis is selectively inactivated in the BAT of our BAT-KO mice, the total glucose uptake by BAT as an organ is increased after insulin stimulation and during acute cold exposure. Interestingly, glucose uptake is increased in heart and gastrocnemius muscle of FAT-KO but not BAT-KO mice. In humans treated with niacin, cold induces shivering [228, 239]. Shivering thermogenesis can compensate for impaired NST for heat production to maintain body temperature. For example, UCP1 KO mice are deficient in NST, but can tolerate cold via shivering after cold acclimation [240]. Therefore, it is important to assess NST in mice [241], which can be done by housing mice under a thermoneutral temperature (30 ^{o}C), followed by injection of NE [241-243]. We observed that FAT-KO, but not BAT-KO mice at thermoneutrality have reduced NST capacity after CL-316,243 injection (see Figure 8 for FAT-KO mice; data not shown for BAT-KO mice), suggesting a critical role of WAT lipolysis in sustaining NST. Consistently, oxygen consumption in primary brown adipocytes from UCP1 knockout mice is normal when the cell culture medium has FFAs, and is suppressed when FFAs are removed from in the culture medium by a high concentration of BSA [244]. In addition, the effect of NE on metabolic rates is enhanced following food intake [245]. Our BAT-KO and FAT-KO mice display higher body temperature when food is present than absent during acute cold exposure. Collectively, our results

together with published data indicate that white adipocyte lipolysis and dietary substrates are essential for NST in the absence of brown adipocyte lipolysis.

While adipose lipolysis deficiency impairs cold adaptation during fasting and may influence cardiac functions, it protects against overnutrition-induced metabolic disorders including glucose intolerance, insulin resistance and hepatic steatosis. This protection may be mediated by increased disposal of glucose for fueling the heart and thermogenesis when adipose lipolysis is deficient. Alternatively, lipolysis deficiency may promote secretion of insulin-sensitizing factors, which may regulate locally and remotely insulin signaling, energy balance and lipid metabolism.

Summary

It was believed that lipolysis of cytosolic LDs in brown adipocytes plays a central role in NST, but this concept has not been examined in vivo in whole animals due to lack of appropriate animal models. In this project, we have filled this gap in the field using mice with lipolysis deficiency in BAT only and those with lipolysis deficiency in both BAT and WAT. We demonstrate that brown adipocyte LD lipolysis is not essential for cold-induced thermogenesis in vivo due perhaps to enhanced WAT browning and increased uptake of circulating thermogenic fuels that are derived from WAT lipolysis and diet. Comparative studies with mice deficient in CGI-58, an intracellular lipolysis activator, in different fat depots (BAT or both BAT and WAT) uncover a critical role of WAT lipolysis in cold-induced thermogenesis during fasting. In the fed state, dietary nutrients can substitute for

WAT lipolysis for thermogenesis, at least for a short period. A proposed model for thermoregulation in mice deficient in lipolysis in brown and/or white adipocytes is summarized in Figure 16.

A limitation of our approach is that it did not provide direct evidence as to the role of WAT lipolysis in thermoregulation. Although there are currently no WAT-specific genetic manipulations, we could, in the future, create a BAT-specific CGI-58 transgenic mice and then cross them with our FAT-KO mice. This way, we will have mice deficient in lipolysis in WAT only. We could then define how WAT lipolysis influences thermogenesis and metabolic health.

While our study has clarified the in vivo significance of adipocyte cytosolic LD lipolysis in thermoregulation, it raises many intriguing questions. What is the molecular mechanism sensing brown adipocyte lipolysis deficiency? How does this mechanism communicates with other metabolic and cellular and pathways to regulate thermogenesis? Is the sympathetic innervation necessary for WAT browning when adipose lipolysis is suppressed? Do lipolysis-deficient brown adipocytes release any “batokines” that are essential for sustaining the whole-body thermogenic capacity? How does adipose lipolysis deficiency affect cardiac health? Are ANP and BNP derived from the heart involved in the browning of WAT deficient in lipolysis? Future studies addressing these questions are warranted.

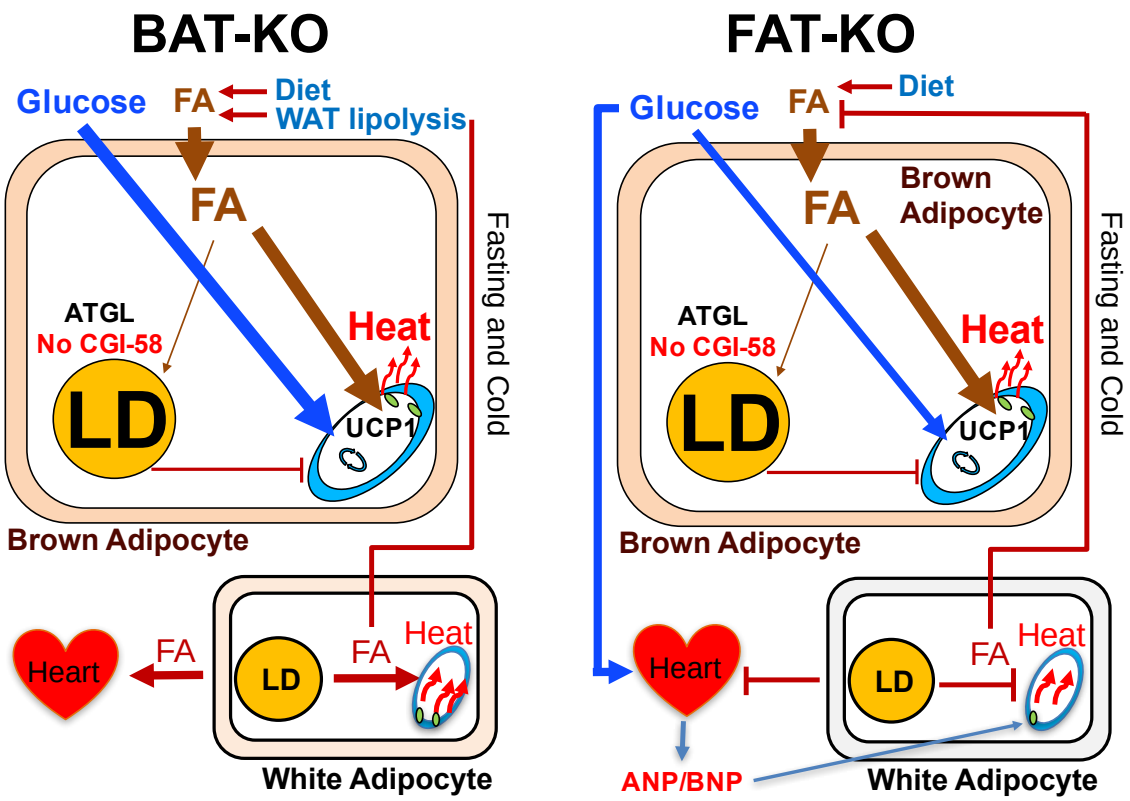

Figure 16. A Proposed Model of Thermoregulation in Mice Deficient in CGI-58 in Brown and/or White Adipocytes.

CGI-58-ablated brown adipocytes enhance their uptake of thermogenic substrates from the blood circulation. These substrates include glucose derived from diet and gluconeogenesis as well as FFAs derived from WAT lipolysis and intravascular lipolysis of dietary fat. Deficiency of CGI-58 in brown adipocytes also induces WAT browning. As a result, mice deficient in BAT lipolysis are able to tolerate cold in both fed and fasted states. When CGI-58 is deficient in both brown and white adipocytes, mice cannot tolerate cold during fasting, but they can tolerate cold when food is present. In addition, adipose lipolysis deficiency increases cardiac uptake of glucose, resulting in cardiac remodeling and

increased expression of ANP and BNP, two cardiac hormones that have been implicated in promotion of WAT browning.

References

1. Lowell, B.B. and B.M. Spiegelman, *Towards a molecular understanding of adaptive thermogenesis.* Nature, 2000. **404**(6778): p. 652-60.
2. Cannon, B. and J. Nedergaard, *Brown adipose tissue: function and physiological significance.* Physiol Rev, 2004. **84**(1): p. 277-359.
3. van Marken Lichtenbelt, W.D., et al., *Cold-activated brown adipose tissue in healthy men.* N Engl J Med, 2009. **360**(15): p. 1500-8.
4. Tran, T.T. and C.R. Kahn, *Transplantation of adipose tissue and stem cells: role in metabolism and disease.* Nat Rev Endocrinol, 2010. **6**(4): p. 195-213.
5. Whittle, A.J., M. Lopez, and A. Vidal-Puig, *Using brown adipose tissue to treat obesity - the central issue.* Trends Mol Med, 2011. **17**(8): p. 405-11.
6. Whittle, A., J. Relat-Pardo, and A. Vidal-Puig, *Pharmacological strategies for targeting BAT thermogenesis.* Trends Pharmacol Sci, 2013. **34**(6): p. 347-55.
7. Carobbio, S., B. Rosen, and A. Vidal-Puig, *Adipogenesis: new insights into brown adipose tissue differentiation.* J Mol Endocrinol, 2013. **51**(3): p. T75-85.
8. Villarroya, F. and A. Vidal-Puig, *Beyond the sympathetic tone: the new brown fat activators.* Cell Metab, 2013. **17**(5): p. 638-43.
9. Villarroya, J., R. Cereijo, and F. Villarroya, *An endocrine role for brown adipose tissue?* Am J Physiol Endocrinol Metab, 2013. **305**(5): p. E567-72.

10. Wu, J., P. Cohen, and B.M. Spiegelman, *Adaptive thermogenesis in adipocytes: is beige the new brown?* Genes Dev, 2013. **27**(3): p. 234-50.

11. Young, S.G. and R. Zechner, *Biochemistry and pathophysiology of intravascular and intracellular lipolysis.* Genes Dev, 2013. **27**(5): p. 459-84.

12. van Marken Lichtenbelt, W.D., et al., *Cold-activated brown adipose tissue in healthy men.* New England Journal of Medicine, 2009. **360**(15): p. 1500-1508.

13. Zingaretti, M.C., et al., *The presence of UCP1 demonstrates that metabolically active adipose tissue in the neck of adult humans truly represents brown adipose tissue.* The FASEB Journal, 2009. **23**(9): p. 3113-3120.

14. Nedergaard, J., T. Bengtsson, and B. Cannon, *Unexpected evidence for active brown adipose tissue in adult humans.* American Journal of Physiology-Endocrinology and Metabolism, 2007. **293**(2): p. E444-E452.

15. Cypess, A.M., et al., *Identification and importance of brown adipose tissue in adult humans.* New England Journal of Medicine, 2009. **360**(15): p. 1509-1517.

16. Virtanen, K.A., et al., *Functional brown adipose tissue in healthy adults.* New England Journal of Medicine, 2009. **360**(15): p. 1518-1525.

17. Shabalina, I.G., et al., *UCP1 in brite/beige adipose tissue mitochondria is functionally thermogenic.* Cell Rep, 2013. **5**(5): p. 1196-203.

18. Ozaki, K., et al., *Carnitine is necessary to maintain the phenotype and function of brown adipose tissue.* Lab Invest, 2011. **91**(5): p. 704-10.

19. Kazak, L., et al., *A creatine-driven substrate cycle enhances energy expenditure and thermogenesis in beige fat.* Cell, 2015. **163**(3): p. 643-55.

20. Cypess, A.M., et al., *Identification and importance of brown adipose tissue in adult humans.* N Engl J Med, 2009. **360**(15): p. 1509-17.

21. Virtanen, K.A., et al., *Functional brown adipose tissue in healthy adults.* N Engl J Med, 2009. **360**(15): p. 1518-25.

22. Young, P., J.R. Arch, and M. Ashwell, *Brown adipose tissue in the parametrial fat pad of the mouse.* FEBS Lett, 1984. **167**(1): p. 10-4.

23. Cousin, B., et al., *Occurrence of brown adipocytes in rat white adipose tissue: molecular and morphological characterization.* J Cell Sci, 1992. **103 (Pt 4)**: p. 931-42.

24. Seale, P., et al., *PRDM16 controls a brown fat/skeletal muscle switch.* Nature, 2008. **454**(7207): p. 961-7.

25. Petrovic, N., et al., *Chronic peroxisome proliferator-activated receptor gamma (PPARgamma) activation of epididymally derived white adipocyte cultures reveals a population of thermogenically competent, UCP1-containing adipocytes molecularly distinct from classic brown adipocytes.* J Biol Chem, 2010. **285**(10): p. 7153-64.

26. Seale, P., et al., *Prdm16 determines the thermogenic program of subcutaneous white adipose tissue in mice.* J Clin Invest, 2011. **121**(1): p. 96-105.

27. Schulz, T.J., et al., *Identification of inducible brown adipocyte progenitors residing in skeletal muscle and white fat.* Proc Natl Acad Sci U S A, 2011. **108**(1): p. 143-8.

28. Wu, J., et al., *Beige adipocytes are a distinct type of thermogenic fat cell in mouse and human.* Cell, 2012. **150**(2): p. 366-76.

29. Shinoda, K., et al., *Genetic and functional characterization of clonally derived adult human brown adipocytes.* Nat Med, 2015. **21**(4): p. 389-94.

30. Jespersen, N.Z., et al., *A classical brown adipose tissue mRNA signature partly overlaps with brite in the supraclavicular region of adult humans.* Cell Metab, 2013. **17**(5): p. 798-805.

31. Guerra, C., et al., *Emergence of brown adipocytes in white fat in mice is under genetic control. Effects on body weight and adiposity.* Journal of Clinical Investigation, 1998. **102**(2): p. 412.

32. Atit, R., et al., *Beta-catenin activation is necessary and sufficient to specify the dorsal dermal fate in the mouse.* Dev Biol, 2006. **296**(1): p. 164-76.

33. Gesta, S., Y.H. Tseng, and C.R. Kahn, *Developmental origin of fat: tracking obesity to its source.* Cell, 2007. **131**(2): p. 242-56.

34. Cinti, S., *Transdifferentiation properties of adipocytes in the adipose organ.* Am J Physiol Endocrinol Metab, 2009. **297**(5): p. E977-86.

35. Sidossis, L. and S. Kajimura, *Brown and beige fat in humans: thermogenic adipocytes that control energy and glucose homeostasis.* J Clin Invest, 2015. **125**(2): p. 478-86.

36. Granneman, J.G., et al., *Metabolic and cellular plasticity in white adipose tissue I: effects of beta3-adrenergic receptor activation.* Am J Physiol Endocrinol Metab, 2005. **289**(4): p. E608-16.

37. Cristancho, A.G. and M.A. Lazar, *Forming functional fat: a growing understanding of adipocyte differentiation.* Nat Rev Mol Cell Biol, 2011. **12**(11): p. 722-34.

38. Vegiopoulos, A., et al., *Cyclooxygenase-2 controls energy homeostasis in mice by de novo recruitment of brown adipocytes.* Science, 2010. **328**(5982): p. 1158-61.

39. Wang, Q.A., et al., *Tracking adipogenesis during white adipose tissue development, expansion and regeneration.* Nat Med, 2013. **19**(10): p. 1338-44.

40. McDonald, M.E., et al., *Myocardin-related transcription factor A regulates conversion of progenitors to beige adipocytes.* Cell, 2015. **160**(1-2): p. 105-18.

41. Long, J.Z., et al., *A smooth muscle-like origin for beige adipocytes.* Cell Metab, 2014. **19**(5): p. 810-20.

42. Cinti, S., *Adipocyte differentiation and transdifferentiation: plasticity of the adipose organ.* J Endocrinol Invest, 2002. **25**(10): p. 823-35.

43. Perwitz, N., et al., *Cannabinoid type 1 receptor blockade induces transdifferentiation towards a brown fat phenotype in white adipocytes.* Diabetes Obes Metab, 2010. **12**(2): p. 158-66.

44. Himms-Hagen, J., et al., *Multilocular fat cells in WAT of CL-316243-treated rats derive directly from white adipocytes.* Am J Physiol Cell Physiol, 2000. **279**(3): p. C670-81.

45. Vitali, A., et al., *The adipose organ of obesity-prone C57BL/6J mice is composed of mixed white and brown adipocytes.* J Lipid Res, 2012. **53**(4): p. 619-29.

46. Barbatelli, G., et al., *The emergence of cold-induced brown adipocytes in mouse white fat depots is determined predominantly by white to brown adipocyte transdifferentiation.* Am J Physiol Endocrinol Metab, 2010. **298**(6): p. E1244-53.

47. Frontini, A., et al., *White-to-brown transdifferentiation of omental adipocytes in patients affected by pheochromocytoma.* Biochim Biophys Acta, 2013. **1831**(5): p. 950-9.

48. Rosenwald, M., et al., *Bi-directional interconversion of brite and white adipocytes.* Nat Cell Biol, 2013. **15**(6): p. 659-67.

49. Lee, Y.H., et al., *In vivo identification of bipotential adipocyte progenitors recruited by beta3-adrenoceptor activation and high-fat feeding.* Cell Metab, 2012. **15**(4): p. 480-91.

50. Zhao, J., B. Cannon, and J. Nedergaard, *alpha1-Adrenergic stimulation potentiates the thermogenic action of beta3-adrenoreceptor-generated cAMP in brown fat cells.* J Biol Chem, 1997. **272**(52): p. 32847-56.

51. Tang, W., et al., *White fat progenitor cells reside in the adipose vasculature.* Science, 2008. **322**(5901): p. 583-6.

52. Sanchez-Gurmaches, J., et al., *PTEN loss in the Myf5 lineage redistributes body fat and reveals subsets of white adipocytes that arise from Myf5 precursors.* Cell Metab, 2012. **16**(3): p. 348-62.

53. Macotela, Y., et al., *Intrinsic differences in adipocyte precursor cells from different white fat depots.* Diabetes, 2012. **61**(7): p. 1691-9.

54. Shan, T., et al., *Distinct populations of adipogenic and myogenic Myf5-lineage progenitors in white adipose tissues.* J Lipid Res, 2013. **54**(8): p. 2214-24.

55. Harms, M. and P. Seale, *Brown and beige fat: development, function and therapeutic potential.* Nat Med, 2013. **19**(10): p. 1252-63.

56. Hu, E., P. Tontonoz, and B.M. Spiegelman, *Transdifferentiation of myoblasts by the adipogenic transcription factors PPAR gamma and C/EBP alpha.* Proceedings of the National Academy of Sciences, 1995. **92**(21): p. 9856-9860.

57. Rosen, E.D. and O.A. MacDougald, *Adipocyte differentiation from the inside out.* Nature reviews Molecular cell biology, 2006. **7**(12): p. 885-896.

58. Kajimura, S., et al., *Initiation of myoblast to brown fat switch by a PRDM16–C/EBP-b transcriptional complex.* Nature, 2009. **460**(7259): p. 1154-1158.

59. Liu, C., et al., *PPARγ in vagal neurons regulates high-fat diet induced thermogenesis.* Cell metabolism, 2014. **19**(4): p. 722-730.

60. Gray, S.L., et al., *Decreased brown adipocyte recruitment and thermogenic capacity in mice with impaired peroxisome proliferator-*

activated receptor (P465L PPARγ) function. Endocrinology, 2006. **147**(12): p. 5708-5714.

61. Ohno, H., et al., *PPARγ agonists induce a white-to-brown fat conversion through stabilization of PRDM16 protein.* Cell metabolism, 2012. **15**(3): p. 395-404.

62. Sears, I.B., et al., *Differentiation-dependent expression of the brown adipocyte uncoupling protein gene: regulation by peroxisome proliferator-activated receptor gamma.* Molecular and cellular biology, 1996. **16**(7): p. 3410-3419.

63. Tai, T.-A.C., et al., *Activation of the nuclear receptor peroxisome proliferator-activated receptor γ promotes brown adipocyte differentiation.* Journal of Biological Chemistry, 1996. **271**(47): p. 29909-29914.

64. Cao, J., et al., *Molecular identification of microsomal acyl-CoA: glycerol-3-phosphate acyltransferase, a key enzyme in de novo triacylglycerol synthesis.* Proceedings of the National Academy of Sciences, 2006. **103**(52): p. 19695-19700.

65. Villanueva, C.J., et al., *Adipose subtype-selective recruitment of TLE3 or Prdm16 by PPARgamma specifies lipid storage versus thermogenic gene programs.* Cell Metab, 2013. **17**(3): p. 423-35.

66. Mottillo, E.P., et al., *Lipolytic products activate peroxisome proliferator-activated receptor (PPAR) alpha and delta in brown adipocytes to match fatty acid oxidation with supply.* J Biol Chem, 2012. **287**(30): p. 25038-48.

67. Mochizuki, N., et al., *A novel gene, MEL1, mapped to 1p36. 3 is highly homologous to the MDS1/EVI1 gene and is transcriptionally activated in t (1; 3)(p36; q21)-positive leukemia cells.* Blood, 2000. **96**(9): p. 3209-3214.

68. Kajimura, S., et al., *Regulation of the brown and white fat gene programs through a PRDM16/CtBP transcriptional complex.* Genes & development, 2008. **22**(10): p. 1397-1409.

69. Cohen, P., et al., *Ablation of PRDM16 and beige adipose causes metabolic dysfunction and a subcutaneous to visceral fat switch.* Cell, 2014. **156**(1): p. 304-316.

70. Schulz, T.J., et al., *Brown-fat paucity due to impaired BMP signalling induces compensatory browning of white fat.* Nature, 2013. **495**(7441): p. 379-383.

71. Qiang, L., et al., *Brown remodeling of white adipose tissue by SirT1-dependent deacetylation of Pparγ.* Cell, 2012. **150**(3): p. 620-632.

72. Trajkovski, M., et al., *MyomiR-133 regulates brown fat differentiation through Prdm16.* Nature cell biology, 2012. **14**(12): p. 1330-1335.

73. Yin, H., et al., *MicroRNA-133 controls brown adipose determination in skeletal muscle satellite cells by targeting Prdm16.* Cell metabolism, 2013. **17**(2): p. 210-224.

74. Mootha, V.K., et al., *Errα and Gabpa/b specify PGC-1α-dependent oxidative phosphorylation gene expression that is altered in diabetic muscle.* Proceedings of the National Academy of Sciences of the United States of America, 2004. **101**(17): p. 6570-6575.

75. Puigserver, P., et al., *Insulin-regulated hepatic gluconeogenesis through FOXO1–PGC-1α interaction.* Nature, 2003. **423**(6939): p. 550-555.

76. Puigserver, P., et al., *A cold-inducible coactivator of nuclear receptors linked to adaptive thermogenesis.* Cell, 1998. **92**(6): p. 829-839.

77. Scarpulla, R.C., *Nuclear control of respiratory gene expression in mammalian cells.* Journal of cellular biochemistry, 2006. **97**(4): p. 673-683.

78. Schreiber, S.N., et al., *The estrogen-related receptor (ERR) functions in PPAR coactivator 1 (PGC-1)-induced mitochondrial biogenesis.* PNAS, 2004. **101**(17).

79. Tiraby, C., et al., *Acquirement of brown fat cell features by human white adipocytes.* Journal of Biological Chemistry, 2003. **278**(35): p. 33370-33376.

80. Cao, W., et al., *p38 mitogen-activated protein kinase is the central regulator of cyclic AMP-dependent transcription of the brown fat uncoupling protein 1 gene.* Molecular and Cellular Biology, 2004. **24**(7): p. 3057-3067.

81. Cao, W., et al., *β-Adrenergic Activation of p38 MAP Kinase in Adipocytes cAMP INDUCTION OF THE UNCOUPLING PROTEIN 1 (UCP1) GENE REQUIRES p38 MAP KINASE.* Journal of Biological Chemistry, 2001. **276**(29): p. 27077-27082.

82. Hallberg, M., et al., *A functional interaction between RIP140 and PGC-1α regulates the expression of the lipid droplet protein CIDEA.* Molecular and cellular biology, 2008. **28**(22): p. 6785-6795.

83. Wang, H., et al., *Liver X receptor α is a transcriptional repressor of the uncoupling protein 1 gene and the brown fat phenotype.* Molecular and cellular biology, 2008. **28**(7): p. 2187-2200.

84. Sun, C., et al., *SIRT1 improves insulin sensitivity under insulin-resistant conditions by repressing PTP1B.* Cell metabolism, 2007. **6**(4): p. 307-319.

85. Pfluger, P.T., et al., *Sirt1 protects against high-fat diet-induced metabolic damage.* Proceedings of the National Academy of Sciences, 2008. **105**(28): p. 9793-9798.

86. Andrade, J.M.O., et al., *Resveratrol increases brown adipose tissue thermogenesis markers by increasing SIRT1 and energy expenditure and decreasing fat accumulation in adipose tissue of mice fed a standard diet.* European journal of nutrition, 2014. **53**(7): p. 1503-1510.

87. Itoh, N. and D.M. Ornitz, *Functional evolutionary history of the mouse Fgf gene family.* Developmental Dynamics, 2008. **237**(1): p. 18-27.

88. Thisse, B. and C. Thisse, *Functions and regulations of fibroblast growth factor signaling during embryonic development.* Developmental biology, 2005. **287**(2): p. 390-402.

89. Hotta, Y., et al., *Fibroblast growth factor 21 regulates lipolysis in white adipose tissue but is not required for ketogenesis and triglyceride clearance in liver.* Endocrinology, 2009. **150**(10): p. 4625-4633.

90. Kleiner, S., et al., *FGF21 regulates PGC-1α and browning of white adipose tissues in adaptive thermogenesis.* Genes & development, 2012. **26**(3): p. 271-281.

91. Li, X., et al., *Inhibition of lipolysis may contribute to the acute regulation of plasma FFA and glucose by FGF21 in ob/ob mice.* FEBS letters, 2009. **583**(19): p. 3230-3234.

92. Arner, P., et al., *FGF21 attenuates lipolysis in human adipocytes–a possible link to improved insulin sensitivity.* FEBS letters, 2008. **582**(12): p. 1725-1730.

93. Owen, B.M., et al., *FGF21 Acts Centrally to Induce Sympathetic Nerve Activity, Energy Expenditure, and Weight Loss.* Cell metabolism, 2014. **20**(4): p. 670-677.

94. Chen, W., et al., *Growth hormone induces hepatic production of fibroblast growth factor 21 through a mechanism dependent on lipolysis in adipocytes.* Journal of Biological Chemistry, 2011. **286**(40): p. 34559-34566.

95. Vernia, S., et al., *The PPARα-FGF21 Hormone Axis Contributes to Metabolic Regulation by the Hepatic JNK Signaling Pathway.* Cell metabolism, 2014. **20**(3): p. 512-525.

96. Chau, M.D., et al., *Fibroblast growth factor 21 regulates energy metabolism by activating the AMPK–SIRT1–PGC-1α pathway.* Proceedings of the National Academy of Sciences, 2010. **107**(28): p. 12553-12558.

97. Kim, K.H., et al., *Autophagy deficiency leads to protection from obesity and insulin resistance by inducing Fgf21 as a mitokine.* Nature medicine, 2013. **19**(1): p. 83-92.

98. Emanuelli, B., et al., *Interplay between FGF21 and insulin action in the liver regulates metabolism.* The Journal of clinical investigation, 2014. **124**(2): p. 515.

99. Dushay, J., et al., *Increased fibroblast growth factor 21 in obesity and nonalcoholic fatty liver disease.* Gastroenterology, 2010. **139**(2): p. 456-63.

100. Hafner, R.P., et al., *Altered relationship between protonmotive force and respiration rate in non-phosphorylating liver mitochondria isolated from rats of different thyroid hormone status.* European Journal of Biochemistry, 1988. **178**(2): p. 511-518.

101. Edelman, I. and F. Ismail-Beigi. *Thyroid thermogenesis and active sodium transport*. in *Recent Progress in Hormone Research: Proceedings of the 1973 Laurentian Hormone Conference*. 2013. Academic Press.

102. Bianco, A.C., X. Sheng, and J. Silva, *Triiodothyronine amplifies norepinephrine stimulation of uncoupling protein gene transcription by a mechanism not requiring protein synthesis.* Journal of Biological Chemistry, 1988. **263**(34): p. 18168-18175.

103. Steinsapir, J., et al., *Substrate-Induced Down-Regulation of Human Type 2 Deiodinase (hD2) Is Mediated through Proteasomal Degradation and*

Requires Interaction with the Enzyme's Active Center 1. Endocrinology, 2000. **141**(3): p. 1127-1135.

104. Bilezikian, J.P. and J.N. Loeb, *The Influence of Hyperthyroidism and Hypothyroidism on α and β-Adrenergic Receptor Systems and Adrenergic Responsiveness*.* Endocrine Reviews, 1983. **4**(4): p. 378-388.

105. Levine, M.A., et al., *Influence of thyroid hormone status on expression of genes encoding G protein subunits in the rat heart.* Journal of Biological Chemistry, 1990. **265**(6): p. 3553-3560.

106. Michel-Reher, M.B., et al., *Tissue-and subunit-specific regulation of G-protein expression by hypo-and hyperthyroidism.* Biochemical pharmacology, 1993. **45**(7): p. 1417-1423.

107. Marrif, H., et al., *Temperature homeostasis in transgenic mice lacking thyroid hormone receptor-α gene products.* Endocrinology, 2005. **146**(7): p. 2872-2884.

108. Yoshimura, M., H. Yasue, and H. Ogawa, *Pathophysiological significance and clinical application of ANP and BNP in patients with heart failure.* Can J Physiol Pharmacol, 2001. **79**(8): p. 730-5.

109. Bordicchia, M., et al., *Cardiac natriuretic peptides act via p38 MAPK to induce the brown fat thermogenic program in mouse and human adipocytes.* J Clin Invest, 2012. **122**(3): p. 1022-36.

110. Birkenfeld, A.L., et al., *Lipid mobilization with physiological atrial natriuretic peptide concentrations in humans.* J Clin Endocrinol Metab, 2005. **90**(6): p. 3622-8.

111. Sengenes, C., et al., *Involvement of a cGMP-dependent pathway in the natriuretic peptide-mediated hormone-sensitive lipase phosphorylation in human adipocytes.* J Biol Chem, 2003. **278**(49): p. 48617-26.

112. Souza, S.C., et al., *Atrial natriuretic peptide regulates lipid mobilization and oxygen consumption in human adipocytes by activating AMPK.* Biochem Biophys Res Commun, 2011. **410**(3): p. 398-403.

113. Gustafson, B. and U. Smith, *The WNT inhibitor Dickkopf 1 and bone morphogenetic protein 4 rescue adipogenesis in hypertrophic obesity in humans.* Diabetes, 2012. **61**(5): p. 1217-24.

114. Bowers, R.R., et al., *Stable stem cell commitment to the adipocyte lineage by inhibition of DNA methylation: role of the BMP-4 gene.* Proc Natl Acad Sci U S A, 2006. **103**(35): p. 13022-7.

115. Tseng, Y.H., et al., *New role of bone morphogenetic protein 7 in brown adipogenesis and energy expenditure.* Nature, 2008. **454**(7207): p. 1000-4.

116. Elsen, M., et al., *BMP4 and BMP7 induce the white-to-brown transition of primary human adipose stem cells.* Am J Physiol Cell Physiol, 2014. **306**(5): p. C431-40.

117. Whittle, A.J., et al., *BMP8B increases brown adipose tissue thermogenesis through both central and peripheral actions.* Cell, 2012. **149**(4): p. 871-85.

118. Schulz, T.J., et al., *Brown-fat paucity due to impaired BMP signalling induces compensatory browning of white fat.* Nature, 2013. **495**(7441): p. 379-83.

119. Martins, L., et al., *A Functional Link between AMPK and Orexin Mediates the Effect of BMP8B on Energy Balance.* Cell Rep, 2016. **16**(8): p. 2231-42.

120. Lopez, M., et al., *Hypothalamic AMPK and fatty acid metabolism mediate thyroid regulation of energy balance.* Nat Med, 2010. **16**(9): p. 1001-8.

121. Martinez de Morentin, P.B., et al., *Estradiol regulates brown adipose tissue thermogenesis via hypothalamic AMPK.* Cell Metab, 2014. **20**(1): p. 41-53.

122. Sellayah, D. and D. Sikder, *Orexin receptor-1 mediates brown fat developmental differentiation.* Adipocyte, 2012. **1**(1): p. 58-63.

123. Sellayah, D., P. Bharaj, and D. Sikder, *Orexin is required for brown adipose tissue development, differentiation, and function.* Cell Metab, 2011. **14**(4): p. 478-90.

124. Nisoli, E., et al., *Mitochondrial biogenesis in mammals: the role of endogenous nitric oxide.* Science, 2003. **299**(5608): p. 896-9.

125. Haas, B., et al., *Protein kinase G controls brown fat cell differentiation and mitochondrial biogenesis.* Sci Signal, 2009. **2**(99): p. ra78.

126. Hoffmann, L.S., et al., *Stimulation of soluble guanylyl cyclase protects against obesity by recruiting brown adipose tissue.* Nat Commun, 2015. **6**: p. 7235.

127. Mitschke, M.M., et al., *Increased cGMP promotes healthy expansion and browning of white adipose tissue.* FASEB J, 2013. **27**(4): p. 1621-30.

128. Sun, K., et al., *Brown adipose tissue derived VEGF-A modulates cold tolerance and energy expenditure.* Mol Metab, 2014. **3**(4): p. 474-83.

129. Seki, T., et al., *Endothelial PDGF-CC regulates angiogenesis-dependent thermogenesis in beige fat.* Nat Commun, 2016. **7**: p. 12152.

130. Nicholls, D.G., *Hamster brown-adipose-tissue mitochondria. The control of respiration and the proton electrochemical potential gradient by possible physiological effectors of the proton conductance of the inner membrane.* European journal of biochemistry/FEBS, 1974. **49**(3): p. 573-583.

131. Rial, E., et al., *Alkylsulfonates activate the uncoupling protein UCP1: implications for the transport mechanism.* Biochim Biophys Acta, 2004. **1608**(2-3): p. 122-30.

132. Nicholls, D.G., *The physiological regulation of uncoupling proteins.* Biochimica et Biophysica Acta (BBA)-Bioenergetics, 2006. **1757**(5): p. 459-466.

133. Ricquier, D. and F. Bouillaud, *The uncoupling protein homologues: UCP1, UCP2, UCP3, StUCP and AtUCP.* Biochem J, 2000. **345 Pt 2**: p. 161-79.

134. Fedorenko, A., P.V. Lishko, and Y. Kirichok, *Mechanism of fatty-acid-dependent UCP1 uncoupling in brown fat mitochondria.* Cell, 2012. **151**(2): p. 400-13.

135. Cannon, B., U. Sundin, and L. Romert, *Palmitoyl coenzyme A: a possible physiological regulator of nucleotide binding to brown adipose tissue mitochondria.* FEBS letters, 1977. **74**(1): p. 43-46.

136. Strieleman, P., C. Elson, and E. Shrago. *MODULATION OF GDP BINDING TO BROWN ADIPOSE-TISSUE MITOCHONDRIA BY COENZYME-A THIOESTERS*. in *FEDERATION PROCEEDINGS*. 1983. FEDERATION AMER SOC EXP BIOL 9650 ROCKVILLE PIKE, BETHESDA, MD 20814-3998.

137. Cannon, B. and J. Nedergaard, *Brown adipose tissue: function and physiological significance.* Physiological reviews, 2004. **84**(1): p. 277-359.

138. Rial, E. and M.M. González-Barroso, *Physiological regulation of the transport activity in the uncoupling proteins UCP1 and UCP2.* Biochimica et Biophysica Acta (BBA)-Bioenergetics, 2001. **1504**(1): p. 70-81.

139. Garlid, K.D., M. Jabůrek, and P. Ježek, *The mechanism of proton transport mediated by mitochondrial uncoupling proteins.* FEBS letters, 1998. **438**(1-2): p. 10-14.

140. Rial, E. and M. González-Barroso, *Physiological regulation of the transport activity in the uncoupling proteins UCP1 and UCP2.* Biochimica et Biophysica Acta (BBA)-Bioenergetics, 2001. **1504**(1): p. 70-81.

141. Brasaemle, D.L., *Thematic review series: adipocyte biology. The perilipin family of structural lipid droplet proteins: stabilization of lipid droplets and control of lipolysis.* J Lipid Res, 2007. **48**(12): p. 2547-59.

142. Bickel, P.E., J.T. Tansey, and M.A. Welte, *PAT proteins, an ancient family of lipid droplet proteins that regulate cellular lipid stores.* Biochim Biophys Acta, 2009. **1791**(6): p. 419-40.

143. Zimmermann, R., et al., *Fat mobilization in adipose tissue is promoted by adipose triglyceride lipase.* Science, 2004. **306**(5700): p. 1383-6.

144. Jenkins, C.M., et al., *Identification, cloning, expression, and purification of three novel human calcium-independent phospholipase A2 family members possessing triacylglycerol lipase and acylglycerol transacylase activities.* J Biol Chem, 2004. **279**(47): p. 48968-75.

145. Villena, J.A., et al., *Desnutrin, an adipocyte gene encoding a novel patatin domain-containing protein, is induced by fasting and glucocorticoids: ectopic expression of desnutrin increases triglyceride hydrolysis.* J Biol Chem, 2004. **279**(45): p. 47066-75.

146. Zechner, R., et al., *Lipolysis: pathway under construction.* Curr Opin Lipidol, 2005. **16**(3): p. 333-40.

147. Lai, C.H., et al., *Identification of novel human genes evolutionarily conserved in Caenorhabditis elegans by comparative proteomics.* Genome Res, 2000. **10**(5): p. 703-13.

148. Schrag, J.D. and M. Cygler, *Lipases and alpha/beta hydrolase fold.* Methods Enzymol, 1997. **284**: p. 85-107.

149. Zhang, L., et al., *Functional analysis of the Escherichia coli genome for members of the alpha/beta hydrolase family.* Fold Des, 1998. **3**(6): p. 535-48.

150. Simon, G.M. and B.F. Cravatt, *Endocannabinoid biosynthesis proceeding through glycerophospho-N-acyl ethanolamine and a role for alpha/beta-hydrolase 4 in this pathway.* J Biol Chem, 2006. **281**(36): p. 26465-72.

151. Subramanian, V., et al., *Perilipin A mediates the reversible binding of CGI-58 to lipid droplets in 3T3-L1 adipocytes.* J Biol Chem, 2004. **279**(40): p. 42062-71.

152. Lass, A., et al., *Adipose triglyceride lipase-mediated lipolysis of cellular fat stores is activated by CGI-58 and defective in Chanarin-Dorfman Syndrome.* Cell Metab, 2006. **3**(5): p. 309-19.

153. Brown, J.M., et al., *CGI-58 facilitates the mobilization of cytoplasmic triglyceride for lipoprotein secretion in hepatoma cells.* J Lipid Res, 2007. **48**(10): p. 2295-305.

154. Miao, H., et al., *Macrophage CGI-58 deficiency activates ROS-inflammasome pathway to promote insulin resistance in mice.* Cell Rep, 2014. **7**(1): p. 223-35.

155. Bergman, R., et al., *Neutral lipid storage disease with ichthyosis: serum apolipoprotein levels and cholesterol metabolism in monocyte-derived macrophages.* J Inherit Metab Dis, 1991. **14**(2): p. 241-6.

156. Liu, P., et al., *Chinese hamster ovary K2 cell lipid droplets appear to be metabolic organelles involved in membrane traffic.* J Biol Chem, 2004. **279**(5): p. 3787-92.

157. Yamaguchi, T., et al., *CGI-58 interacts with perilipin and is localized to lipid droplets. Possible involvement of CGI-58 mislocalization in Chanarin-Dorfman syndrome.* J Biol Chem, 2004. **279**(29): p. 30490-7.

158. Yamaguchi, T., et al., *CGI-58 facilitates lipolysis on lipid droplets but is not involved in the vesiculation of lipid droplets caused by hormonal stimulation.* J Lipid Res, 2007. **48**(5): p. 1078-89.

159. Granneman, J.G., et al., *Functional interactions between Mldp (LSDP5) and Abhd5 in the control of intracellular lipid accumulation.* J Biol Chem, 2009. **284**(5): p. 3049-57.

160. Londos, C., et al., *Role of PAT proteins in lipid metabolism.* Biochimie, 2005. **87**(1): p. 45-9.

161. Martin, S. and R.G. Parton, *Lipid droplets: a unified view of a dynamic organelle.* Nat Rev Mol Cell Biol, 2006. **7**(5): p. 373-8.

162. Wolins, N.E., D.L. Brasaemle, and P.E. Bickel, *A proposed model of fat packaging by exchangeable lipid droplet proteins.* FEBS Lett, 2006. **580**(23): p. 5484-91.

163. Lefevre, C., et al., *Mutations in CGI-58, the gene encoding a new protein of the esterase/lipase/thioesterase subfamily, in Chanarin-Dorfman syndrome.* Am J Hum Genet, 2001. **69**(5): p. 1002-12.

164. Fischer, J., et al., *The gene encoding adipose triglyceride lipase (PNPLA2) is mutated in neutral lipid storage disease with myopathy.* Nat Genet, 2007. **39**(1): p. 28-30.

165. Radner, F.P., et al., *Growth retardation, impaired triacylglycerol catabolism, hepatic steatosis, and lethal skin barrier defect in mice lacking comparative gene identification-58 (CGI-58).* J Biol Chem, 2010. **285**(10): p. 7300-11.

166. Igal, R.A. and R.A. Coleman, *Acylglycerol recycling from triacylglycerol to phospholipid, not lipase activity, is defective in neutral lipid storage disease fibroblasts.* J Biol Chem, 1996. **271**(28): p. 16644-51.

167. Igal, R.A. and R.A. Coleman, *Neutral lipid storage disease: a genetic disorder with abnormalities in the regulation of phospholipid metabolism.* J Lipid Res, 1998. **39**(1): p. 31-43.

168. Granneman, J.G., et al., *Perilipin controls lipolysis by regulating the interactions of AB-hydrolase containing 5 (Abhd5) and adipose triglyceride lipase (Atgl).* J Biol Chem, 2009. **284**(50): p. 34538-44.

169. Brown, J.M., et al., *CGI-58 knockdown in mice causes hepatic steatosis but prevents diet-induced obesity and glucose intolerance.* J Lipid Res, 2010. **51**(11): p. 3306-15.

170. Singh, R., et al., *Autophagy regulates lipid metabolism.* Nature, 2009. **458**(7242): p. 1131-5.

171. Sahu-Osen, A., et al., *CGI-58/ABHD5 is phosphorylated on Ser239 by protein kinase A: control of subcellular localization.* J Lipid Res, 2015. **56**(1): p. 109-21.

172. Liew, C.W., et al., *Ablation of TRIP-Br2, a regulator of fat lipolysis, thermogenesis and oxidative metabolism, prevents diet-induced obesity and insulin resistance.* Nature medicine, 2013. **19**(2): p. 217-226.

173. Fajas, L., et al., *E2Fs regulate adipocyte differentiation.* Developmental cell, 2002. **3**(1): p. 39-49.

174. Tseng, Y.-H., et al., *Prediction of preadipocyte differentiation by gene expression reveals role of insulin receptor substrates and necdin.* Nature Cell Biology, 2005. **7**(6): p. 601-611.

175. Laplante, M. and D.M. Sabatini, *mTOR signaling in growth control and disease.* Cell, 2012. **149**(2): p. 274-293.

176. Wullschleger, S., R. Loewith, and M.N. Hall, *TOR signaling in growth and metabolism.* Cell, 2006. **124**(3): p. 471-484.

177. Chakrabarti, P., et al., *Mammalian target of rapamycin complex 1 suppresses lipolysis, stimulates lipogenesis, and promotes fat storage.* Diabetes, 2010. **59**(4): p. 775-781.

178. Polak, P., et al., *Adipose-specific knockout of raptor results in lean mice with enhanced mitochondrial respiration.* Cell metabolism, 2008. **8**(5): p. 399-410.

179. Holt, L.S., Kenneth, *Grb10 and Grb14: enigmatic regulators of insulin action-and more?* Biochem. J, 2005. **388**: p. 393-406.

180. Lim, M.A., H. Riedel, and F. Liu, *Grb10: more than a simple adaptor protein.* Front Biosci, 2004. **9**: p. 387-403.

181. Hsu, P.P., et al., *The mTOR-regulated phosphoproteome reveals a mechanism of mTORC1-mediated inhibition of growth factor signaling.* Science, 2011. **332**(6035): p. 1317-1322.

182. Yu, Y., et al., *Phosphoproteomic analysis identifies Grb10 as an mTORC1 substrate that negatively regulates insulin signaling.* Science, 2011. **332**(6035): p. 1322-1326.

183. Liu, M., et al., *Grb10 promotes lipolysis and thermogenesis by phosphorylation-dependent feedback inhibition of mTORC1.* Cell metabolism, 2014. **19**(6): p. 967-980.

184. Yang, X., et al., *The G(0)/G(1) switch gene 2 regulates adipose lipolysis through association with adipose triglyceride lipase.* Cell Metab, 2010. **11**(3): p. 194-205.

185. El-Assaad, W., et al., *Deletion of the gene encoding G0/G 1 switch protein 2 (G0s2) alleviates high-fat-diet-induced weight gain and insulin resistance, and promotes browning of white adipose tissue in mice.* Diabetologia, 2015. **58**(1): p. 149-57.

186. Zandbergen, F., et al., *The G0/G1 switch gene 2 is a novel PPAR target gene.* Biochem J, 2005. **392**(Pt 2): p. 313-24.

187. Lu, X., X. Yang, and J. Liu, *Differential control of ATGL-mediated lipid droplet degradation by CGI-58 and G0S2.* Cell Cycle, 2010. **9**(14): p. 2719-25.

188. Ma, T., et al., *Mice lacking G0S2 are lean and cold-tolerant.* Cancer Biol Ther, 2014. **15**(5): p. 643-50.

189. Ahmadian, M., et al., *Desnutrin/ATGL is regulated by AMPK and is required for a brown adipose phenotype.* Cell metabolism, 2011. **13**(6): p. 739-748.

190. Haemmerle, G., et al., *Defective lipolysis and altered energy metabolism in mice lacking adipose triglyceride lipase.* Science, 2006. **312**(5774): p. 734-7.

191. Ström, K., et al., *Attainment of brown adipocyte features in white adipocytes of hormone-sensitive lipase null mice.* PLoS One, 2008. **3**(3): p. e1793.

192. Bartelt, A., et al., *Brown adipose tissue activity controls triglyceride clearance.* Nat Med, 2011. **17**(2): p. 200-5.

193. Davies, B.S., et al., *GPIHBP1 is responsible for the entry of lipoprotein lipase into capillaries.* Cell Metab, 2010. **12**(1): p. 42-52.

194. Stahl, A., et al., *Insulin causes fatty acid transport protein translocation and enhanced fatty acid uptake in adipocytes.* Developmental cell, 2002. **2**(4): p. 477-488.

195. Doege, H. and A. Stahl, *Protein-mediated fatty acid uptake: novel insights from in vivo models.* Physiology, 2006. **21**(4): p. 259-268.

196. Richards, M.R., et al., *Oligomerization of the murine fatty acid transport protein 1.* Journal of Biological Chemistry, 2003. **278**(12): p. 10477-10483.

197. Stuhlsatz-Krouper, S.M., N.E. Bennett, and J.E. Schaffer, *Substitution of alanine for serine 250 in the murine fatty acid transport protein inhibits*

long chain fatty acid transport. Journal of Biological Chemistry, 1998. **273**(44): p. 28642-28650.

198. Wu, Q., et al., *FATP1 is an insulin-sensitive fatty acid transporter involved in diet-induced obesity.* Molecular and cellular biology, 2006. **26**(9): p. 3455-3467.

199. Wu, Q., et al., *Fatty acid transport protein 1 is required for nonshivering thermogenesis in brown adipose tissue.* Diabetes, 2006. **55**(12): p. 3229-3237.

200. Harmon, C.M. and N.A. Abumrad, *Binding of sulfosuccinimidyl fatty acids to adipocyte membrane proteins: Isolation and ammo-terminal sequence of an 88-kD protein implicated in transport of long-chain fatty acids.* The Journal of membrane biology, 1993. **133**(1): p. 43-49.

201. Harmon, C.M., P. Luce, and N.A. Abumrad, *Labelling of an 88 kDa adipocyte membrane protein by sulpho-N-succinimidyl long-chain fatty acids: inhibition of fatty acid transport.* Biochemical Society Transactions, 1992. **20**: p. 811-811.

202. Harmon, C.M., et al., *Labeling of adipocyte membranes by sulfo-N-succinimidyl derivatives of long-chain fatty acids: inhibition of fatty acid transport.* The Journal of membrane biology, 1991. **121**(3): p. 261-268.

203. Ibrahimi, A., et al., *Expression of the CD36 homolog (FAT) in fibroblast cells: effects on fatty acid transport.* Proceedings of the National Academy of Sciences, 1996. **93**(7): p. 2646-2651.

204. Bastie, C.C., et al., *CD36 in myocytes channels fatty acids to a lipase-accessible triglyceride pool that is related to cell lipid and insulin responsiveness.* Diabetes, 2004. **53**(9): p. 2209-2216.

205. Nickerson, J.G., et al., *Greater transport efficiencies of the membrane fatty acid transporters FAT/CD36 and FATP4 compared with FABPpm and FATP1 and differential effects on fatty acid esterification and oxidation in rat skeletal muscle.* Journal of Biological Chemistry, 2009. **284**(24): p. 16522-16530.

206. van Oort, M.M., et al., *Insulin-induced translocation of CD36 to the plasma membrane is reversible and shows similarity to that of GLUT4.* Biochimica et Biophysica Acta (BBA)-Molecular and Cell Biology of Lipids, 2008. **1781**(1): p. 61-71.

207. Luiken, J.J., et al., *Insulin induces the translocation of the fatty acid transporter FAT/CD36 to the plasma membrane.* American Journal of Physiology-Endocrinology And Metabolism, 2002. **282**(2): p. E491-E495.

208. Putri, M., et al., *CD36 is indispensable for thermogenesis under conditions of fasting and cold stress.* Biochem Biophys Res Commun, 2015. **457**(4): p. 520-5.

209. Dallner, O.S., et al., *β3-adrenergic receptors stimulate glucose uptake in brown adipocytes by two mechanisms independently of glucose transporter 4 translocation.* Endocrinology, 2006. **147**(12): p. 5730-5739.

210. Olsen, J.M., et al., *Glucose uptake in brown fat cells is dependent on mTOR complex 2–promoted GLUT1 translocation.* The Journal of cell biology, 2014. **207**(3): p. 365-374.

211. Emanuelli, B., et al., *Interplay between FGF21 and insulin action in the liver regulates metabolism.* The Journal of clinical investigation, 2014. **124**(2): p. 0-0.

212. Marette, A. and L.J. Bukowiecki, *Stimulation of glucose transport by insulin and norepinephrine in isolated rat brown adipocytes.* American Journal of Physiology-Cell Physiology, 1989. **257**(4): p. C714-C721.

213. Guerra, C., et al., *Brown adipose tissue–specific insulin receptor knockout shows diabetic phenotype without insulin resistance.* Journal of Clinical Investigation, 2001. **108**(8): p. 1205.

214. Bartelt, A., et al., *Brown adipose tissue activity controls triglyceride clearance.* Nature medicine, 2011. **17**(2): p. 200-205.

215. Virtue, S., et al., *A new role for lipocalin prostaglandin d synthase in the regulation of brown adipose tissue substrate utilization.* Diabetes, 2012. **61**(12): p. 3139-47.

216. Guo, F., et al., *Deficiency of liver Comparative Gene Identification-58 causes steatohepatitis and fibrosis in mice.* Journal of lipid research, 2013. **54**(8): p. 2109-2120.

217. Kong, X., et al., *IRF4 is a key thermogenic transcriptional partner of PGC-1α.* Cell, 2014. **158**(1): p. 69-83.

218. Eguchi, J., et al., *Transcriptional control of adipose lipid handling by IRF4.* Cell metabolism, 2011. **13**(3): p. 249-259.

219. Wei, E., W. Gao, and R. Lehner, *Attenuation of adipocyte triacylglycerol hydrolase activity decreases basal fatty acid efflux.* J Biol Chem, 2007. **282**(11): p. 8027-35.

220. Etherton, T., E. Thompson, and C. Allen, *Improved techniques for studies of adipocyte cellularity and metabolism.* Journal of lipid research, 1977. **18**(4): p. 552-557.

221. Temel, R.E., et al., *Hepatic Niemann-Pick C1–like 1 regulates biliary cholesterol concentration and is a target of ezetimibe.* The Journal of clinical investigation, 2007. **117**(7): p. 1968-1978.

222. Classics Lowry, O., et al., *Protein measurement with the Folin phenol reagent.* J biol Chem, 1951. **193**: p. 265-75.

223. Daikoku, T., et al., *Specific elevation of transcript levels of particular protein subtypes induced in brown adipose tissue by cold exposure.* Biochimica et Biophysica Acta (BBA)-Bioenergetics, 2000. **1457**(3): p. 263-272.

224. Shimizu, Y., et al., *Increased expression of glucose transporter GLUT-4 in brown adipose tissue of fasted rats after cold exposure.* American Journal of Physiology-Endocrinology And Metabolism, 1993. **264**(6): p. E890-E895.

225. Yu, X.X., et al., *Cold elicits the simultaneous induction of fatty acid synthesis and β-oxidation in murine brown adipose tissue: prediction from*

differential gene expression and confirmation in vivo. The FASEB Journal, 2002. **16**(2): p. 155-168.

226. Virtue, S., et al., *A new role for lipocalin prostaglandin d synthase in the regulation of brown adipose tissue substrate utilization.* Diabetes, 2012. **61**(12): p. 3139-3147.

227. Wang, X. and R. Wahl, *Responses of the insulin signaling pathways in the brown adipose tissue of rats following cold exposure.* PloS one, 2014. **9**(6): p. e99772.

228. Labbé, S.M., et al., *In vivo measurement of energy substrate contribution to cold-induced brown adipose tissue thermogenesis.* The FASEB Journal, 2015. **29**(5): p. 2046-2058.

229. Cao, H., et al., *Identification of a lipokine, a lipid hormone linking adipose tissue to systemic metabolism.* Cell, 2008. **134**(6): p. 933-944.

230. Ryu, V., et al., *Brown adipose tissue has sympathetic-sensory feedback circuits.* The Journal of Neuroscience, 2015. **35**(5): p. 2181-2190.

231. Ou, J., et al., *Loss of abhd5 promotes colorectal tumor development and progression by inducing aerobic glycolysis and epithelial-mesenchymal transition.* Cell Rep, 2014. **9**(5): p. 1798-811.

232. Xie, P., et al., *Muscle-Specific Deletion of Comparative Gene Identification-58 (CGI-58) Causes Muscle Steatosis but Improves Insulin Sensitivity in Male Mice.* Endocrinology, 2015. **156**(5): p. 1648-58.

233. Zhou, D., et al., *CD36 level and trafficking are determinants of lipolysis in adipocytes.* The FASEB Journal, 2012. **26**(11): p. 4733-4742.

234. Mossenbock, K., et al., *Browning of white adipose tissue uncouples glucose uptake from insulin signaling.* PLoS One, 2014. **9**(10): p. e110428.

235. Yan, J., et al., *Increased glucose uptake and oxidation in mouse hearts prevent high fatty acid oxidation but cause cardiac dysfunction in diet-induced obesity.* Circulation, 2009. **119**(21): p. 2818-28.

236. Brandt, R.R., et al., *Atrial natriuretic peptide in heart failure.* Journal of the American College of Cardiology, 1993. **22**(4s1): p. A86-A92.

237. Bordicchia, M., et al., *Cardiac natriuretic peptides act via p38 MAPK to induce the brown fat thermogenic program in mouse and human adipocytes.* The Journal of clinical investigation, 2012. **122**(3): p. 1022-1036.

238. Lafontan, M., et al., *Control of lipolysis by natriuretic peptides and cyclic GMP.* Trends in Endocrinology & Metabolism, 2008. **19**(4): p. 130-137.

239. Blondin, D.P., et al., *Inhibition of Intracellular Triglyceride Lipolysis Suppresses Cold-Induced Brown Adipose Tissue Metabolism and Increases Shivering in Humans.* Cell Metab, 2017. **25**(2): p. 438-447.

240. Ukropec, J., et al., *UCP1-independent thermogenesis in white adipose tissue of cold-acclimated Ucp1-/- mice.* J Biol Chem, 2006. **281**(42): p. 31894-908.

241. Cannon, B. and J. Nedergaard, *Nonshivering thermogenesis and its adequate measurement in metabolic studies.* J Exp Biol, 2011. **214**(Pt 2): p. 242-53.

242. Golozoubova, V., B. Cannon, and J. Nedergaard, *UCP1 is essential for adaptive adrenergic nonshivering thermogenesis.* Am J Physiol Endocrinol Metab, 2006. **291**(2): p. E350-7.

243. Depocas, F., G. Zaror-Behrens, and S. Lacelle, *Noradrenaline-induced calorigenesis in warm- or cold-acclimated rats. In vivo estimation of adrenoceptor concentration of noradrenaline effecting half-maximal response.* Can J Physiol Pharmacol, 1980. **58**(9): p. 1072-7.

244. Li, Y., et al., *Taking control over intracellular fatty acid levels is essential for the analysis of thermogenic function in cultured primary brown and brite/beige adipocytes.* EMBO Rep, 2014. **15**(10): p. 1069-76.

245. Feldmann, H.M., et al., *UCP1 ablation induces obesity and abolishes diet-induced thermogenesis in mice exempt from thermal stress by living at thermoneutrality.* Cell Metab, 2009. **9**(2): p. 203-9.